NASA CR-159708

DOE/NASA/0100-79/1
Distribution Category UC-94a

High Temperature Thermal Energy Storage in Steel and Sand

Robert H. Turner

December 15, 1979

Prepared for
NASA Lewis Research Center
Cleveland, Ohio
and
U.S. Department of Energy
Through an agreement with
National Aeronautics and Space Administration
by
Jet Propulsion Laboratory
California Institute of Technology
Pasadena, California

(JPL PUBLICATION 80-35)

NASA CR-159708

DOE/NASA/0100-79/1
Distribution Category UC-94a

High Temperature Thermal Energy Storage in Steel and Sand

Robert H. Turner

December 15, 1979

Prepared for
NASA Lewis Research Center
Cleveland, Ohio
and
U.S. Department of Energy
Through an agreement with
National Aeronautics and Space Administration
by
Jet Propulsion Laboratory
California Institute of Technology
Pasadena, California

(JPL PUBLICATION 80-35)

Prepared by the Jet Propulsion Laboratory, California Institute of Technology, for the NASA Lewis Research Center and the U.S. Department of Energy through an agreement with the National Aeronautics and Space Administration.

The JPL Solar Thermal Power Systems Project is sponsored by the U.S. Department of Energy and forms a part of the Solar Thermal Program to develop low-cost solar thermal electric generating plants.

ABSTRACT

This study evaluates the technical and economic potential for high temperature (343°C, 650°F) thermal energy storage (TES) in hollow steel ingots, pipes embedded in concrete, and for pipes buried in sand. The intended TES application is integration into a steam power plant, perhaps to provide an otherwise baseload plant.

It was determined that concrete would separate from pipes due to thermal stresses, causing unacceptable thermal resistances. Therefore, for study, concrete was replaced by sand, which is free from thermal stresses. The original hollow steel ingot concept underwent a series of evolutionary changes, and it was finally decided that all variations were not cost effective compared to the sand-pipe approach. Therefore, the sand-pipe thermal storage unit (TSU) was evaluated in depth to assess the approximate tube spacing requirements consistent with different system performance characteristics and also attendant system costs. A series of performance cost curves were generated from which tube spacing and tube diameter performance comparisons were obtained. The curves served as inputs for the cost analysis.

The major conclusion of the study is that for large TSUs which do not require fast response times, the sand-pipe approach offers attractive possibilities. A pipe diameter about 9 cm (3.5 in) and pipe spacing of approximately 25 cm (10 in), with sand filling the interspaces, appears appropriate. Such a TSU system designed for 8 hours charge/discharge cycle has an energy unit storage cost (C_E) of $2.63/kWhr-t and a power unit storage cost (C_P) of $42/kW-t (in 1977 dollars).

LIST OF SYMBOLS

A	Area, (m^2 or ft^2)
C_E	Energy Unit Storage Cost, or TSU energy related costs per unit energy, ($/kWhr)
C_p	Specific heat, (kWhr-t/kg-^oC or Btu/lb-^oF)
C_P	Power Unit Storage Cost, or TSU power related costs per unit power, ($/kW)
C_T	Total Capital Costs, ($/kW) $C_T = C_P + C_E t$
D_i	Pipe diameter, (cm or in)
D_o	Spacing between pipes, (cm or in)
f	Friction factor in pipe, (dimensionless)
g_c	Constant
h	Convective heat transfer coefficient, (cal/hr-cm^2-^oC or Btu/hr-ft^2-^oF)
L	Flow length, (m or ft)
$\dot{M}$	Fluid flowrate, (kg/sec or lb/sec)
P	Pressure, (kPa or psi)
PP	Pump Power, (kW)
Q	Heat quantity, (kWhr-t or Btu)
r	Radial distance from axial centerline, (cm)
Re	Reynold's numbers, (dimensionless)
t	Time, (hr, min, or sec)
T	Temperature, (^oC or dimensionless, distinction made clear in text)
V	Fluid velocity through pipe, (m/sec or ft/sec)
x	Axial distance from a given starting reference point, (m)
α	Thermal diffusivity, (m^2/hr or ft^2/hr)
η	Efficiency, (dimensionless)

λ Dimensionless location

ν Kinematic viscosity, (m^2/sec or ft^2/sec)

ρ Density, (kg/m^3 or lb/ft^3)

τ TSU time factor, the TSU energy storage capacity divided by TSU power transfer capacity

TABLE OF CONTENTS

SUMMARY

LIST OF SYMBOLS

I. INTRODUCTION ---------- 1-1

II. SELECTION OF STORAGE CONCEPT ---------- 2-1

A. Hollow Steel Ingot ---------- 2-1

B. Steel Sandwich Pressure Containing Thermal Storage Unit (TSU) ---------- 2-4

C. Four Slab Square Hollow-Steel TSU ---------- 2-6

D. Thick Wall Pipe Containing Water TSU ---------- 2-8

E. Sand-Pipe TSU ---------- 2-8

F. Selection of the Appropriate TSU Concept for In-Depth Analysis ---------- 2-10

III. THE SAND-PIPE THERMAL STORAGE UNIT ---------- 3-1

IV. THERMAL ANALYSIS AND PRELIMINARY ECONOMICS ---------- 4-1

A. Computer Code ---------- 4-5

B. Thermal Analysis Results ---------- 4-6

V. ECONOMICS AND THE SAND-PIPE TSU ---------- 5-1

A. General Considerations ---------- 5-1

B. Economics of a Sand-Pipe TSU ---------- 5-7

VI. RESULTS AND DISCUSSION ---------- 6-1

APPENDIXES

A. Numerical Differencing of the Transient Heat Conduction Equation in Cylindrical Coordinates; Derivation of Equation 4.1 ---------- A-1

B. Heat Capacity Weighted Average Temperature for a Cylindrical Section ---------- B-1

C. Computer Code Listing of the Thermal Analysis in Section IV ---------- C-1

D. Derivation of Dimensionless Parameter ---------- D-1

E. Pipe and Sand Cost Sample Calculation ---------- E-1

Figures

2.1 Original Concept for Hollow Steel Ingot TSU ---------- 2-2

2.2 Electroslag Welded Steel Sandwich TSU with Interior Passage ---------- 2-5

2.3 Four Slab Square Hollow-Steel TSU ---------- 2-7

3.1 Sand-Pipe Thermal Storage Unit Overall Configuration ---------- 3-2

3.2 Steel Retaining Wall Configuration Design ---------- 3-4

4.1 Zone of Thermal Influence (Actual and Approximate) and Pipe/Sand Matrix ---------- 4-2

4.2 Finite Difference Geometry (Cross-Section) ---------- 4-3

4.3 Finite Difference Geometry (Side View) ---------- 4-3

4.4 Thermal Charge vs Time: I.D. = 3.8 cm ---------- 4-11

4.5 Thermal Charge vs Time: I.D. = 6.35 cm ---------- 4-12

4.6 Thermal Charge vs Time: I.D. = 8.9 cm ---------- 4-13

4.7 Thermal Charge vs Time - Indicating Impact of Variable Velocity on Performance ---------- 4-15

4.8 Dimensionless Fluid Outlet Temperature, I.D. = 3.8 cm ---------- 4-17

4.9 Dimensionless Fluid Outlet Temperature, I.D. = 6.35 cm ---------- 4-18

4.10 Dimensionless Fluid Outlet Temperature, I.D. = 8.9 cm ---------- 4-19

4.11 Heating Fluid Residual Thermal Power vs Time - Velocity is a Parameter ---------- 4-20

4.12 System Average Temperature Fraction vs Axial Position, D_o = 25.4 cm ---------- 4-22

4.13 System Average Temperature Fraction vs Axial Position, D_o = 20.3 cm ---------- 4-23

4.14 Fluid Temperature Fraction vs Axial Position at Different Times, Case 10 ---------- 4-24

4.15 Fluid Temperatures Fraction vs Axial Position at Different Times, Case 6 ---------- 4-25

4.16 Fluid Temperatures Fraction vs Axial Position at Different Times, Case 9 ---------- 4-26

5.1 TSU Energy and Power Related Costs vs System Capabilities ---------- 5-2

Tables

2.1 Comparison of Candidate Concepts ---------- 2-11

3.1 TSU Capital Cost ---------- 3-6

4.1 Sand-Pipe TSU System, Parametric, Cost and Performance Data ---------- 4-9

4.2 Economic Relationships ---------- 4-34

4.3 Friction Pressure Drop and Pump Work ---------- 4-36

SECTION I

INTRODUCTION

Thermal energy storage (TES) systems have the potential to make possible fuel substitution, fuel savings, and capital savings in many application areas. For large power plants, a thermal storage unit (TSU) must be able to store and return heat at high temperatures. Another practical requirement is that the TSU must be able to receive and return its full thermal charge within a specified time, probably measured in a few hours for a daily charge-discharge cycle.

Various approaches using solids as the prime storage medium were considered. Because the intended TES application is integration with a steam power plant to confer load following capability, pressurized water or steam is a logical heat transport fluid to charge and discharge the solid storage mass. Two solids were originally planned for consideration as storage media; steel and concrete. The original steel ingot heat storage concept underwent a series of evolutionary changes and was eliminated from selection because of high cost. The concrete was disqualified because of technical limitations and replaced by ordinary sand. The factors and considerations which lead to the final concept selection (sand-pipe TSU) are described below.

A system temperature limit of 343°C (650°F) was selected for this study to allow utilization of relatively low cost carbon steel, both in large ingot form and also in pipe form, because the strength of carbon steel deteriorates at temperatures above 343°C (650°F). To facilitate system comparisons, the charging and discharging medium was considered to be pressurized liquid water, without a phase change. Therefore, only the sensible heat of the water is available for system charging and heat storage. Because this is basically a feasibility study, no attempt was made at performance and economic optimization, although parametric variations allow an indication of cost trends for different design specifications.

The original steel ingot TES concept consisted of many long square cross-section steel castings with axial holes to provide for heat transfer from a pressurized transport fluid. It was originally thought that such steel ingots with holes could be obtained at 33¢/kg (15¢/lb), which would have provided a cost-attractive system. Thermal stress analysis indicated that the header attachment problem was not insurmountable. Surveys of industrial suppliers of steel products have revealed that such a piece would cost $1.32/kg (60¢/lb), because placing the hole in the ingot is an expensive and difficult process. Therefore, the idea was discarded in favor of a steel "sandwich," consisting of two long 18.3 m (60 ft) steel slabs approximately 1 m (3 ft) wide and 20 cm (8 in) thick. These would be separated by electroslag welded dividers 2.5 cm (1 in) thick which would form a thin but wide channel which would contain pressurized water. Such a unit could be fabricated for 70¢/kg (32¢/lb) and would provide more heat transfer area than the hollow ingot. An improved design was

evolved which could be fabricated as a square from four such slabs. This design provided a large internal cavity which could store appreciable amounts of water, thus allowing the water to contribute to the heat balance and reduce the overall system cost. This four-slab square would also cost 70¢/kg (32¢/lb), but less steel would be needed than for the sandwich because of the water that the structure would contain. Finally, if the square were made into a thick, pressure-bearing steel pipe, less steel would be required, but such pipe would cost $1.32/kg (60¢/lb). Therefore, two concepts have emerged where steel contains pressurized water in a cyclical storage mode and both steel and water contribute to the energy storage; the thick square pipe (@70¢/kg, 32¢/lb) and the thinner cylindrical pipe (@$1.32/kg, 60¢/lb).

The other technique proposed for study was concrete poured around pressure bearing pipes. The pipe matrix would resemble a shell and tube heat exchanger, except the pipes would be spaced every few inches. To charge the system with heat, hot pressurized water would flow through the pipes and heat would diffuse into the concrete. Energy is recovered by passing pressurized cold water through the same pipes. The cold water displaces the hot water already stored in the pipes and becomes heated by the surrounding concrete. Tube spacing determines system performance, but thermal stress analysis showed that concrete would eventually separate from the fluid bearing tubes, causing very high thermal resistances between the concrete and pipes. This condition would severely impair performance. For this reason, concrete was disqualified and replaced by common sand, because with loose sand no stress could occur between the storage medium and pressure containment pipes. Also, sand would be less expensive than concrete, both to procure and handle. The sand would, however, require come kind of containment structure or pit, whereas the concrete unit is self-containing.

Comparing the three candidate concepts mentioned above (the thick square pipe, cylindrical pipe, and sand and pipe), it was found that for a large system with several hours available for charging and discharging (as would be the case for daily cycle in a power plant) the TES system cost divided by the system usable heat capacity for both hollow steel approaches would be about $14/kWhr-t. The sand-pipe system energy cost is closer to $2.60/kWhr-t. Therefore, the steel storage concepts were abandoned and effort was focused on the sand-pipe TSU.

A thermal analysis was conducted on the sand-pipe storage configuration to assess approximate tube spacing requirements consistent with different system performance requirements and also attendant system costs. From the computer outputs, a series of performance curves were generated from which tube spacing versus performance information was obtained. The curves served as inputs for the cost analysis.

SECTION II

SELECTION OF STORAGE CONCEPT

Although two approaches were originally considered as attractive TES candidates, hollow steel ingots and concrete poured around steel pipes, each underwent an evolutionary process forced either by economics or technical considerations. The evolution steps are described along with the rationale for various changes.

A. HOLLOW STEEL INGOT

The original steel-solid TES concept consisted of many long square cross-section steel ingots with axial holes to provide for heat transfer from a transport fluid. One of the potential advantages of steel-solid TES for the intended application is direct contact of the application fluid with the storage medium, obviating the need for intermediate heat transport fluids or heat exchangers. In addition if the storage medium can serve as containment for the transfer fluid, which is generally pressurized, the requirement for a separate container could be eliminated. These desirable attributes lead to the hollow steel ingot TES concept which is conceptualized in Figure 2.1. The TES system is comprised of many steel ingots, each with a hole in the axial direction through which the pressurized water passes. Each ingot functions as a very thick wall pipe capable of high pressure containment. A subsystem of headers and control valves allows the fluid to pass through the ingot bundle in a serpentine path which can be optimized by the operator. Such a stacked ingot system is depicted in Figure 2.1 which features ingots 18 m (60 ft) long with square front cross-section area of 0.092 sq m (one sq ft). The maximum length is chosen from the more limiting of two criteria: the maximum length of a suitable ingot which can be mill fabricated, and the maximum length which can be transported by rail or truck.

It was orginally thought that the steel ingots with holes could be obtained at 33¢/kg (15¢/lb) which would have provided a very cost attractive system. Thermal stress analysis indicated that the header attachment problem was not insurmountable. However, surveys of industrial suppliers of steel products revealed that the steel would cost more and, more significantly, producing a longitudinal hole would be a difficult and expensive process.

A number of methods were investigated for producing the steel storage system ingots (0.3 m x 0.3 m x 18.3 m or 1 ft x 1 ft x 60 ft, plain carbon steel). The methods investigated were: (1) continuously casting the steel, then piercing a circular hole by drawing the bar around a mandrel, (2) "trepanning" a hole down the entire length, and (3) centrifugally casting a large hollow-cored cylinder and either hot or cold working into the rectilinear shape desired.

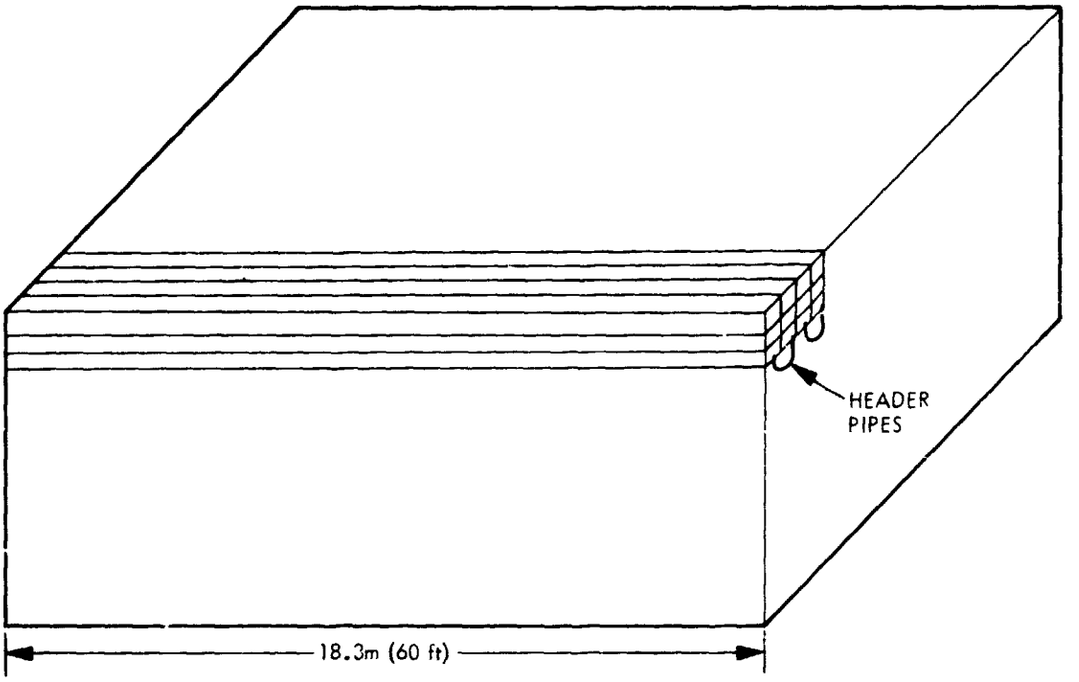

STEEL INGOTS STACKED TO FORM THERMAL STORAGE SYSTEM

(INSULATION, VALVES, WEATHERPROOFING, SENSORS AND OTHER MISCELLANEOUS ITEMS NOT SHOWN)

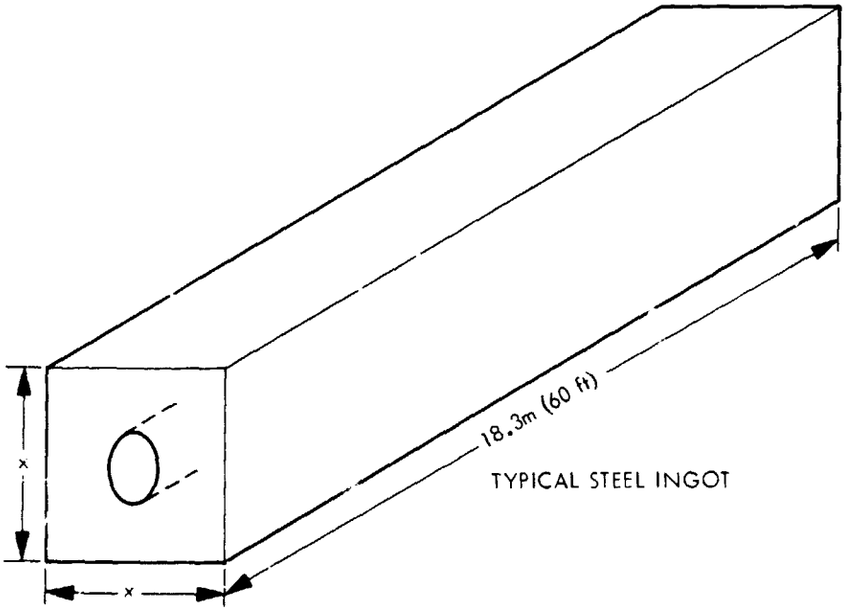

TYPICAL STEEL INGOT

Figure 2.1. Original Concept for Hollow Steel Ingot TSU

The continuous casting/piercing operation was found to be impossible for this application. Carbon steel can be continuously cast, but it is done so that the length is limited to about 6 m (20 ft). Republic Steel indicates that they can cast a 20 cm (8 in) square cross section, but this must be rolled down to a 10 cm (4 in) square to have the mechanical properties of billets produced by other means. The piercing process is designed to produce seamless tubing. The bar stock to be pierced must be round in cross section, since it is carried and rotated on rollers as the stock is drawn around a piercing mandrel. The maximum wall thickness is under 2.5 cm (1 in) because the metal must plastically deform around the mandrel.

Trepanning is a deep hole drilling operation that can be done by many companies providing the length of the workpiece does not exceed about 6 m (20 ft). It was recommended that a "forging quality" billet be used (approximately 46¢/kg = 21¢/lb) which has been stress relieved by annealing or normalizing. Defects in the steel are detrimental to the drilling operation. The ends of the billet must be faced in order to facilitate clamping and to provide a seal for pressurized oil which is used for chip removal. Also, the billet might have to be straightened prior to drilling, depending on the dimensional tolerance of the billet. A 6 m billet could be drilled from both ends if a 3 mm (1/8 in) mismatch of the holes at the center is tolerable. An estimate for this work from the Clark and Wheeler Company in Los Angeles was $2500 for set-up charge and $625 per 6 m unit (6.25¢/lb). Other estimates ran higher, with the combined steel and trepanning costs estimated at around 90-110¢/kg (40-50¢/lb).

Another idea pursued to obtain the necessary steel unit configuration was to take round centrifugally cast steel pipe and roll it into the correct shape. Pipe with O.D.s of 35 cm to 40 cm (14 in or 16 in) can be obtained, but there is restriction of the ratio of the O.D. to the I.D. induced by fabrication techniques, so that a minimum I.D. of about 15 cm (6 in) is available. In addition, the hole must be bored to remove poor quality steel deposited around the interior wall, the result of having to "feed metal" as it solidifies. Under high temperature and pressure this metal could scale and contaminate the piping system. A much more serious drawback is that the process of working the cast pipe into a square section is not an established procedure. Companies exist that can cold work the cast pipe, but the pipe maintains a circular cross section. Working the pipe into a square could conceivably be done but, because none of the companies contacted had done this previously, they were reluctant to supply cost estimates. As a reference, centrifugally cast plain carbon steel pipe costs about 90¢/kg (40¢/lb) with a 35 cm O.D. and 15 cm I.D.

The steel extrusion process, with a hole punched out around a mandrel, can be fabricated by only one steel producer in the United States, Cameron Iron Company in Houston. Cameron stated that such hollow steel ingots would cost approximately $1.30/kg (59¢/lb); this assumes full shop load, maximum number of melts, no chemistry limit, and mass production. Because this appears to be the least expensive way to obtain a long steel ingot with axial hole, the concept

illustrated in Figure 2.1 costs a minimum of $1.30/kg (59¢/lb) for steel, or almost 4 times more than originally expected. Transportation in any case is likely to be 7.7¢/kg (3.5¢/lb) by rail.

B. STEEL SANDWICH PRESSURE CONTAINING TSU

An alternative to the hollow steel ingot is to form a "sandwich" consisting of two thick steel slabs which are spaced apart (by perhaps 2.5 cm) and welded at the edges by an electroslag welding technique (Figure 2.2). Pressurized water flows in the open channel between the two slabs, heating or cooling the steel, Steel billets of at least 9000 kg (10 tons) can be fabricated on the West Coast, and billets of 18000 kg (20 tons) can be made at larger mills in the East. The steel costs, for these larger sizes, are about 44¢/kg (20¢/lb) for plain carbon steel (33¢/kg for smaller sizes). Shipping costs for the steel are about $65/ton (7.2¢/kg).

Welding massive steel plates can be accomplished by electroslag welding. The workpiece is held vertically and the weld is made from bottom to top. Heat is obtained from the resistance of current in an electrically conductive molten flux. Electrodes are continuously fed into a molten pool of slag which is formed between the pieces to be welded. The temperature of the molten pool is sufficient to melt the surfaces of the workpiece. Water cooled copper slides confine the molten metal and slag, and help to solidify the molten metal. The electrodes and slide move upward at a specified rate, thus forming a progressive weld. This process is capable of depositing 136 kg (300 lb) of weld material per man-hour. If the welding were done on a production basis, it is possible that welding could be accomplished at 23-45 kg/man-hr (50-100 lb/man-hr). Kaiser Steel indicated that rates can be computed at approximately $20/man-hr. Therefore, based on 23 kg/man-hr (50 lb/man-hr), the welding would cost 88¢/kg (40¢/lb) of deposited weld material. Parallel square rods would be welded to one slab, prior to joining the two slabs together, in order to hold them in place. This welding as well as the header welding could be accomplished by many U.S. installations.

Several steel companies (U.S. Steel, Kaiser, Republic) were considered in order to get a specific breakdown of the billet costs. For a plain carbon steel billet the breakdown is as follows:

Base Steel Price: approximately 33-35¢/kg (15-16¢/lb). This price appears to be consistent from one steel company to the next.

"Process" charge: includes costs for specific thickness, width, length, quantity, mechanical properties, etc. The estimates ranged from approximately 7.7¢/kg (3.5¢/lb) for a 30 cm by 30 cm by 7.6 m (1 ft x 1 ft x 25 ft) billet, to 11¢/kg (5¢/lb) for a 20 cm by 120 cm by 8.5 m (8 in x 4 ft x 28 ft) billet.

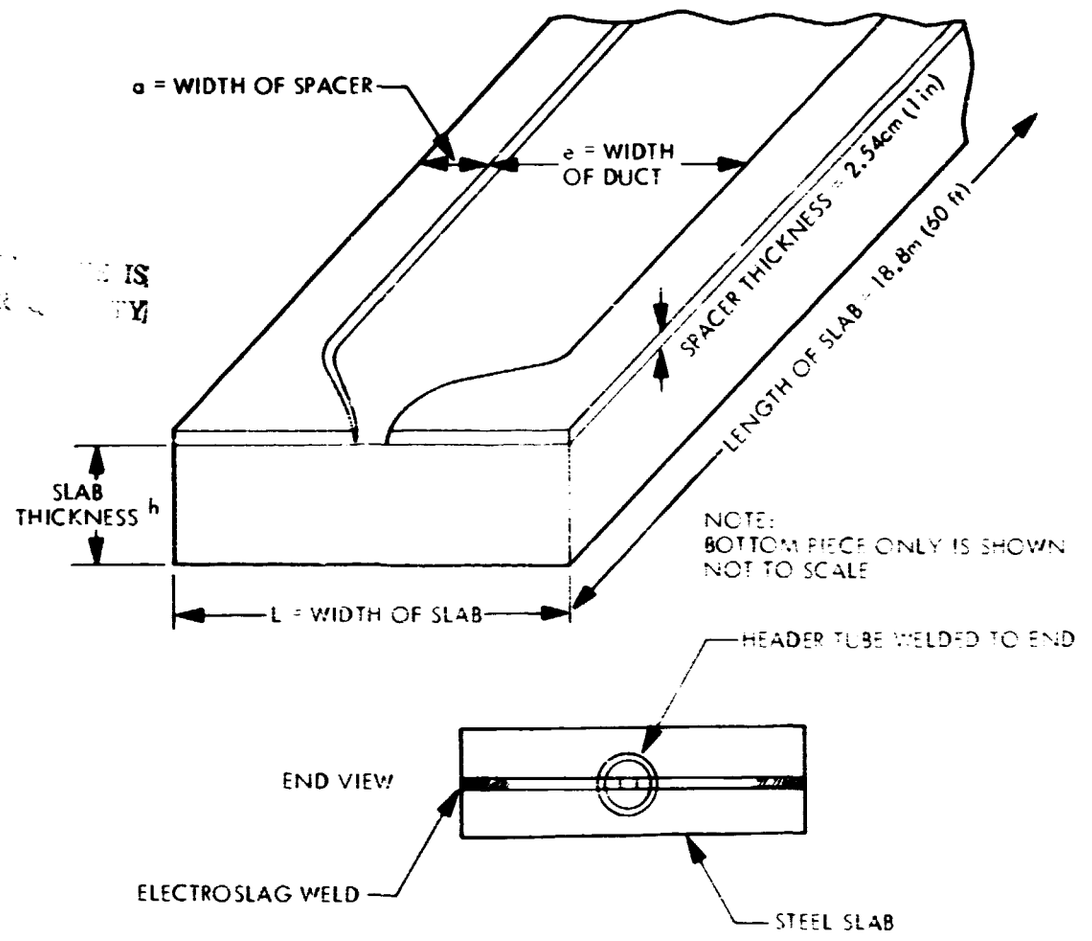

NOTES:
*ESTIMATE COST IS 70.5c/kg (32c/lb)
*FLUID PASSES THROUGH THE DUCT, DIRECTLY CONTACTING STEEL SLAB

Figure 2.2. Electroslag Welded Steel Sandwich TSU with Interior Passage

Shipping charge: for an order of 54000/kg (60 tons) or more, the estimates ranged from 5.5¢/kg (2.5¢/lb) for steel shipped from mills located in the western region shipping to the West Coast, to approximately 8.8¢/kg (4¢/lb) for steel shipped from the East to the West Coast.

The price of steel from foreign countries is generally lower than domestic steel. It appears that, on the West Coast, the cost of Japanese steel is 7-10% lower than the cost of domestic steel, European steel is about 15% lower than domestic, and Korean and Taiwanese steel is about 2[illegible]% lower. The domestic, European, and Japanese steel are of approximately the same quality, while the Korean and Taiwanese steel is somewhat lower in quality.

From the above information, it appears that for the sandwich approach illustrated in Figure 2.2, the cost of each completed unit will be about 70¢/kg (32¢/lb). There does not appear to be any disqualifying fabrication problems. Stress calculations showed that, for carbon steel exposed to a maximum temperature of 371°C (700°F), the slab thickness should be at least 15 cm (6 in) for an internal duct width of 50 cm (20 in) in order to avoid pressure-induced bowing with 13790 kPa (2000 psia) pressure inside the channel. Although the sandwich approach appears to be technically feasible and cost two-thirds as much as the hollow steel ingot, additional investigation showed that other geometries are more cost effective, and so the sandwich concept evolved to the geometry described below.

C. FOUR SLAB SQUARE HOLLOW-STEEL TSU

The steel slab sandwich with a small spacing between the slabs to allow pressurized flow (Figure 2.2) was modified to the square configuration depicted in Figure 2.3. The slabs for the four sides are identical to those in the sandwich, but the addition of a large central area which can contain pressurized water allows a significant reduction in cost of energy storage compared to the sandwich configuration. This is because the liquid water is the transport medium and also serves as part of the storage medium; the water contains a significant portion of the stored heat. Because the water inventory is low in cost, the steel cost of the square ingot system is estimated to cost 67% of the sandwich configuration for a given quantity of heat storage. Furthermore, thermal resistance into and out of the steel is reduced, so the system will respond faster. Pressure drops should be considerably less due to the large flow cross-section. The electroslag weld technique is identical for either the sandwich or hollow TSU, and the fabricated cost of either approach is estimated at 70¢/kg (32¢/lb). For all of these reasons, the sandwich configuration in Figure 2.2 was abandoned in favor of the hollow square configuration in Figure 2.3. At the end of each section, a formed header with square end narrows down to a small circular orifice, which allows for water introduction and extraction. Stacking individual units into a system used the same procedure as previously described for the sandwiches and single piece square ingots.

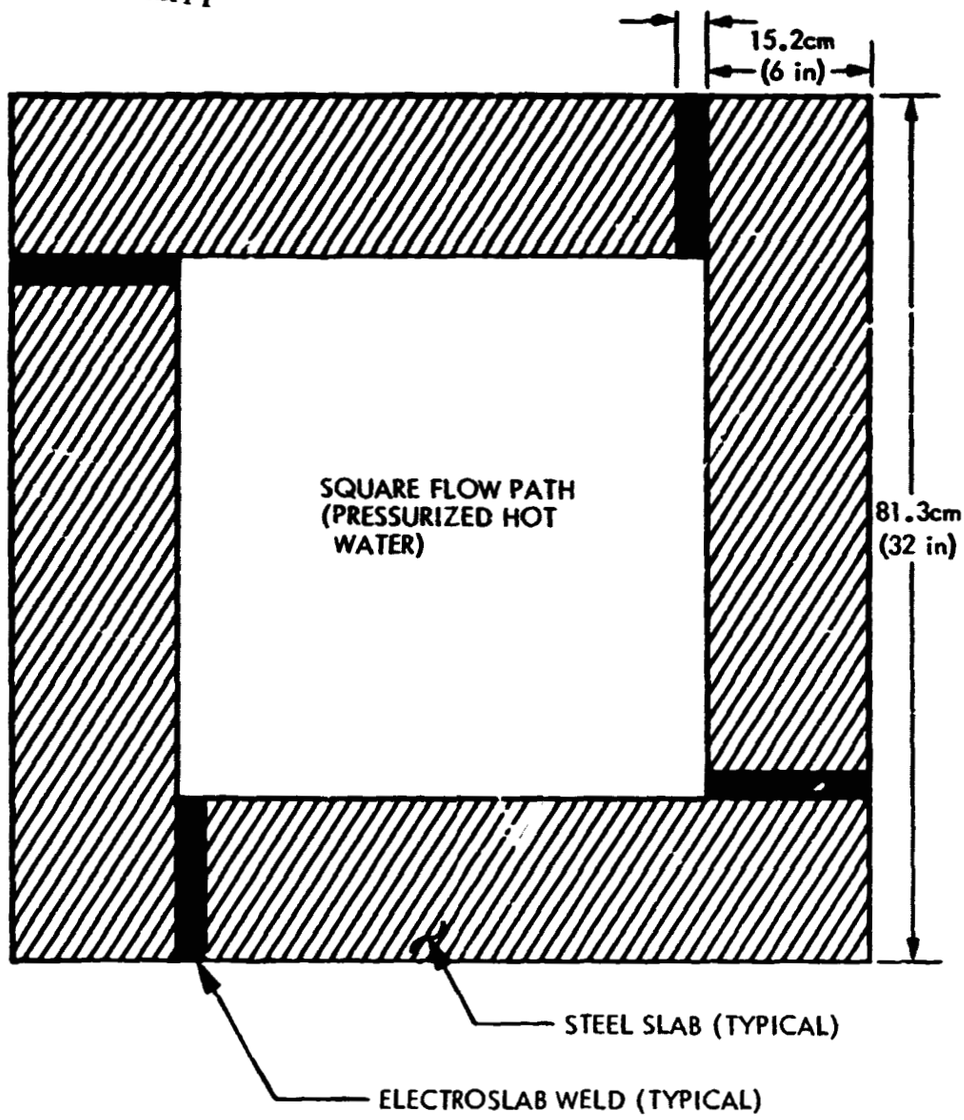

NOTES:

(1) THE DIMENSIONS ARE APPROPRIATE FOR INTERNAL WATER PRESSURE OF 17,235 kPa (2500 psia) AND TEMPERATURE OF 343°C (650°F).

(2) HEADERS WELDED TO ENDS CHANNEL FLOW DOWN TO A SMALL DIAMETER CYLINDRICAL PIPE SHAPE.

(3) PRESSURIZED WATER INSIDE THE SQUARE FLOWPATH STORES AN APPRECIABLE AMOUNT OF THE THERMAL ENERGY.

(4) ESTIMATED COST OF STEEL SYSTEM IS 70.54/kg (32¢/lb), EXCLUSIVE OF HEADERS.

Figure 2.3. Four Slab Square Hollow-Steel TSU

D. THICK WALL PIPE CONTAINING WATER TSU

The slabs which form the welded square configuration in Figure 2.3 must be 15 cm (6 in) thick in order to avoid outward bowing when 13790 kPa (2000 psia) pressure is internally contained. This suggests the idea of using large diameter thick pipes to contain water, because the pipe thickness can be smaller for a circular geometry than for a square geometry. Also, it is relatively simple to design such a pipe to conform to local pressure vessel codes, whereas a sizeable safety factor may have to be introduced if the welded square cross-section configuration were selected. The minimum wall thickness equation for a cylindrical pressure vessel (ASME Boiler and Pressure Vessel Code) and the pipe thickness equation (ANSI - Code for Pressure Piping) are identical. Therefore, the only code that needs to be satisfied is the ANSI code for pressure piping. Calculations using the pipe thickness equation to determine the minimum allowable thickness indicate that, for pressures in the 13790 kPa (2000 psia) range and temperatures less than 343°C (650°F) for carbon steel pipes, the minimum pipe thickness to outer diameter ratio is about 1:10. A 91 cm (36 in) O.D. pipe has a required minimum thickness of 9.1 cm. Because the pipe is relatively thin compared to the square configuration of Figure 2.3, most of the heat will be stored in the water rather than in the steel, so the response time for heat input or extraction will be considerably faster for the circular pipe.

It appears that only six steel mills in the United States can make pipe over 61 cm (24 in) diameter. Babcock and Wilcox uses a piercing and drawing technique, Cameron Steel of Houston uses an extrusion technique, and Tower Iron Works uses the rolled and welded technique. The Babcock and Wilcox Band W process lists a price of $1.32/kg (60¢/lb) based on pipes of A106 seamless carbon steel of 6.7 m (22 ft) length, the longest they can produce, with square ends. Ninety-one cm (36 in) O.D. is the largest in their catalogue, and wall thicknesses are available up to 15.4 nominal cm (6.06 in). Their price includes ultrasonic testing. Rolled ends, which reduce radius, would cost more. The cost of extruded pipe from Cameron is $1.30/kg (59¢/lb); this is the mill price without a middleman markup. The cost of pipe greater than 61 cm (2 ft) diameter and meeting pressure codes is therefore about $1.32/kg (60¢/lb).

E. SAND-PIPE TSU

The original TES study approach was to consider both the hollow steel ingot and also concrete encased pipes. For the hollow steel ingot, it was felt that the relatively high cost steel would allow direct contact between the transport fluid (pressurized water) and the storage medium (steel), while the high thermal diffusivity of steel would allow for fast system response. At the other end of the cost spectrum, for the concrete encased pipes, it was anticipated that inexpensive solid (concrete) could serve as a storage medium if the concrete volume were interpenetrated with pressure-containing pipes.

The tube spacing and, thus, system cost would be dictated by the required heat input and extraction rates. The concrete encased pipe approach underwent a parallel evolution to the steel approach, although the geometry did not change.

A considerable amount of effort was expended on the concrete encased pipe approach, and it was found that concretes exist which can endure up to 510°C (950°F). The cost of the concrete would probably be controlled by transportation costs. Although the thermal expansion coefficients of concrete and steel are similar, a careful thermal stress analysis showed that the concrete would separate from the tubes due to thermal cycling. This tube separation would cause high thermal resistances between the concrete and pipes, which would impair performance to an unacceptable extent. During cooling, the steel pipe will tend to shrink prior to the concrete, placing the concrete in tension. Concrete is very weak in tension, although reasonably strong in compression.

During heating, hoop stresses induced by the steel pipe expansion may give rise to failure in the concrete due to shear stresses. This disqualifying feature of concrete caused its abandonment for this study.

The way to overcome the stress problem inherent in the concrete storage system is to substitute sand for the concrete (Figure 3.1, Section III). With loose sand, stresses between the storage medium and pressure containments do not appear. Due to thermal cycling, the sand will probably settle, thermal performance should improve as voids are eliminated and the sand is more tightly pressed against the pipes, reducing thermal resistance. Sand settling from the top would be filled in with more sand. Also, sand is less expensive than concrete, both to procure and to handle. However, the sand requires some kind of containment structure or pit, whereas the concrete unit does not. The published thermal diffusivity of sand is half that of concrete, so a greater tube density than for concrete is required. The sand storage medium is inexpensive, widely available, probably non-degradable, nonflammable, nontoxic, requires no pressure container and is safe. The only adverse properties appear to be the low thermal diffusivity and the requirement for containment. A possible alternative is to have encapsulated phase change material units, spheres or pipes, mixed in the sand to increase the effective heat capacity and reduce volume and pipe length. But such encapsulation approaches would alter the basic premise of very low storage medium cost, and as such are not considered further in this study.

Because the sand-pipe TSU is described in detail in Section III, a system description is not made here. The system performance is described in Section IV, and the economic performance for different conditions is considered in Section V.

F. SELECTION OF THE APPROPRIATE TSU CONCEPT FOR IN-DEPTH ANALYSIS

To choose the "best" TSU from several candidates depends upon the application and the total system into which it is to be integrated. The application system considered here is a large steam power plant, which can be thermally powered by conventional fossil fuel, a nuclear core or solar input. It is assumed that pressurized water of the required quantity is available both for transferring heat to and from the TSU, and for direct storage. Therefore, the TSU must be capable of containing pressurized water, probably in excess of 14000 kPa (2000 psia) pressure. Also, it is expected that the large TSU will function in a daily cycle, so a few hours of each day are available to charge the system from the heat source, and later the system is discharged over a few hours to augment the heat source in producing power, perhaps by feedwater preheating. The condition for a solar power plant is more severe than for the conventional power plant, because for the solar power plant, the system must be able to drive the prime mover without benefit of an external guaranteed heat source. In each case, it is assumed that pressurized liquid water is available at 315°C (600°F) for charging, and the system can swing through a total temperature cyclic excursion of 222°C (400°F).

Of the five concepts considered above, only three need to be considered for economic attractiveness, for reasons already described. Table 2.1 calculations are presented for two systems, the four-slab square of Figure 2.3 (System 1) and the large thick pipe (System 2). The sand-pipe approach (System 3) is analyzed in detail in Section IV. The economic results, expressed in $/kWhr-t and taken from Tables 4.1 (Section IV) and 4.2 (Section IV) is shown at the bottom line of Table 2.1. Although in Table 2.1 the weight of steel is much greater in System 1 than for System 2, the cost of each system is almost equal, due to lower steel cost for the heavier system. This appears to be coincidental and is due to prevailing steel, processing, and labor rates. In Table 2.1, peripherals such as valving, headers, controls, insulation, foundation, etc., are not considered because the bulk of the cost will be for the steel itself. System 1 stores 59% of heat in the water and 41% must be transferred to and from the steel, whereas System 2 features a 34%/66% water/steel heat storage ratio. Therefore, System 1 will provide a faster system response than System 2. It is stressed that the fluid which transports and stores the heat has an impact on the system economics. If oil were used instead of pressurized water, there would be additional cost factors. Heat exchangers would be necessary and heat capacities would be different resulting in different system sizes, and cost comparisons such as that shown in Table 2.1.

The most significant result from Table 2.1 is the energy cost ($/kWhr-t). For the considered conditions, Systems 1 and 2 cost about the same, $14/kWhr-t, whereas the sand-pipe approach costs about $3/kWhr-t. The result can be anticipated from Table 4.1 (Section IV). The $3/kWhr-t cost for sand-pipe TSU considers the entire system including containment, controls, contigency, etc. This result is not completely unexpected; if the large pipe approach of System 1 had sand

Table 2.1. Comparison of Candidate Concepts

NOTE: All physical parameters are per linear meter.
Water pressure = 2000 psia (13,788 kPa).

Considered Parameter	Square Foot Piece Pipe System 1	Thick Walled Pipe System 2	Sand-Pipe System 3
Volume of steel	(4.34 ft^3/ft) 0.403 m^3/m	(2.48) 0.230 m^3/m	
Weight of steel (ρ_s = 7850 kg/m^3)	(2126 lb/ft) 3100 kg/m	(1216) 1773 kg/m	
Heat stored in steel (C_p = 0.28 Joules/gram dT = 222°C)	(102,000 Btu/ft) 98 kWhr-t/m	(58,400) 56 kWhr-t/m	
Volume of water	(2.78 ft^3/ft) 0.258 m^3/m	(4.59) 0.426 m^3/m	
Weight of water (ρ_w = 913 kg/m^3)	(158 lb/ft) 230 kg/m	(261) 380 kg/m	
Heat stored in water (C_p = 2.6 Joules/gram dT = 222°C)	(69,600 Btu/ft) 67 kWhr-t/m	(114,800) 110 kWhr-t/m	
Heat stored in system	(171,600 Btu/ft) 165 kWhr-t/m	(173,200) 166 kWhr-t/m	
Percent of heat in steel/water	59%/41%	34%/66%	
Cost for steel	($680/ft @ 32¢/lb) $2231/m @ 70¢/kg	($730/ft @ 60¢/lb) $2395/m @ 132¢/kg	
Energy cost	$4.00/10 Btu = $13.66/kWhr-t	$4.22/$10^3$ Btu = $14.41/kWhr-t	Approx $3/kWhr-t

NOTES

System 1 is the four slab square hollow steel TSU formed from four slabs (filled with interior water) (Figure 2.3).

System 2 is a 0.91 m (3 ft) O.D. thick wall circular pipe with wall thickness 8.9 cm (3.5 in) filled with water.

System 3 is the sand-pipe (with water interior) TSU, described and analyzed in following sections.

packed around the outer pipe diameter so that the low cost sand could participate in the heat storage function, then the system cost would naturally be reduced. However, as will be explained in Section IV, although the sand system costs less, the penalty for introducing sand is lowered system response because considerable time is required for heat to diffuse into and out of the sand, which is characterized by a low thermal diffusivity. If immediate system response is not required in all parts of the TSU, as is the case where a 6 hour charge and discharge time may be necessary, then a lower cost system with appropriate response may be suitable. Therefore, Systems 1 and 2 are rejected from further consideration, and the remainder of this study will describe and analyze the sand-pipe TSU approach.

SECTION III

THE SAND-PIPE THERMAL STORAGE UNIT

In Section II the process was described which led to selection of the sand-pipe TES concept as the most cost efficient system from among various candidate approaches for storage. The considered application is storage in a large power plant with charge and discharge times measured in the several hour range. The approach makes use of sand and pressurized water as the storage medium, with pressure containing pipes buried within the sand volume. The pipe intensiveness is equivalent to a large heat exchanger area, so no heat exchanger is required between pressurized fluid which flows within the pipes and the power cycle working fluid (pressurized steam or water). The storage transport fluid is identical with the power plant working cycle fluid. The intention is to use an inexpensive and widely available storage medium (sand and water) and calculate that the cost will not be excessive for placing pressure pipes throughout the sand volume in order to input or extract the heat. It will be shown in Sections IV and V that this is equivalent to low energy-related costs with a relatively moderate power-related cost although sand containment and insulation costs are both energy related. As the system power-to-energy ratio requirement decreases, the concept becomes more attractive, because a lower pipe density is possible. The expected low operation and maintenance expense is a positive feature of the concept.

The desirability of adding metal chips or spines to the sand was briefly considered. This would increase the thermal diffusivity of the solid, which would allow increased tube spacing, and therefore dollar savings. But a preliminary calculation showed that a 50-50 mix of sand and steel chips would increase the sand thermal conductivity (and also the thermal diffusivity) by a factor of two, and the steel chips may be too costly. Therefore, in the interest of keeping the considered system simple, only sand is considred in this study.

One possible design for the sand-pipe TSU is shown in Figure 3.1. The sand, which is above ground and piled to a height consistent with the amount of heat storage desired, is retained on two sides by concrete walls, because concrete appears to offer the least costly method for such containment. The remaining two opposing walls are thin corrugated steel plates. The concrete-steel plate structure is above ground to provide pipe replacement capability. Holes in the steel plate are spaced to align hot water bearing pipes which pass through the sand volume. Header pipes are welded to the pipes just outside the steel retaining wall. Insulation on the top and sides reduces heat loss. Analyses in the next sections indicate that for the considered application pipe diameters should be about 8.9 cm (3.5 in), and spacing distances should be 20 to 25 cm (8 to 10 in). The design consists of two opposing corrugated sheet steel walls 3 mm (1/8 in) thick with holes punched on horizontal centers. The other

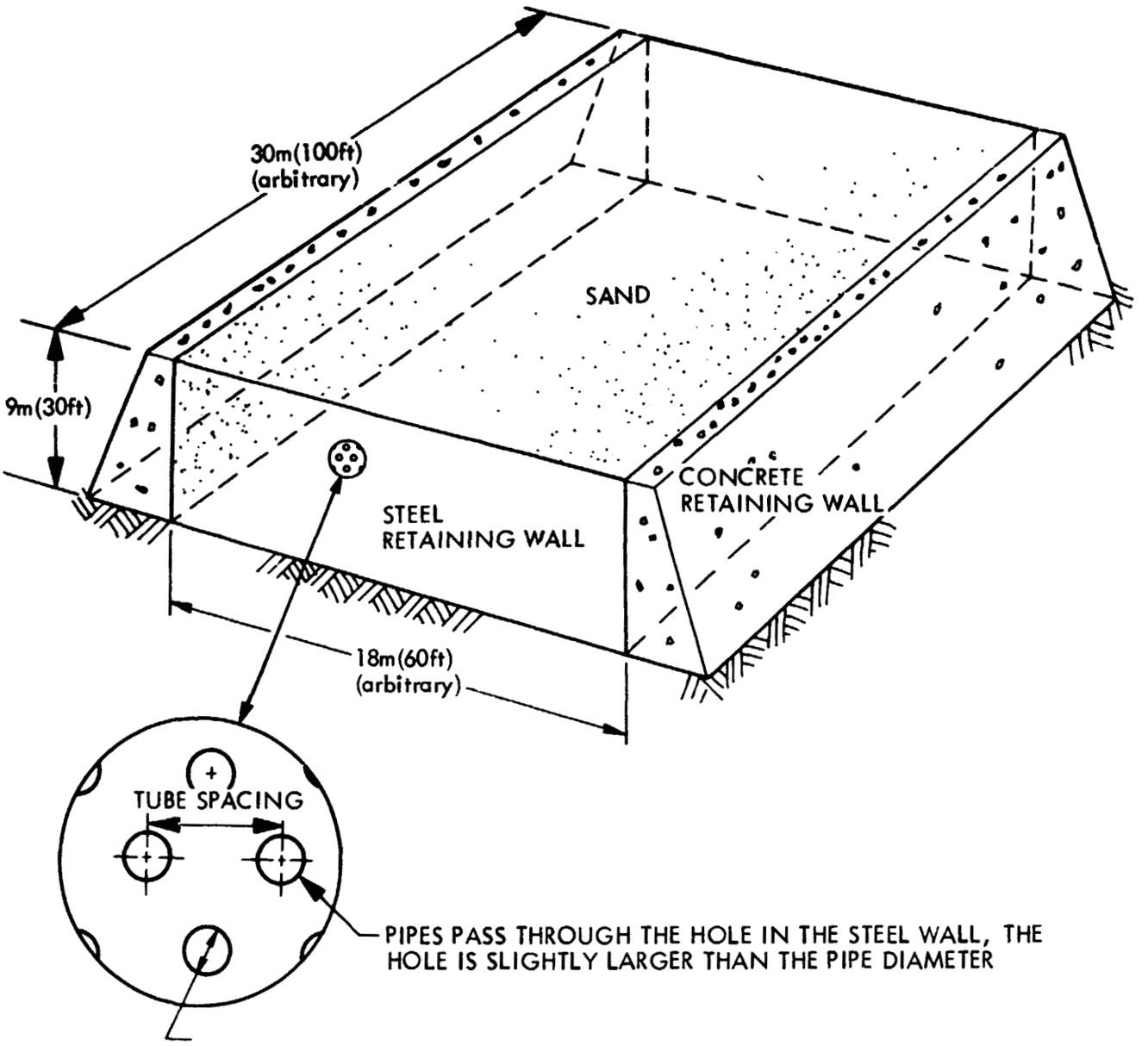

Figure 3.1. Sand-Pipe Thermal Storage Unit Overall Configuration

two walls made of concrete are unspecified as to geometrical details due to their simplicity, and so the design concentrates on the steel retaining walls and their support structure. Load analysis based on maximum bending moment indicates that columns must be placed vertically every 1.5 m (5 ft) to minimize outward bowing of the sheet steel. Because the horizontal pressure on the wall decreases linearly toward the top, alternate columns are designed shorter (6.6 m = 22 ft) as compared to the longer beam columns (9 m = 30 ft, Figure 3.2). Utilizing fundamental stress analysis techniques, the section moduli (cross sectional shape and dimension) of the beam columns are calculated and designed. In addition, tie rods which connect the two steel walls together for beam support are designed considering the maximum applied force at the support points. There are 26 tie rods which restrain the two opposing steel walls from falling outward (Figure 3.2). The tie rods are, as the name implies: rods which tie two beams together on opposing walls for stability against the outward acting hydrostatic pressure of sand. In this sand-pipe thermal storage unit, the concrete walls stand by themselves, although tie rods could also provide increased stability. However, the steel-end wall structures including the column beams need support from within to prevent outward collapse. So the tie rods, which are essentially thick wires, penetrate the sand volume and tie opposing beam columns together to help support the steel wall structure. The tie rods are as long as the distance between the two opposing metal walls and are spaced the same as beam column intervals. The tie rods are calculated to be 3.8 cm (1.5 in) in diameter to contain the sand pressure against the steel walls. The footing is calculated considering the combined load of the I-beams, sheet steel, sand, and pipes. The footing is calculated to be 1.22 m (4 ft) wide and continuous throughout the wall span.

A heat conduction calculation demonstrates the necessity for thermal insulation on the outside of the steel plates. If the heat leakage rate is limited through the insulation to be no more than 1% of the inputted heat rate, 15 cm (6 in) of mineral wood insulation thickness is found to be adequate. A telephone survey given to commercial insulation vendors indicates there is a labor and material cost of $\$1410/m^3$ ($\$40/ft^3$) for mineral wood insulation and weatherproofing. The approximate cost for insulating the steel walls and headers and top is $228,000 for the design considered in Figure 3.1.

In the charging mode, hot pressurized water enters the TSU, and heat is transferred from hot water through the pipe wall where it diffuses through the sand volumes, heating the sand. In the heat extraction mode, cool pressurized water enters the hot system via the same tubes and displaces the hot fluid previously contained. In addition, heat is transferred by conduction from the sand through the pipe wall to the cool fluid. The fluid is heated and is discharged from the module. The pipes serpentine to allow long flow paths, and heat is stored both in the sand and the liquid transport fluid.

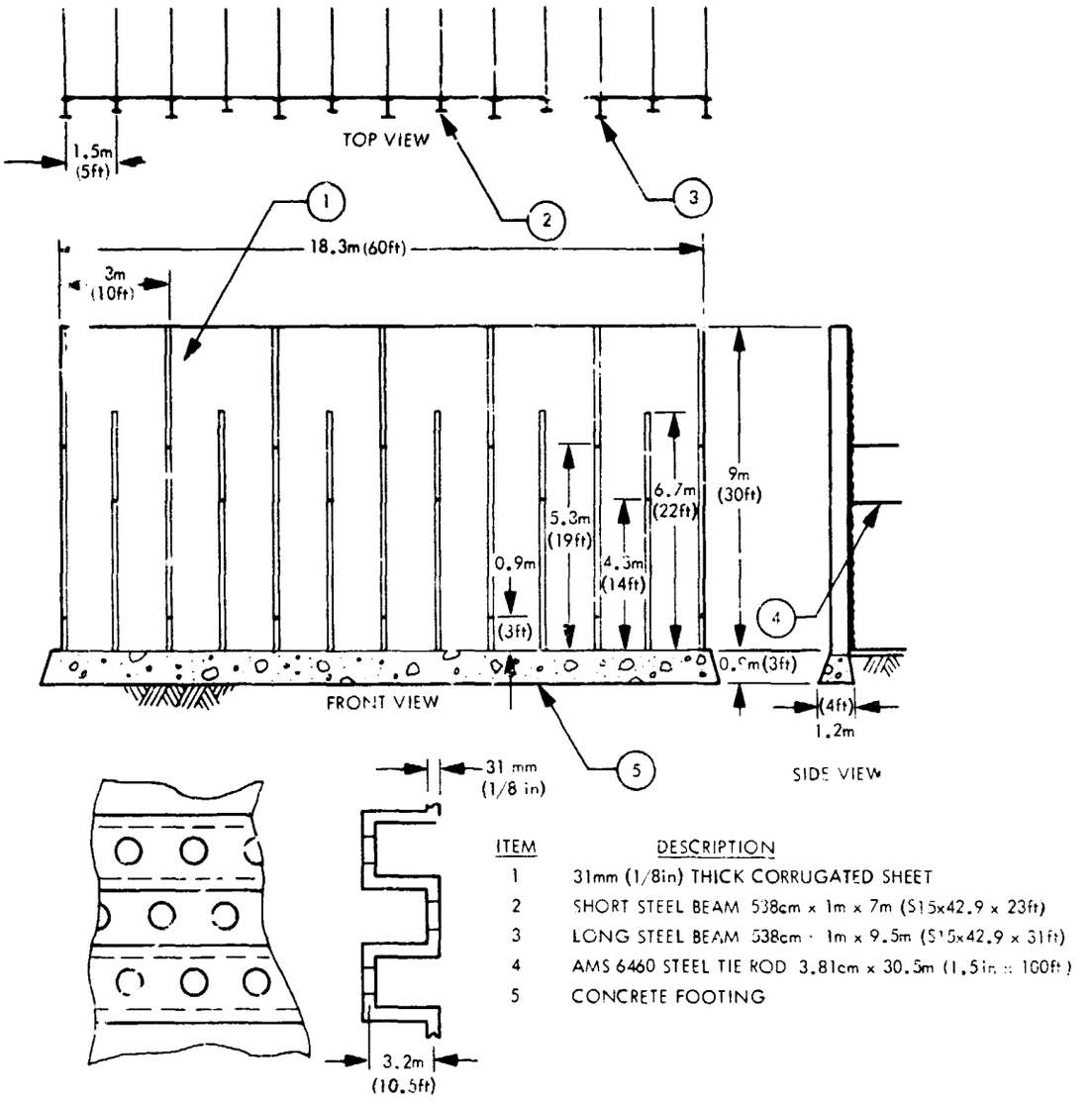

Figure 3.2. Steel Retaining Wall Configuration and Design

A limiting factor in the extraction or input of thermal energy to or from the stationary sand-pipe TSU is the low thermal diffusivity of the storage material, sand. This may mandate a high pipe density, which manifests as a relatively high pipe cost. Because the cost for the sand and accompanying concrete retaining structure, including insulation, is less than the cost of the pipes, the overall system cost is strongly dependent upon tube spacing. Power related costs dominate TSU cost, primarily due to the pipe expense. Power related cost items include pipes and header system, controls, sensors, and valves. Pumps and filters are not considered here as part of the TSU expense because they are already present requirements in any system. However, pump work and pressure drop through the TSU will be evaluated in subsequent calculations because they are vital factors for system integration and operational cost assessment. The energy related costs include sand, containment and insulation. A simple First Law of Thermodynamics type calculation is generally sufficient to size the sand volume, thus essentially resolving the sand and container costs. However, a Second Law type thermal analysis is needed to evaluate the minimum tube spacing or range of spacings which will satisfy the power input and extraction requirements. For example, it may be desired that the total energy from the system be extracted in six hours, which would be consistent with one given tube spacing. A 9 hour cycle would allow a greater tube spacing and a less expensive system. The thermal analysis (presented in Section IV of this report) will evaluate the time temperature history of the storage unit with given specified geometrical parameters (i.e., pipe diameter and centerline spacing between the pipes). A 6 hour cycle is chosen here as a convenient reference point. The temperature distribution as a function of time will indicate whether the tube spacing will satisfy the 6 hour charging/discharging time; if not, other sets of geometrical data input will continue until the criteria is satisfied. The resulting tube spacing will then be used to determine the cost of the pipes and the system. The thermal analysis will be described in the next section and the cost analysis in Section V.

In addition to the costs for sand and pipes, examination of Table 3.1 shows that there will be other energy related TSU costs. The two concrete retaining walls, the two reinforced steel retaining walls with internal tie rods, and insulation and weatherproofing must be installed. Anticipating results from Section IV, the system geometry indicated in Figure 3.1 (5100 m^3 = 180,000 ft^3 of useful storage volume) will store 355 MWhr-t for a 8.9 cm (3.5 in) pipe with 25 cm (10 in) of sand (Case 10 from Table 4.1, Section IV) with 6 hours of charging; for 8 hours the system can store 398 MWhr-t. This would represent 49 flowpaths in parallel, each 1524 m (5000 ft) long.

In Figure 3.1 the area of steel walls, including a multiplication factor of two for the corrugation, is 669 m^2 (7200 ft^2), and for 3 mm (1/8 in) thick wall the steel volume is 2.12 m^3 (75 cu ft), which weighs 17,000 kg (37,500 lbs). The factor of two is probably too great for the corrugation correction but is used here to be conservative (1.5 is probably more practical). It would cost

Table 3.1. TSU Capital Cost

Pipe Diameter = 8.9 cm (3.5 in); Pipe Spacing = 25 cm (10 in)
Pipe and Sand Cost Taken from Case 10 of Table 4.1
Total Pipe Length here is 66 x 1524 m = 100,600 m (330,000 ft)

Item	Type Cost	Cost	Percent of Sub-Total
Pipes and Headers	Power Related	($20,100) (66) = $1,327,000	52.3
Controls and Sensors*	Power Related	Small — Assume 25% of Pipe Cost $332,000	
Valves*	Power Related	Small	13.1
Pipe Spacers*	Power Related	Small	
Power Related Sub-Cost =		$1,659,000	65.4
Sand	Energy Related	($2393) (66) = $158,000	6.2
Steel and Concrete Containment, Insulation, and Weatherproofing	Energy Related	$722,000	28.4
Energy Related Sub-Cost =		$ 880,000	34.6
TSU SUB-TOTAL COST =		$2,539,000	100
Contingency (30% of Subtotal) =		$ 762,000	
TSU TOTAL COST =		$3,301,000	

*Because controls, sensors, valves and pipe spacers are system specific, a close estimate is not available for a general case. Twenty-five percent of pipe cost, or $331,000 provides a safe and conservative (high) approximation.

about $2.2/kg ($1/lb) to purchase and install the steel, so the cost for steel walls is $37,500. The total I-beam length is 433 m (1420 ft), and at 37 kg/m (25 lb/ft) the I-beams weigh 32,500 kg (71,000 lb). At $2.2/kg ($1/lb) for installed cost, the I-beams cost $71,000. There are 26 tie rods, each 30 m (100 ft) long and 3.8 cm (1.5 in) diameter. These weigh 7250 kg (15,950 lb), and at $2.2/kg ($1/lb) cost $16,000. The total cost for the two steel walls is $124,000, as summarized below:

Steel Wall Breakdown

Item	Size or Magnitude	Cost, $
Corrugated Steel	669 m^2 = 17,000 kg (7200 ft^2 = 37,500)	37,000
Reinforcing I-Beams	443 m = 32,500 kg (1420 ft = 71,000 lb)	71,000
Tie Rods	793 m = 7,250 kg (2600 ft = 16,000 lb)	16,000
	Cost for Two Steel Walls	124,000

Assume that the concrete wall is 1.5 m (5 ft) wide at the bottom and 61 cm (2 ft) wide at the top. Then, for 61 m (200 ft) length the volume is 593 m^3 (21,000 ft^3), and at 150 lb/ft^3 for concrete, the wall weight is 1 million kg (2.1 million lb). At 22¢/kg (10¢/lb) to build the concrete wall, it costs $310,000. Note that although the cost for steel wall is around the same as that for concrete wall per linear foot, the concrete wall requires little or no insulation and weatherproofing, and so is less expensive than steel walls. The costs for sand containment and insulation are summarized below:

TSU Costs for Sand Containment, Insulation and Weatherproofing and Geometry Dimensions

Item	Cost
Steel Wall	$124,000
Concrete Wall	$310,000
Insulation and Weatherproofing	$288,000
TOTAL	$722,000

The tabulation shows that for the considered geometry the subtotal cost of the TSU components necessary for sand containment, insulation and weatherproofing amounts to around $722,000, with almost half required for insulation and weatherproofing.

For the internal pipe and sand geometry described by Case 10 of Table 4.1 (Section IV), namely pipe diameter of 8.9 cm (3.5 in) and pipe spacing of 25 cm (10 in), each 1524 m (5000 ft) section can store 5.67 MWhr-t of energy with 6 hours of charging for considered conditions. There are 66 such flow paths which would fit within the containment described in Figure 3.1. The costs of pumps, filters, PH control deaeration, etc. are not assessed against the TSU because they would already be part of the power plant. The costs of installed pipes and headers (from Table 3.1) were obtained from a telephone survey of engineering construction firms. Because controls, sensors, valves and pipe spacers are very system specific, a close estimate is not available for a general case. Therefore, in Table 3.1, these items were assumed to have an installed cost of 25% of the pipe cost, or $331,000, which was to provide a safe and conservative (high) approximation. In Table 3.1, a "contingency factor" of 30% of the subtotal was added as an insurance that this cost estimation exercise is not overly optimistic (on the low side). Part of the contingency figure might be used to provide spare parts stored on site for quick maintenance as necessary.

From Table 3.1 the sand and pipe cost totals $1,485,000 and the total TSU cost is estimated at $3,301,000. Therefore,

$$\frac{\text{TSU Total Cost}}{\text{Pipe and Sand Cost}} = \frac{\$3,301,000}{\$1,485,000} = 2.22$$

In Section IV, various pipe and sand costs will be estimated for different operational conditions and TSU system costs will be estimated by multiplying pipe and sand cost by 2.22. It is recognized that there is an economy to large scale, because the containment costs relate to exterior area; as a system gets larger, the volume increases faster than the area. However, using this factor should give a reasonable estimate of the total TSU cost for the requirements of an engineering screening concept study.

Various TSU economic parameters of interest are C_p (capital cost of power related equipment in $/kW), C_E (Capital Cost of Energy related equipment in $/kWhr) and C_T (total TSU capital cost in $/kW). The above quantities are related by

$$C_T = C_P + C_E\, t \qquad (3.1)$$

where t is the rated TSU hours of storage capacity. To use the Equation 3.1, it is necessary to separate the total TSU system cost into power related items and energy related items. These parameters will be discussed in Section V. To calculate C_p, the percentage of the total TSU cost is needed which is spent for power related cost . For C_E the fraction required for energy related costs is needed. From Table 3.1 before contingency, 65% of total TSU cost is power related and 35% is energy related. Contingency will probably be

directed more towards power related items than energy related items. Therefore, another rule of thumb which will be used in the estimate of the next section is that power related costs are double the costs of energy related costs (power costs = 2/3 of total; energy costs = 1/3 of total).

SECTION IV

THERMAL ANALYSIS AND PRELIMINARY ECONOMICS

Figure 4.1 shows some of the modeling assumptions employed in the thermal analysis. Adjacent tubes are staggered in a hexagonal arrangement when viewed from the end, although for analytical purposes, the hexagonal zone of thermal influence is approximated by a cylindrical zone surrounding the pipe. The unsteady state heat conduction equation in cylindrical coordinates is used with the appropriate boundary conditions to evaluate the time/temperature distribution in the cylindrical section as a function of radial and axial distance. Axial (along the tube) conduction effects are neglected, as heat diffusion predominates in the radial direction. As the fluid moves along the pipe, it loses (or gains) heat to (or from) the surrounding sand. Thus, the fluid temperature decreases (or increases) from its original input valve as the fluid moves along in the pipe. To account for this, a First Law calculation (a heat balance between the fluid and the solid) is made at short intervals to continually show the effects of decreasing fluid temperature. Equation 4.1 is the numerical analog solution to the transient heat conduction problem in the radial direction. The finite difference technique leading to Equation 4.1 is described in Appendix A.

$$T_\eta^{m+1} = 1/2\ T_{\eta+1}^{\ m}\ (1 + \frac{r}{2r_\eta}) + T_{\eta-1}^{\ m}(1 - \frac{r}{2r_\eta}) \qquad (4.1)$$

where,

the superscripts refer to time step

the subscripts refer to space step (radial)

T = temperature, r = radial distance from axial centerline

The geometry for this finite differencing scheme is shown in Figure 4.2. Equation 4.1 is used to generate the temperature distribution for a given radial location at each time step from previous time step information and boundary conditions. Once the distribution is calculated, the revised fluid temperature is calculated from

$$T_{fluid,\ \eta+1} = T_{fluid,\eta} - T_{axial}$$

where T_{axial} is calculated from the heat balance on the axial element x for a time step t. The next axial element will then have the fluid running through it with a different temperature, which changes for every time step, and the process is repeated until the entire length of the storage unit is transversed. Some key parameters for the cylindrical section analyzed are shown in Figure 4.3. A crucial aspect of the thermal analysis is the application of

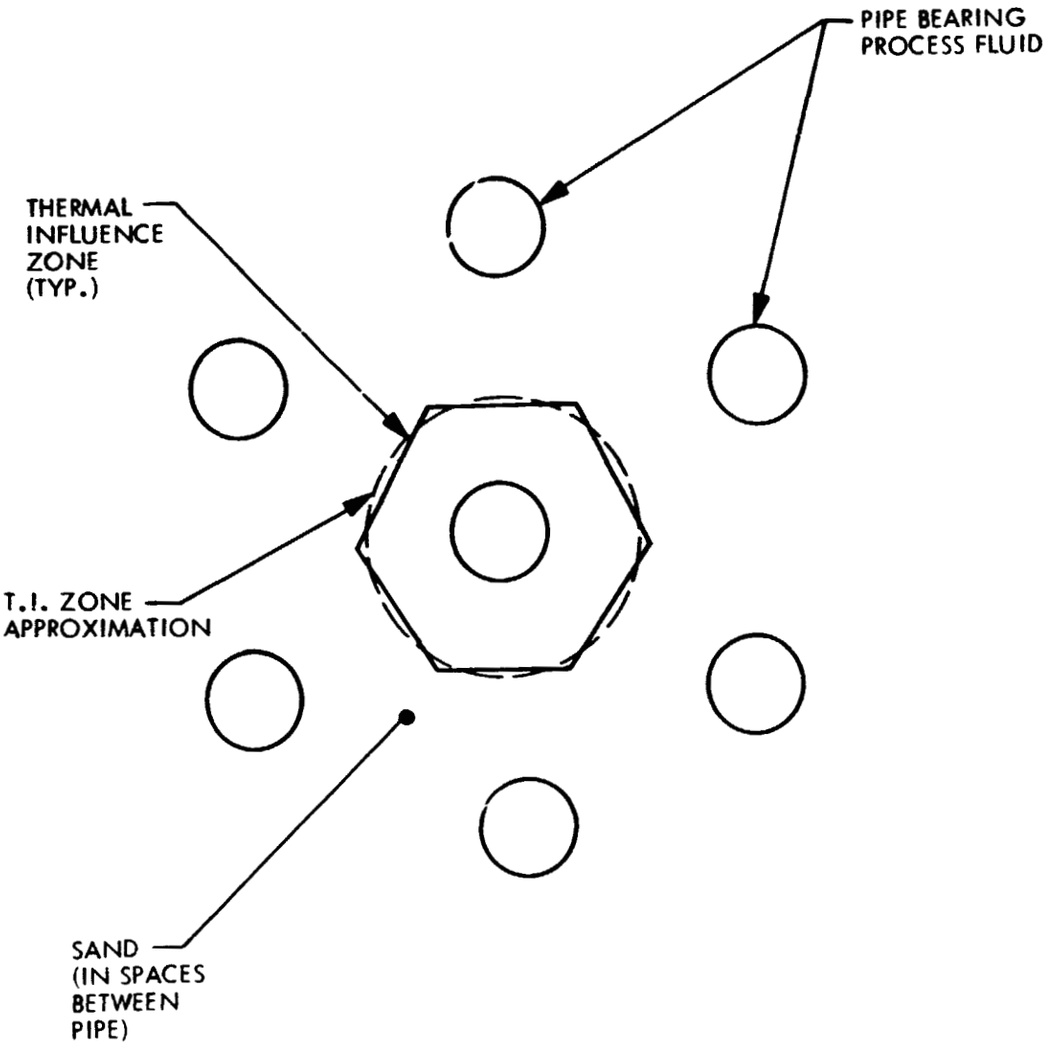

Figure 4.1. Zone of Thermal Influence (Actual and Approximate) and Pipe/Sand Matrix

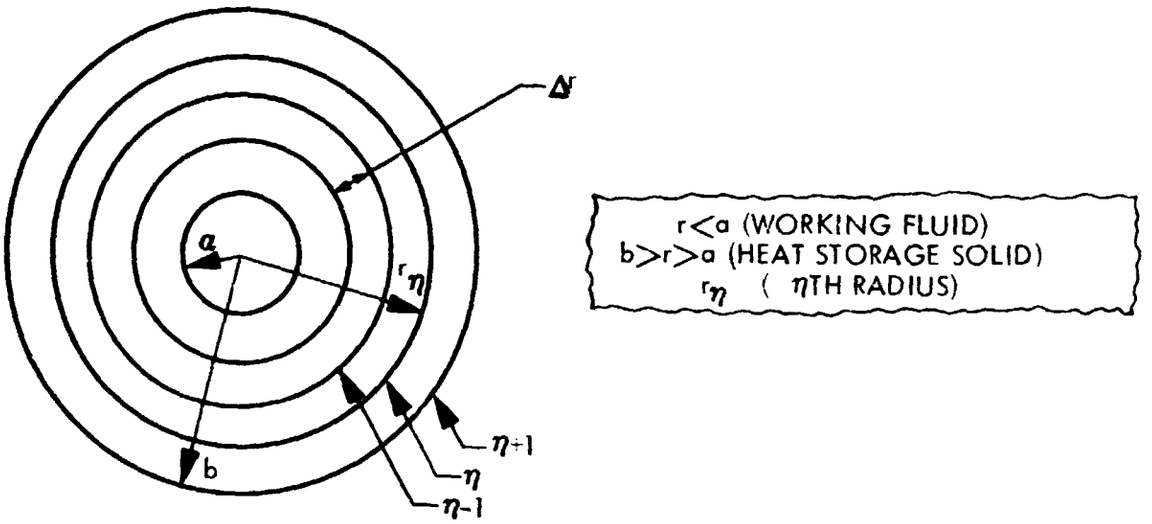

Figure 4.2. Finite Difference Geometry (Cross-Section)

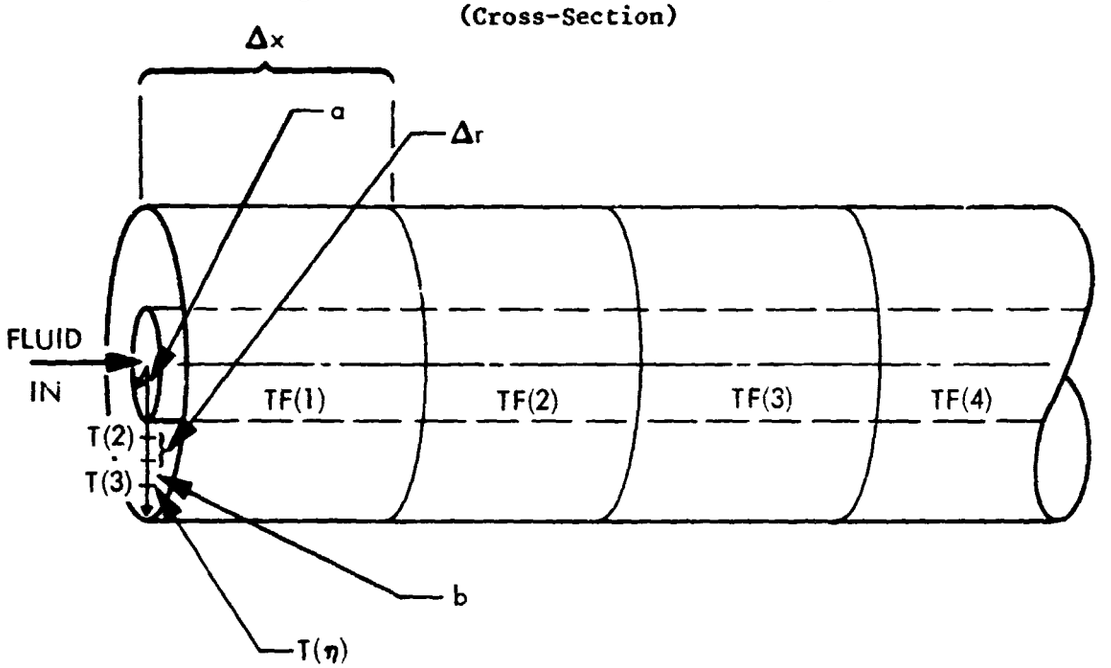

TF ( ) - FLUID TEMP. ARRAY
T ( ) - SOLID TEMP. ARRAY
Δr - RADIAL STEP
Δx - AXIAL STEP
a - PIPE RADIUS
b - THERMAL ZONE RADIUS
η - ηTH RADIAL STEP

Figure 4.3. Finite Difference Geometry (Side View)

appropriate boundary conditions to the considered problem. Consider the fluid running through the pipes. By convection, heat is transferred from the fluid to the pipe wall. The pipe, being relatively thin and having a high thermal conductivity, offers a negligible heat transfer resistence and is considered to be at a single wall temperature. Heat is transferred within the sand by conduction. The pressure of the sand against the pipes promotes heat transfer between sand and pipes at the interface.

The boundary condition which related to zero flux at the outer wall (system symmetry) is

$$\frac{\gamma T}{\gamma r}_{r=b} = 0 \qquad \text{where } b = \text{thermal influence radius}$$

which can be represented simply as

$$T_{\eta+1} = T_{\eta} \tag{4.2}$$

The initial condition necessary for the bounding of the differential equation is

$$T \text{ (time zero)} = F(x) \tag{4.3}$$

In the computer runs, F(x) was taken to be zero, corresponding to a system initially at a total discharge state.

By formulating the problem so that Equation 4.1 can be used, which places a restriction on the value of the time step, it is possible to calculate all temperatures for the next time step from those of the present time step, except for the surface temperature T_1; the new temperature at r = b is determined from Equation 4.2. The difference between old and new temperatures is a measure of heat which has conducted into the solid during a considered time step at a given axial location. Thus, the heat which has been conducted in is known, except for the first radial element which has the unknown surface temperature T_1. T_1 is related to T_{fluid} at that location and for the next time step both are unknown, although they are mathematically related and can be solved simultaneously. The heat stored in a cylindrical element at any considered time is

$$Q = \frac{\pi}{2} \rho_{sand} C_{p\ sand}\, \Delta X i{=}1 \left(r_{i+1}^2 - r_i^2\right) \left[T_{i+1}^{New} + T_i^{New} - T_{i+1}^{Old} - T_i^{Old}\right] \tag{4.4}$$

$$= K_1 T_1^{New} + K_2$$

where the subscripted variables can be recognized by inspection of Figure 4.3. The conduction heat rate in Equation 4.4 is equated to fluid heat lost during the time step.

Volume heat-capacity average integrated temperatures were calculated for the solid, and also for the solid plus the flowing fluid to indicate the state of the charge of the system. Rather than defining a criterion such as the time required to have location (r,x) be at a temperature T(r,x) = 0.5 (nondimensional temperature where 1.0 is the maximum temperature), a single volumetric heat capacity weighted temperature $\bar{T}$ which represents the entire storage unit was found to be more useful. Appendix B gives the details of the derivation. The result is

$$\bar{T} = \frac{\rho_{sand} (B^2 - A^2) C_{p_{sand}} \bar{T}_s + \rho_{water} A^2 C_{p_{water}} T_{water}}{(B^2 - A^2) \rho_{sand} C_{p_{sand}} + A^2 \rho_{water} C_{p_{water}}} \qquad (4.5)$$

where

A = pipe radius

B = sand equivalent thermal influence radius

ρ = density

C_p = heat capacity

with $\bar{T}_s$ defined as

$$\bar{T}_s = \frac{\frac{1}{2}T_1 (r_1 + \frac{1}{4}\Delta r) + T_2 r_2 + \ldots + T_I r_I + \ldots + \frac{1}{2}T_N (r_N - \frac{1}{4}\Delta r)}{\frac{1}{2}r_1 + r_2 + r_3 + \ldots + r_I + \ldots + \frac{1}{2}r_N}$$

where

T_I = temperature at points within solid

r_I = radii

$\bar{T}_s$ = volume weighted average solid temperature

Δr = radial space step; all r are equal

A. COMPUTER CODE

The thermal analysis described above was coded in FORTRAN and exercised on a digital computer for input parameters of interest. The listing is given as Appendix C. The variable names for the inputs are documented in the comments to the code as part of Appendix C. The code will briefly be described here. After inputting the solid and fluid properties and inputting the physical geometry and fluid flow conditions as well as the finite differencing parameters, internal constants are calculated and the temperature arrays are initialized.

Then, for each time step the radial temperature distribution is calculated along with the heat transferred, fluid temperature drop, and total heat to system transferred since time zero. The volumetric heat capacity weighted temperatures are also calculated in the main loop for each time step. The program continues until a specified time limit (which orginally inputted) is reached. At each time step the temperature distribution and the volume weighted temperatures are printed.

The computer code was checked for correctness and accuracy by comparing the temperature output distribution with a Schmidt plot (graphical heat transfer conduction analysis) for the constant temperature fluid boundary case. A check through of about thirty time steps showed agreement between the plot and the program output. The first axial space grid, which always "sees" a constant fluid temperature, checked with the appropriate transient conduction solution given in the literature.

B. THERMAL ANALYSIS RESULTS

The results of the thermal analysis are now described for a sand heat storage system. For purposes of generality and ease of discussion, an excess temperature difference ratio T is generally used instead of the actual temperature; thus

$$T = \frac{Temp - T_{min}}{T_{max} - T_{min}} \qquad (4.6)$$

where

T = excess temperature difference ratio $\quad 0 \leq T \leq 1.0$

$Temp$ = local temperature at a given location and time (^{o}F)

T_{min} = minimum possible system temperature corresponding to discharged state (^{o}F)

T_{max} = maximum temperature of charging fluid, and so maximum potential system charge temperature (^{o}F)

The advantage of using T instead of Temp to describe local conditions is that T can only vary between zero and unity, which allows easier presentation of results. Hereafter, T is referred to as "temperature" unless otherwise specified. The analysis considers in every case the initial condition where the entire sand-pipe system is in a state of total discharge (T = 0 everywhere). At time equal to zero, pressurized hot water enters the system at location x = 0, displacing cold water, and allowing heat to conduct into the sand. Temperature-time histories for different tube diameter and tube spacing conditions are plotted against axial locations. The

volume-weighted average solid temperature at each axial point is computed along with the fluid temperature distribution. A system state of charge is also defined as the arithmetic average temperature of the volume weighted temperatures at all axial locations. This state of charge parameter is used along with fluid distribution to determine which candidate systems (in terms of pipe diameter and centerline spacing) have better technical and economic performance potential relative to each other for various requirements. The curves presented below could just as well refer to a discharging system, originally at T = 1 everywhere (through which fluid flows at incoming temperature T = 0) by inverting the temperature scale in the figures (i.e., replacing T = 0 by T = 1, and T = 1 by T = 0).

The physical and system properties used in the computer analysis are listed below:

$T_{water\ in}$ = 315°C (600°F), the inlet water temperature

$T_{initial}$ = 93°C (200°F), the initial solid temperature

Fluid Density = 913 kg/m^3 (57 lb/ft^3)

Fluid Specific Heat = 4.61 kJ/kg°C (1.1 Btu/lb-°F)

Fluid viscosity = 1.875 x 10^{-6} kg/m-sec (1.26 x 10^{-6} lb/ft-sec)

Solid (sand) density = 160 kg/m^3 (100 lb/ft^3)

Solid Thermal Conductivity = 0.346 w/m-°C (0.20 Btu/hr-ft-°F)

Solid Thermal Diffusivity = 9.29 x 10^{-4} m^2/hr (0.01 ft^2/hr)

It is recognized that fluid properties change as the pressure on the fluid increases. The specific heat of water in particular increases as the pressure increases. The intention of having 222°C (400°F) maximum temperature drop is to estimate absolute heat input rates for a given system. Also, the maximum water temperature could increase to above 315°C (600°F) by increasing the pressure. Furthermore, there is no restriction to using water inside the pressurized pipes; steam could condense to provide the heat at a near constant elevated temperature if this were attractive from systemical considerations. Because the total storage system charge potential is proportional to the overall temperature swing potential, if a difference greater that 222°C (400°F) had been considered, then the system economics which will be described below would have been proportionally improved and vice versa. The calculations and results describe one way that the sand and water storage device could work, and assumptions tended to be conservative (leading to a less advantageous economic result). Other charge and discharge strategies might lead to improved economic performance over that indicated by passing pressurized water through the system and arbitrarily setting a 222°C (400°F) temperature swing potential.

The difference between the systems considered here arise from differences in tube diameter and tube centerline spacing. As expected, a larger pipe costs more that a smaller pipe, but contains more water and provides more heat transfer surface. Also, for a given tube diameter, greater distance between tube centerlines (see Figure 4.1) results in longer charge times and more sluggish system response, but lower system cost. Table 4.1 indicates the parametric analysis that was done for ten cases at flow velocity of 0.3 m/sec (1 fps) representing a range of tube outer diameters 3.8 cm to 8.9 cm (1.5 in to 3.5 in) and tube spacings 10 cm to 25 cm (4 in to 10 in). Cases 11 and 12 consider flow velocities of 0.9 m/sec (3 fps) and 3 m/sec (10 fps), respectively, for the Case 8 geometry. In every case, a 100% charge would represent a total system cycled swing of 222°C (400°F) average temperature difference between a totally charged and discharged condition. Table 4.1 also summarizes the results of the calculations, which will be described.

The system states of charge versus time for various conditions are indicated in Figures 4.4 through 4.6, where in each case a flow length of 1530 m (5000 ft) is considered, and a total temperature swing of 222°C (400°F) would constitute a totally charged system. A typical interpretation is afforded by consideration of Figure 4.4, which features a pipe outer diameter of 3.8 cm (1.5 in) and pipe centerline spacings of 10 cm, 15 cm, and 20 cm (4 in, 6 in, and 8 in). After 8 hours (480 minutes) of charging the 1530 m (5000 ft) long system, initially at temperature T = 0 but heated by pressurized water at T = 1, the 10 cm (4 in) spaced system (Case 1) has attained a 100% charge while the 15 cm (6 in) spaced system (Case 2 has a 75.5% charge and the 20 cm (8 in) spaced system (Case 3) has accepted only 50% of its maximum possible charge. The total energy potential charge in MWhr-t for each curve is idicated in parentheses by each curve. For a cylindrical water column with diameter 3.8 cm and length 1530 m, pressurized to 13.8 MPa or 13,790 kPa (2000 psia), changing the temperature 222°C (400°F) stores around 0.44 MWhr-t of heat, and this value is common to each of the three curves in Figure 4.4 (Cases 1, 2, and 3 in Table 4.1). For the 10 cm (4 in) sand annulus, an additional 0.88 MWhr-t can be stored, bringing the total storage potential to 1.32 MWhr-t as indicated in parentheses by the D_o = 10 cm (4 in) curve in Figure 4.4. Larger sand annuli naturally have greater heat capacity, resulting in a less expensive system. However, Figure 4.4 clearly shows that the larger tube spacing distances are associated with longer times to achieve charging, and so some tradeoffs of technical efficiency versus dollar investment become obvious.

If an infinite amount of time is available to charge a system with a pipe diameter of 3.8 cm (1.5 in), then nearly twice as much pipe length (actually 2.578/1.324 = 1.95 times as much) would have to be provided for the 10 cm (4 in) spacing case (Case 1) as for the 15 cm (6 in) case (Case 2) to store a given quantity of heat. Because the majority of the TSU system cost is for the pipes (as is shown in Table 4.1), one might expect the closer spaced system to cost approximately twice as much. However, if there is insufficient time for the system to accept 100% charge, then the system chargeability

Case	D_i Tube Dia. cm (in)	D_o Spacing Between Tubes cm (in)	V Fluid Vel. in Tubes m/sec (fps)	Q_S Heat Storable in Sand kWhr-t (Btu/10^6)	Q_F Heat Storable in Fluid kWhr-t (Btu/10^6)	Q_{total} Heat Storable in TSU System $/kWhr-t kWhr-t (Btu x 10^6)	% Heat Storable in Sand	Pi Inst Co $
1	3.8 (1.5)	10 (4)	0.30 (1.0)	885 (3.02)	439 (1.50)	1324 (4.52)	67%	$ 7,
2	3.8 (1.5)	15 (6)	0.30 (1.0)	2139 (7.30)	439 (1.50)	2578 (8.79)	83%	$ 7,
3	3.8 (1.5)	20 (8)	0.30 (1.0)	3855 (13.16)	439 (1.50)	4294 (14.65)	90%	$ 7,
4	6.3 (2.5)	10 (4)	0.30 (1.0)	630 (2.15)	1242 (4.24)	1875 (6.39)	34%	$13,
5	6.3 (2.5)	15 (6)	0.30 (1.0)	1886 (6.44)	1242 (4.24)	3128 (10.67)	60%	$13,
6	6.3 (2.5)	20 (8)	0.30 (1.0)	3614 (12.34)	1242 (4.24)	4856 (16.57)	74%	$13,
7	6.3 (2.5)	25 (10)	0.30 (1.0)	5884 (20.09)	1242 (4.24)	7126 (24.31)	83%	$13,
8	8.9 (3.5)	15 (6)	0.30 (1.0)	1513 (5.17)	2450 (8.36)	3963 (13.52)	38%	$20,
9	8.9 (3.5)	20 (8)	0.30 (1.0)	3307 (11.29)	2449 (8.36)	5756 (19.64)	57%	$20,
10	8.9 (3.5)	25 (10)	0.30 (1.0)	5447 (18.70)	2449 (8.36)	7926 (27.06)	69%	$20,
11	8.9 (3.5)	25 (10)	0.90 (3.0)	3307 (11.29)	2449 (8.36)	5756 (19.64)	57%	$20,
12	8.9 (3.5)	25 (10)	3.0 (10)	3307 (11.29)	2449 (8.36)	5756 (19.64)	57%	$20,

*3.8 cm (1.5 in) installed pipe costs $5.02/m ($1.53/ft)
6.35 cm (2.5 in) installed pipe costs $8.60/m ($8.62/ft)
8.9 cm (3.5 in) installed pipe costs $13.19/m ($4.02/ft)

**TSU system cost is 2.22 times pipe and
***Energy Cost Ratio (C_E) = 1/3 (TSU Syst
See Section III for discussion of 1/3

% Heat orable in Sand	Pipe Installed* Cost $	Sand Cost @ 20/m $	Pipe and Sand Cost $	TSU System Cost** $	$/kWhr-t Cost if 100% Charge***	% Charge 6 hr.	$/kWhr-t 6 hr	% Charge 8 hr	$/kWhr-t 8 hr
67%	$ 7,650	$ 375	$ 8,025	$17,816	4.49	96%	4.67	100%	4.49
83%	$ 7,650	$ 920	$ 8,570	$19,025	2.46	63%	3.90	75.5%	3.26
90%	$ 7,650	$1,684	$ 9,334	$20,721	1.61	40%	4.03	50%	3.22
34%	$13,100	$ 266	$13,366	$29,673	5.28	100%	5.28	100%	5.28
60%	$13,100	$ 811	$13,911	$30,882	3.29	97%	3.50	98%	3.56
74%	$13,100	$1,575	$14,675	$32,579	2.24	71%	3.15	81%	2.77
83%	$13,100	$2,557	$15,657	$34,759	1.63	51%	3.20	60.5%	2.69
38%	$20,100	$ 648	$20,748	$46,061	3.87	100%	3.87	100%	3.87
57%	$20,100	$1,411	$21,511	$47,754	2.77	90%	3.08	95.6%	2.89
69%	$20,100	$2,393	$22,493	$49,934	2.10	71.5%	2.94	80%	2.63
57%	$20,100	$1,411	$21,511	$ 7,75[illegible]	2.77	96.5%	2.87	99%	2.80
57%	$20,100	$1,411	$21,511	$47,754	2.77	98%	2.83	100%	2.77

2.22 times pipe and sand cost (see Section III)

C_E) = 1/3 (TSU System Cost)/Heat Storage Capability; discussion of 1/3 factor.

Table 4.1. Sand-Pipe TSU System, Parametric, Cost and Performance Data

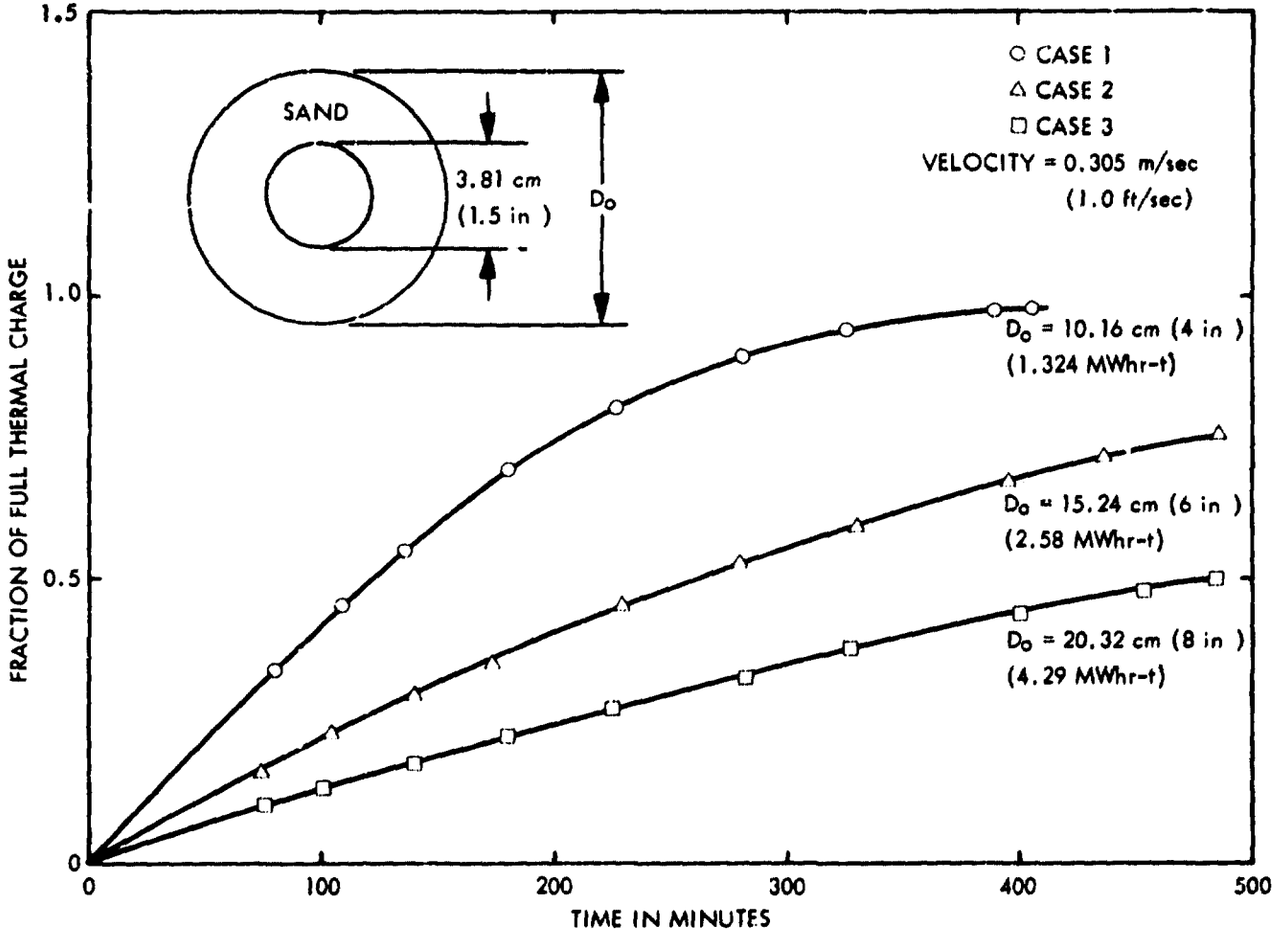

Figure 4.4. Thermal Charge vs Time: I.D. = 3.8 cm

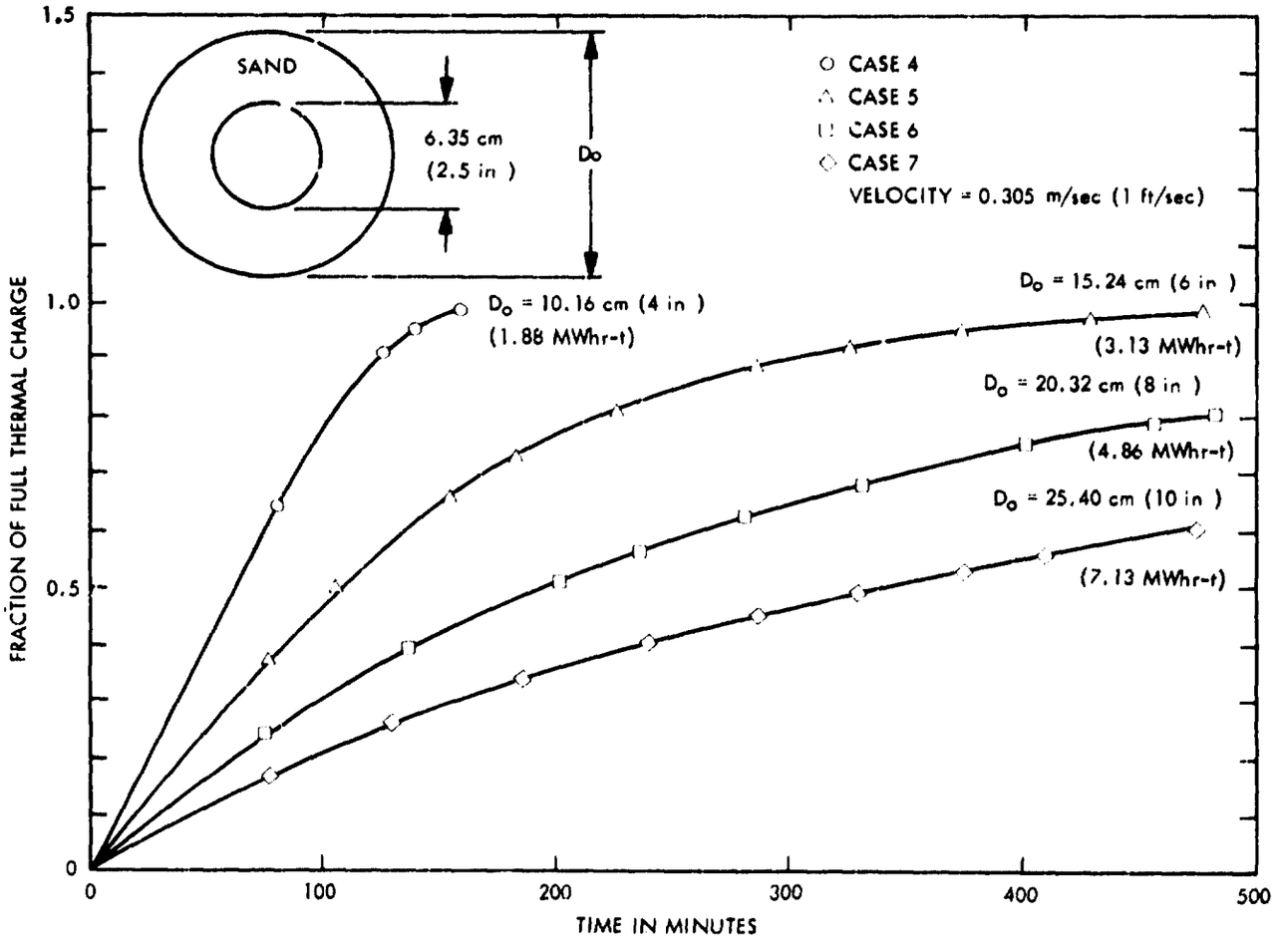

Figure 4.5. Thermal Charge vs Time: I.D. = 6.35 cm

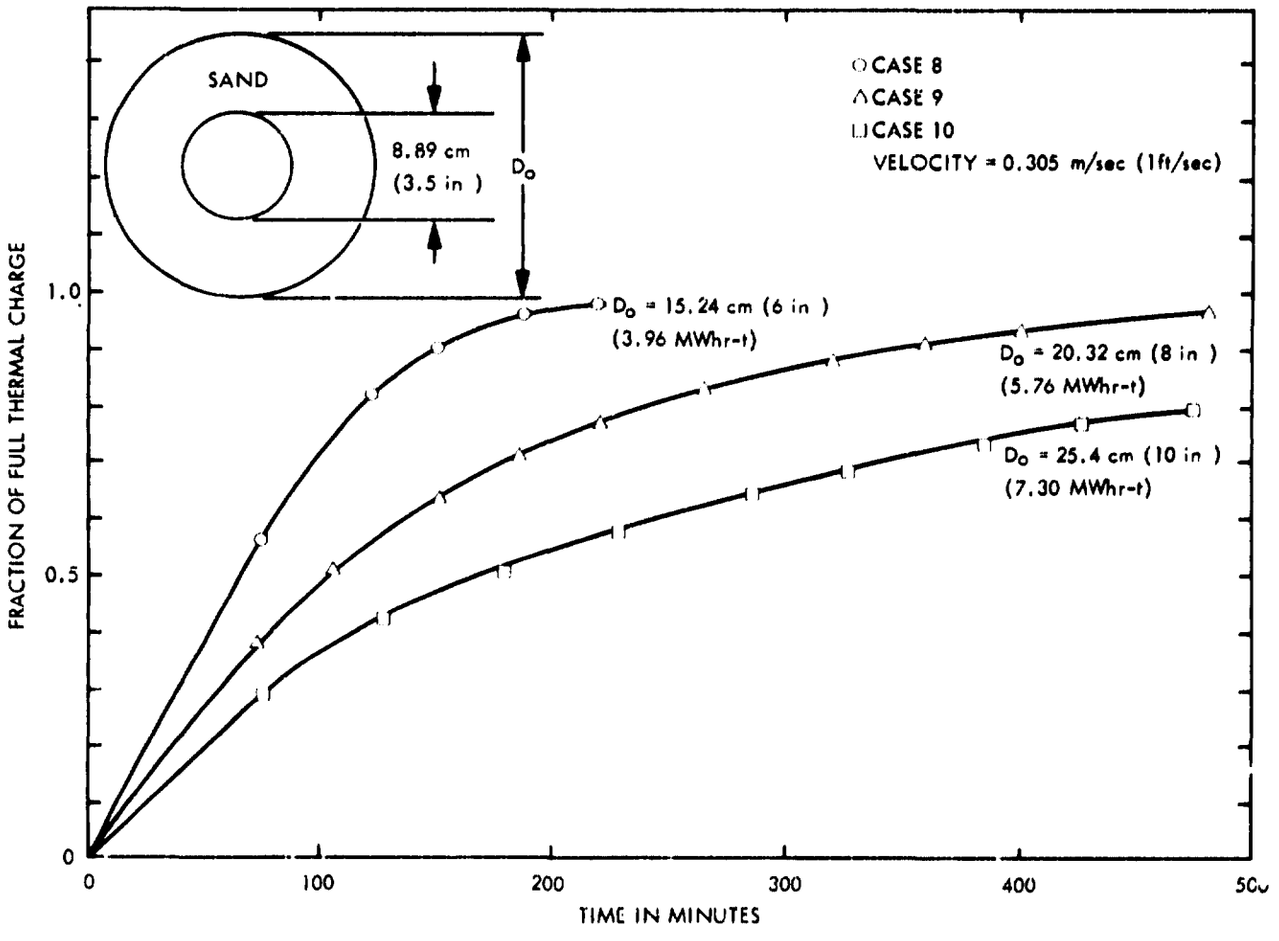

Figure 4.6. Thermal Charge vs Time: I.D. = 8.9 cm

(state of charge) must be taken into account. Generally, when comparing two systems (cases) which feature the same tube diameter but different tube spacing, the relative pipe lengths are related by the following type relationship

$$\frac{\text{Pipe Length (Case 1)}}{\text{Pipe Length (Case 2)}} = \frac{\text{(Q-Total, 2) (\% Charge of 2)}}{\text{(Q-Total, 1) (\% Charge of 1)}} \quad (4.7)$$

The Equation 4.7 is the first step to comparing system tube lengths and costs for different cases, and Figures 4.4, 4.5, and 4.6 are required to determine the percentage of charge at a given time. For example, exercising Equation 4.6 for Cases 1 and 2 at an 8 hour charge cycle, the percentage charge of 1 is 1.00 and the percentage charge of 2 is 0.755. From Table 4.1 the Q-Total for Case 1 is 1.324 MWhr-t, and for Case 2 the Q-Total is 2.578 MWhr-t. Using Equation 4.7 for an 8 hour charge time is represented as follows

$$\frac{\text{Pipe Length (Case 1)}}{\text{Pipe Length (Case 2)}} = \frac{(2.578)\ (0.755)}{(1.324)\ (1.000)} = 1.47$$

which indicates (that for an 8 hour charge period), 47% more length (and therefore greater cost) will be necessary if a Case 1 configuration is used instead of Case 2. But this result and Equation 4.7 are both time dependent, for if infinite time were allowed then the ratio would be 1.95, and if only three hours were available then the ratio would have been 1.03. The close spacing cases are attractive only when fast response times are required. When longer charge times are available, the advantages of close tube spacing are lost and these cases become more expensive. This is a general and expected result, and illustrates why care must be exercised in selecting a given tube diameter and spacing for a given application, because the optimal configuration to satisfy one system requirement may be the wrong configuration for another. The analytical arguments attendant for Figure 4.4, for the 3.8 cm (1.5 in) tube diameter, also apply for Figures 4.5 and 4.6 for diameters of 6.3 cm (2.5 in) and 8.9 cm (3.5 in), respectively.

Another fundamental (and perhaps intuitively obvious) conclusion is that a higher fluid velocity promotes a faster charging rate, evidenced in Figure 4.7, because the mass and heat flow into the system is higher. The convective heat transfer coefficient is also increased by the higher velocity, but that effect is secondary and will not be discussed. The convective heat transfer coefficient between the pressurized water and tube inner wall used in this analysis is, $h = 488$ cal/hr cm^2 ^oC (1000 Btu/hr-ft^2-^oF). There are two performance tradeoff considerations: 1) higher velocities increase the rate of system charge (Figure 4.7), 2) also a general increase in the pressure drop and associated pump work requirements, although it will be shown below that pressure drops are not too severe for water velocities less than 3 m/sec (10 fps).

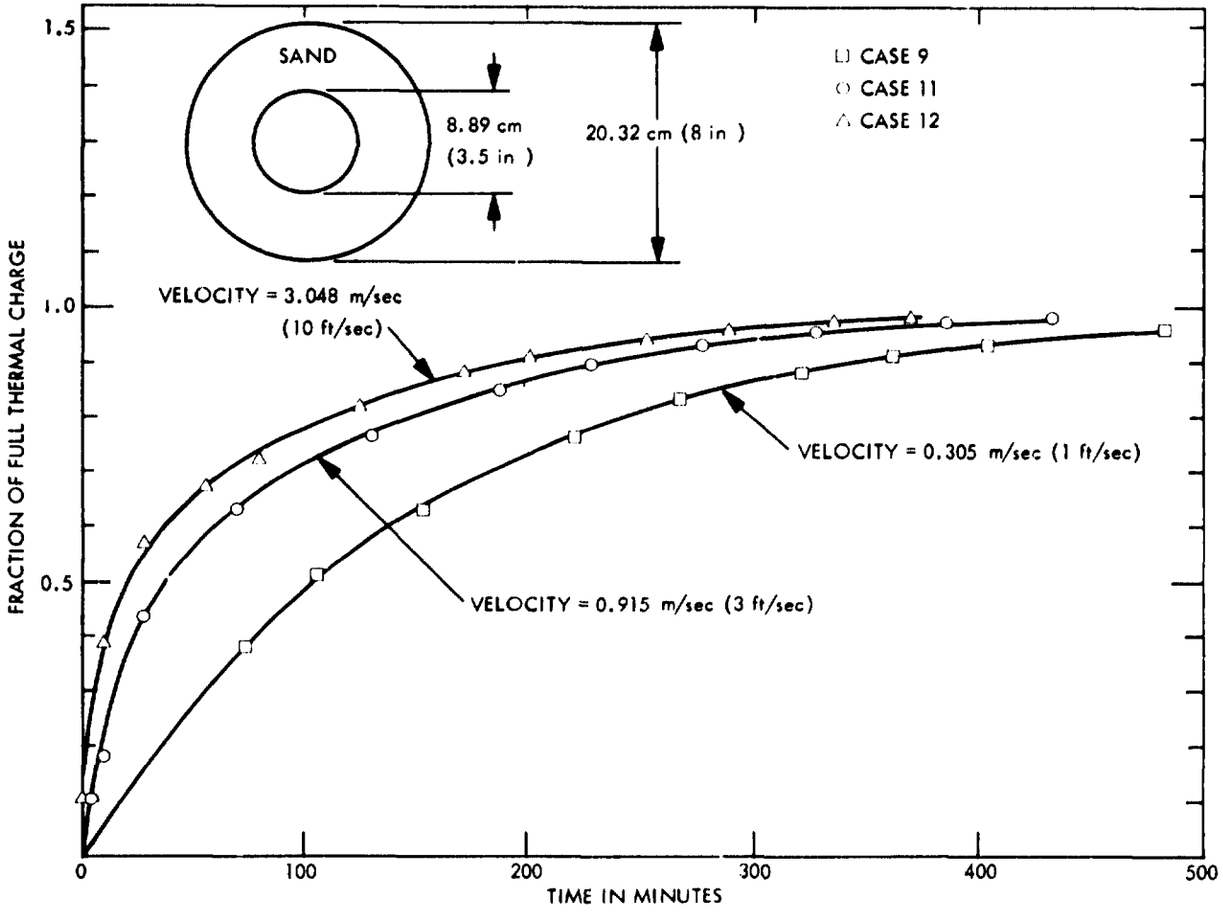

Figure 4.7. Thermal Charge vs Time - Indicating Impact of Variable Velocity on Performance

From a system basis, the total heat input to an initially discharged system (T = 0 everywhere) can be measured by monitoring the instantaneous temperature difference between fluid inlet and outlet temperatures. Thermal power input results for ten cases considered in Table 4.1 are shown in Figures 4.8 (for D_i = 3.8 cm = 1.5 in), 4.9 (for D_i = 6.3 cm = 2.5 in), and 4.10 (for D_i = 8.9 cm = 3.5 in). In each case, the water entry velocity is 0.3 m/sec (1 fps), the flow length is L = 1530 m (5000 ft), and the pipes are initially filled with water at T = 0. At time zero, water at temperature T = 1 begins to displace the cold water at x = 0, and behind the advancing hot-cold front (assumed to be sharp here) heat begins to be transferred to the sand, cooling the water. After 5000 sec (83 min), the advancing hot-cold front reaches the exit section at x = L = 1530 m (5000 ft), and the temperature of the outlet water can begin to rise, provided all of its heat has not been lost to sand. Comparative inspection of Figures 4.8, 4.9 and 4.10 reveal several general trends. Generally, systems with smaller diameter pipes have a slower system response than those with larger pipe diameters for a given tube spacing. This is because, for a larger pipe, a larger fraction of the heat is stored in water, rather than sand, and so less heat must be transferred to the sand. At the same time, larger pipes feature a greater heat transfer area, which promotes heat exchange from fluid to sand. Another expected result is that for a given pipe diameter, larger spacing inhibits charging rate and therefore the system utilization factor for a given charge time. In the three figures the heat rates are based on a total possible temperature difference of 220°C (400°F), and if the temperature difference potential were changed, then the heat flux would be proportionately altered. The outlet fluid temperature and the heat flux acceptance rates are important in determining the percentage of achieved system charge.

Figures 4.8, 4.9 and 4.10 can also be used to determine the fluid outlet temperature by using the ordinate at the right. For the case where L = 1530 m (5000 ft) and V = 0.3 m/sec (1 fps), it is apparent that the fluid outlet temperature will be zero up to 83.3 min (5000 sec) and that the system heat retention rate is also constant at some maximum level. Therefore, the fluid outlet temperature ordinate is inverted in magnitude, with zero corresponding to maximum heat rate and T(fluid) = 1 corresponding to zero thermal power retention.

Figure 4.11 shows the impact of velocity on the heat charge rate and also on fluid outlet temperature for a given configuration. For a given flow length, higher water velocity is associated with faster system response, namely faster charging rates and increased fluid outlet temperatures at early times. Because increased fluid velocity through a pipe increases friction pressure drop and pump work, the technical performance improvement must be balanced against increased pump work costs. Also, because the same quantity of heat is stored regardless of velocity and heat acceptance rate, the areas under each of the three curves in Figure 4.11 are all equal.

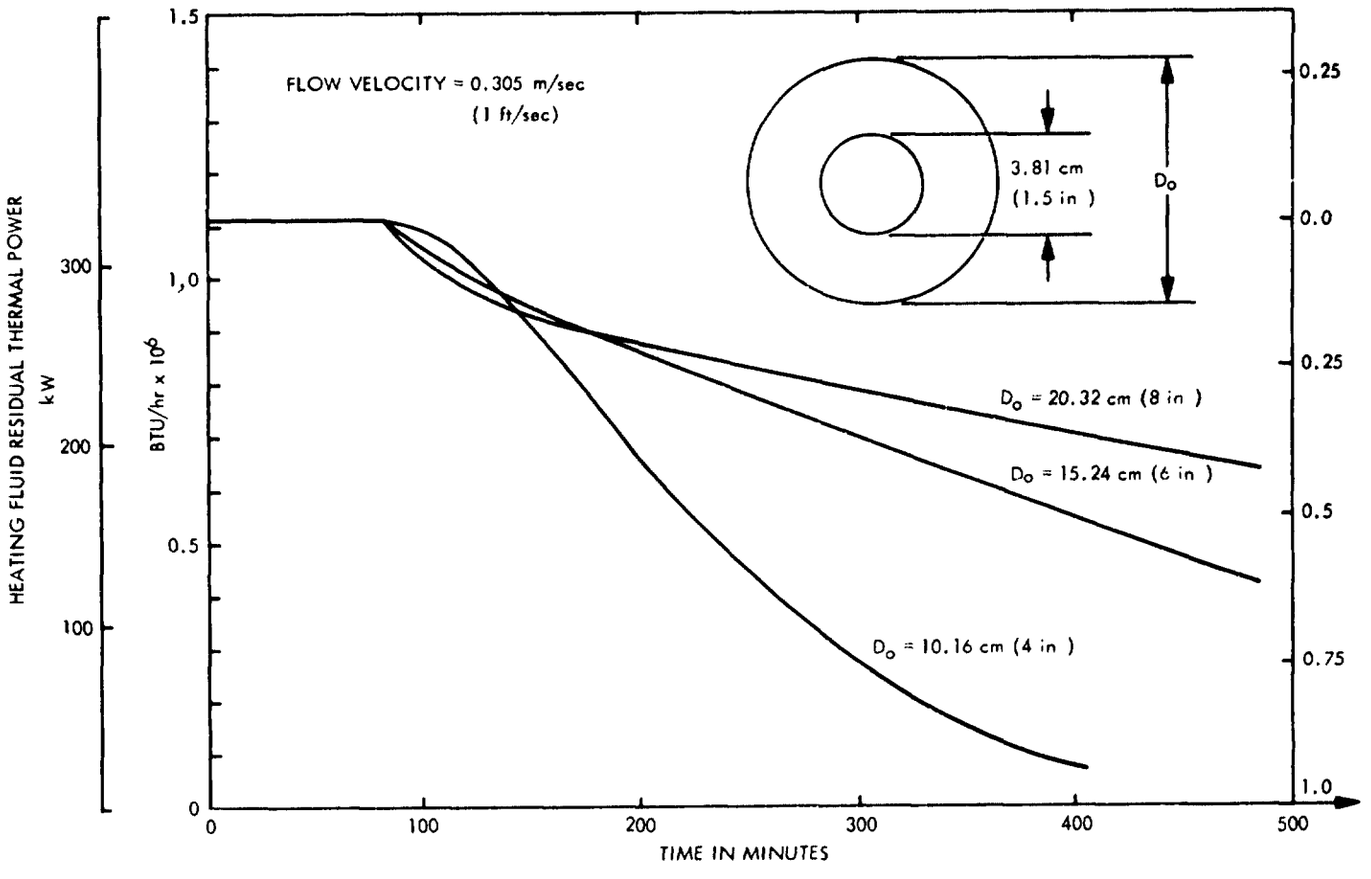

Figure 4.8. Dimensionless Fluid Outlet Temperature, I.D. = 3.8 cm

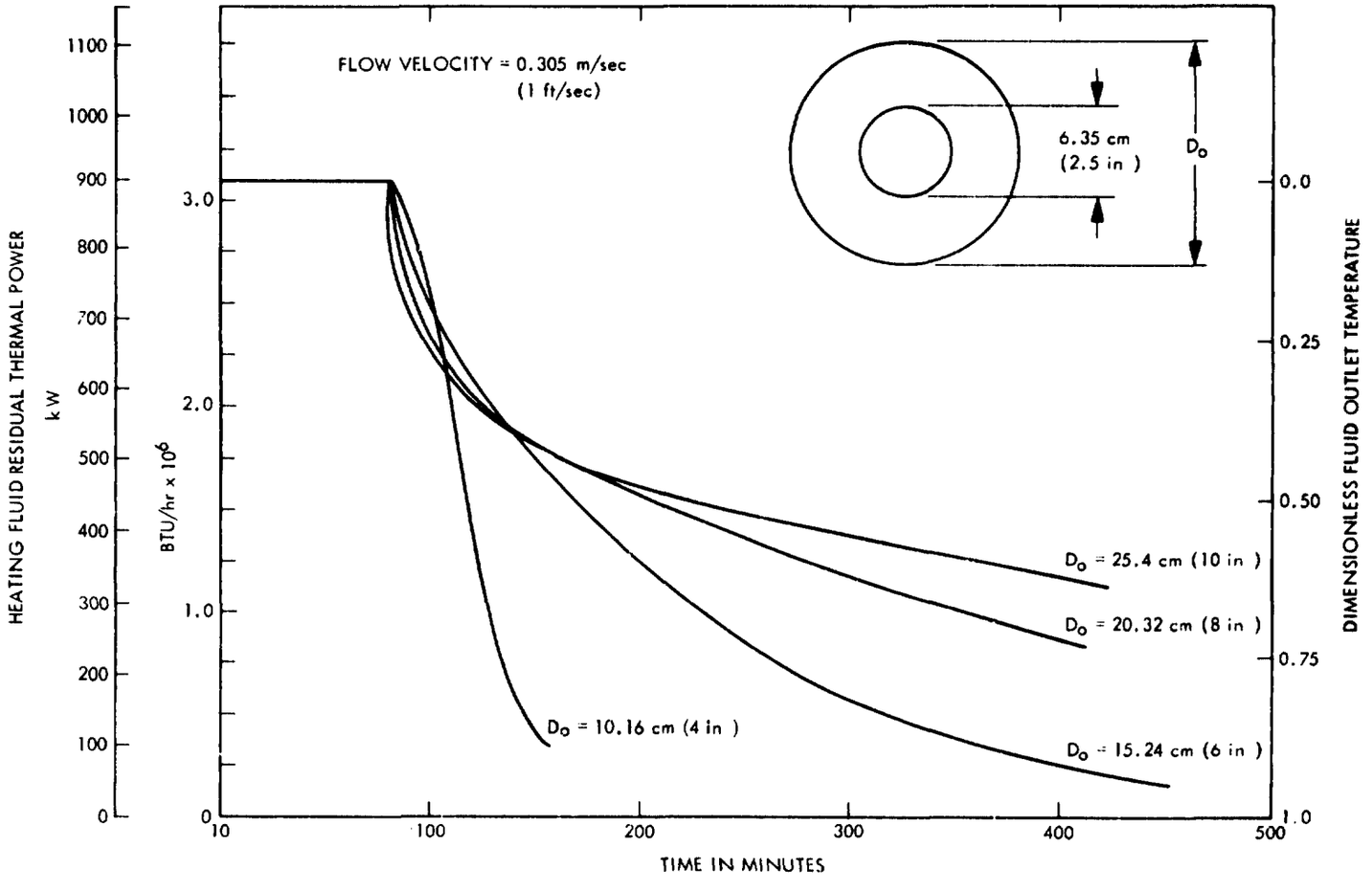

Figure 4.9. Dimensionless Fluid Outlet Temperature, I.D. = 6.35 cm

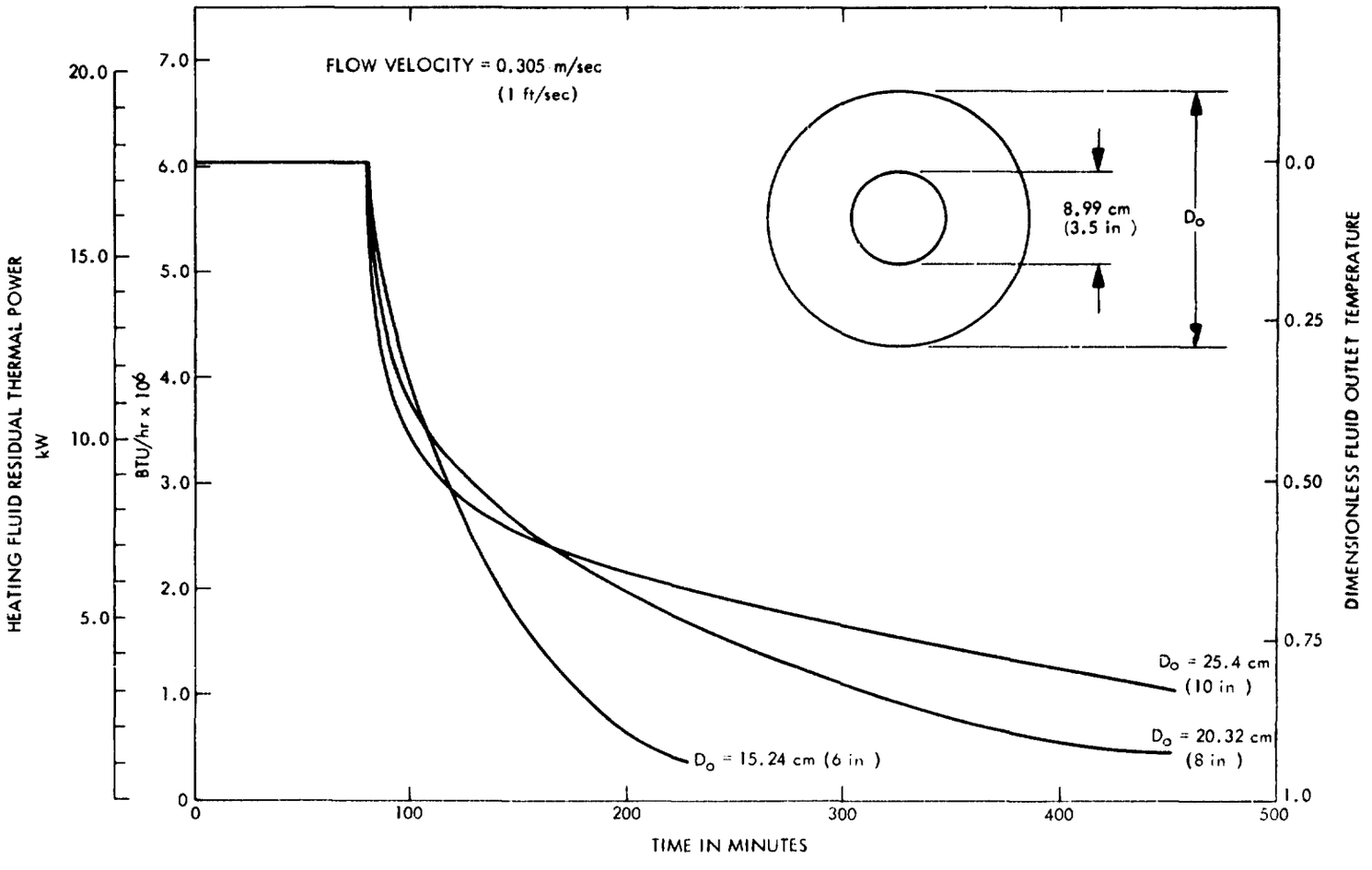

Figure 4.10. Dimensionless Fluid Outlet Temperature, I.D. = 8.9 cm

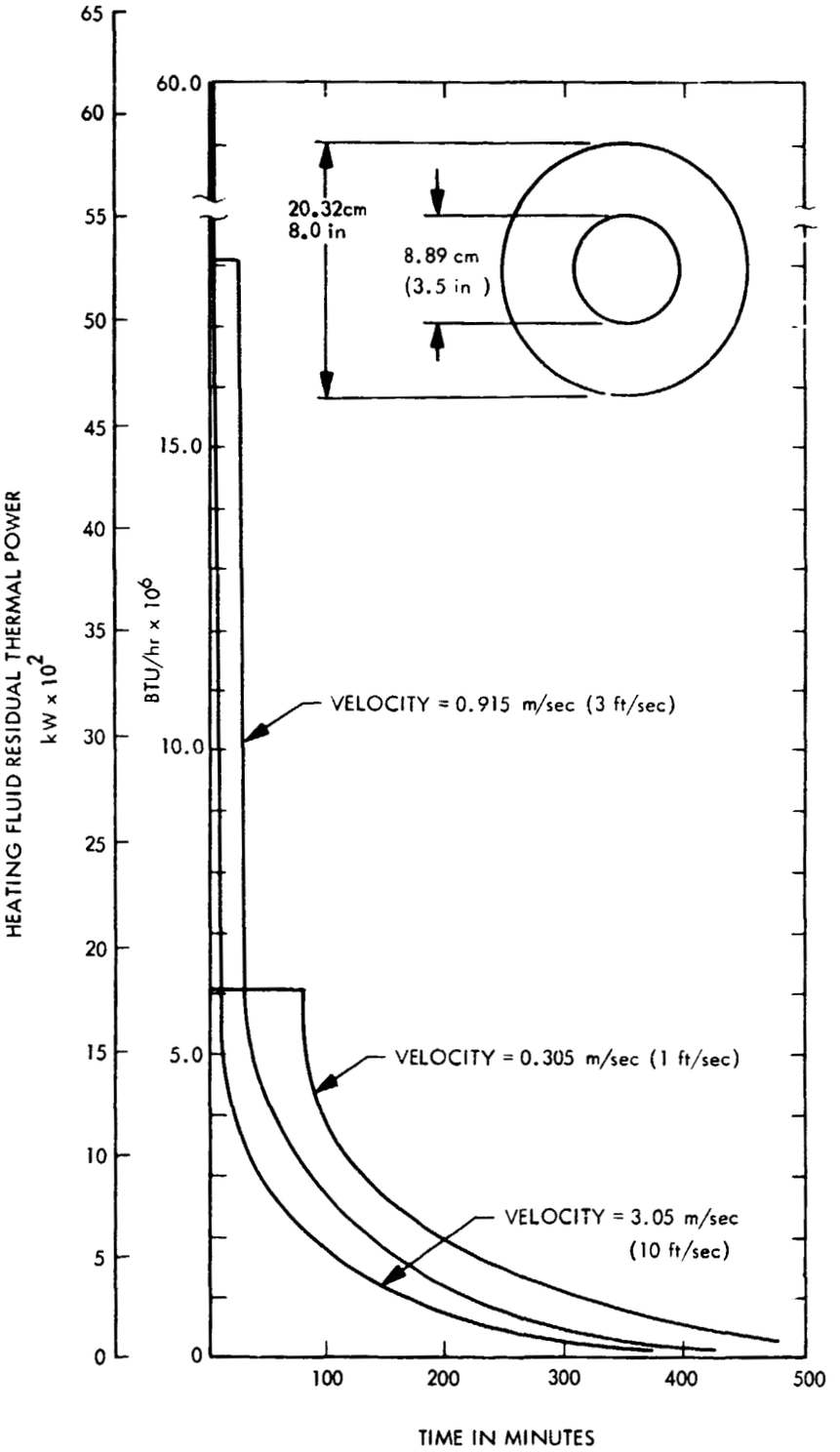

Figure 4.11. Heating Fluid Residual Thermal Power vs Time Velocity is a Parameter

The practical problem of selecting a suitable geometry (tube diameter and tube spacing within the sand matrix) for a given charge rate acceptance requirement can be approached, but not entirely decided, by inspection of Figures 4.8 through 4.10 for 0.3 m/sec (1 fps). Other similar curves would have to be generated if velocities other than 0.3 m/sec (1 fps) were to be considered. For example, if only 2 hours (120 min) were available for system charging, then Case 4 (D_o = 10 cm = 4 in with D_i = 63 cm = 2.5 in, Figure 4.5) would be the most likely candidate from those considered. Figure 4.5 indicates that this configuration accepts about 90% of total possible charge in 2 hours at a near steady rate, and Table 4.1 indicates that for maximum charge only 34% of heat is stored in sand (with the remainder of 66% in the water). Case 8, with D_o = 15 cm (6 in) and D_i = 8.9 cm (3.5 in), accepts 82% of total charge in 2 hours, and this might be a fair alternative to Case 4, depending upon which case is most economically attractive. But it is clear that neither Case 4 or 8 is appropriate if we consider a 6 or 8 hour available charge period, because the capability of quick charge cannot be used to advantage. For longer charge times increased tube spacing is acceptable, and because system cost drops rapidly as tube spacing increases, this cost differential would be a driving criterion. For 8 hour available charge times we would be tempted to select the least expensive configuration which achieves at least 80% of total charge, but not 100%. Thus, Case 5 (D_i = 6.3 cm = 2.5 in and D_o = 15 cm = 6 in), L = 1524 m (5000 ft) on Figure 4.5 accepts 90% of possible charge after 5 hours and for the next 3 hours approaches asymptotically total charge, Case 5 might be acceptable for 5 hours but would be too costly for an 8 hour charge time. Case 6 (D_i = 6.3 cm = 2.5 in and D_o = 20 cm = 8 in) accepts 80% charge in 8 hours and would be less costly than Case 5. Also attractive in the D_i = 8.9 cm (3.5 in) category might be Case 9 (D_o = 20 cm = 8 in) and Case 10 (D_o = 25 cm = 10 in).

Chargeability is one necessary technical criterion for configuration selection. A second factor is favorable temperature distribution of heat stored in a system. Storage efficiencies are greatest when some parts of the thermal storage unit are hot and some are cold because this represents minimum degradation of heat inputted to storage, and also provides the condition for which heat can be recovered at temperatures approximating input conditions with attendant higher post-storage conversion efficiencies.

The development of axial temperature profiles with time (Figures 4.12 through 4.16) for candidate configurations is useful because they indicate which part of a system is accepting heat and which is not. Although a somewhat arbitrary reference length of 1530 m (5000 ft) was chosen for the computer simulation, the effect of a shorter system flow length is easily determined from these figures. For an 8 hour charge period, the chargeability for Case 10 (D_i = 8.9 cm = 3.5 in and D_o = 25 cm = 10 in) is 80% and features relatively constant thermal power rate (Figure 4.6) and the energy cost looks promising at $2.63/kWhr-t (Table 4.1). Let us analyze Case 10 in some detail. The system average temperature (including average solid and fluid effect)

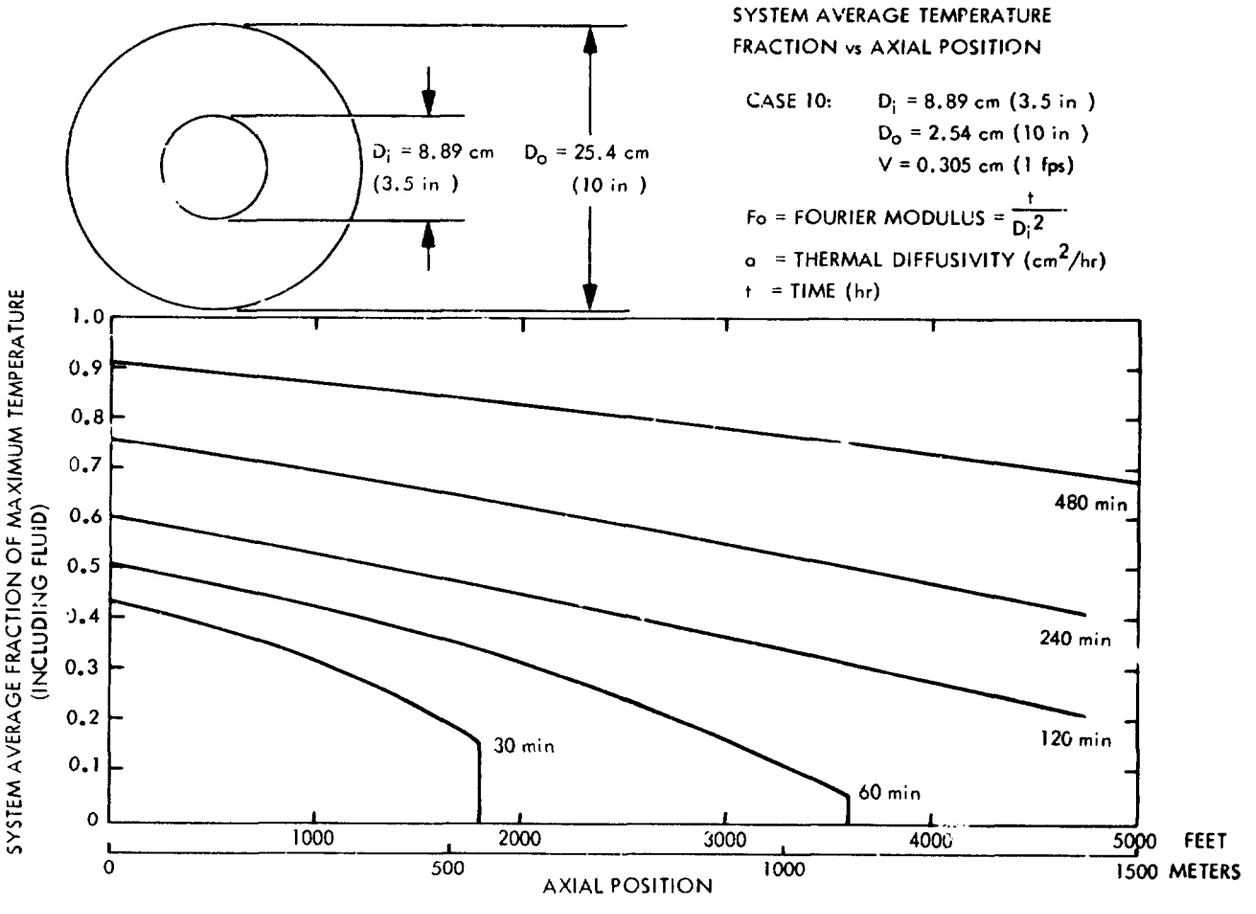

Figure 4.12. System Average Temperature Fraction vs Axial Position, D_o = 25.4 cm

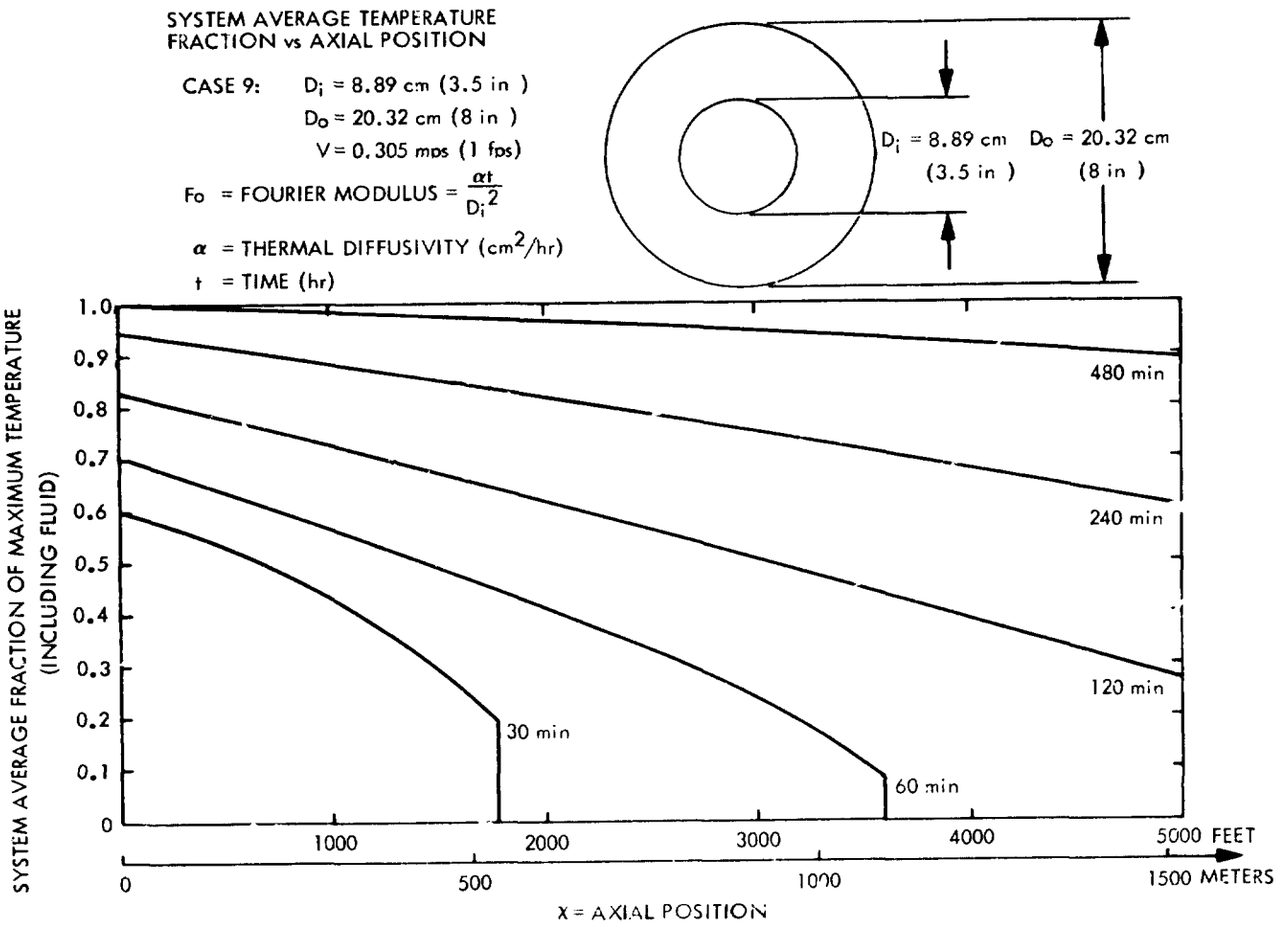

Figure 4.13. System Average Temperature Fraction vs Axial Position, D_o = 20.3 cm

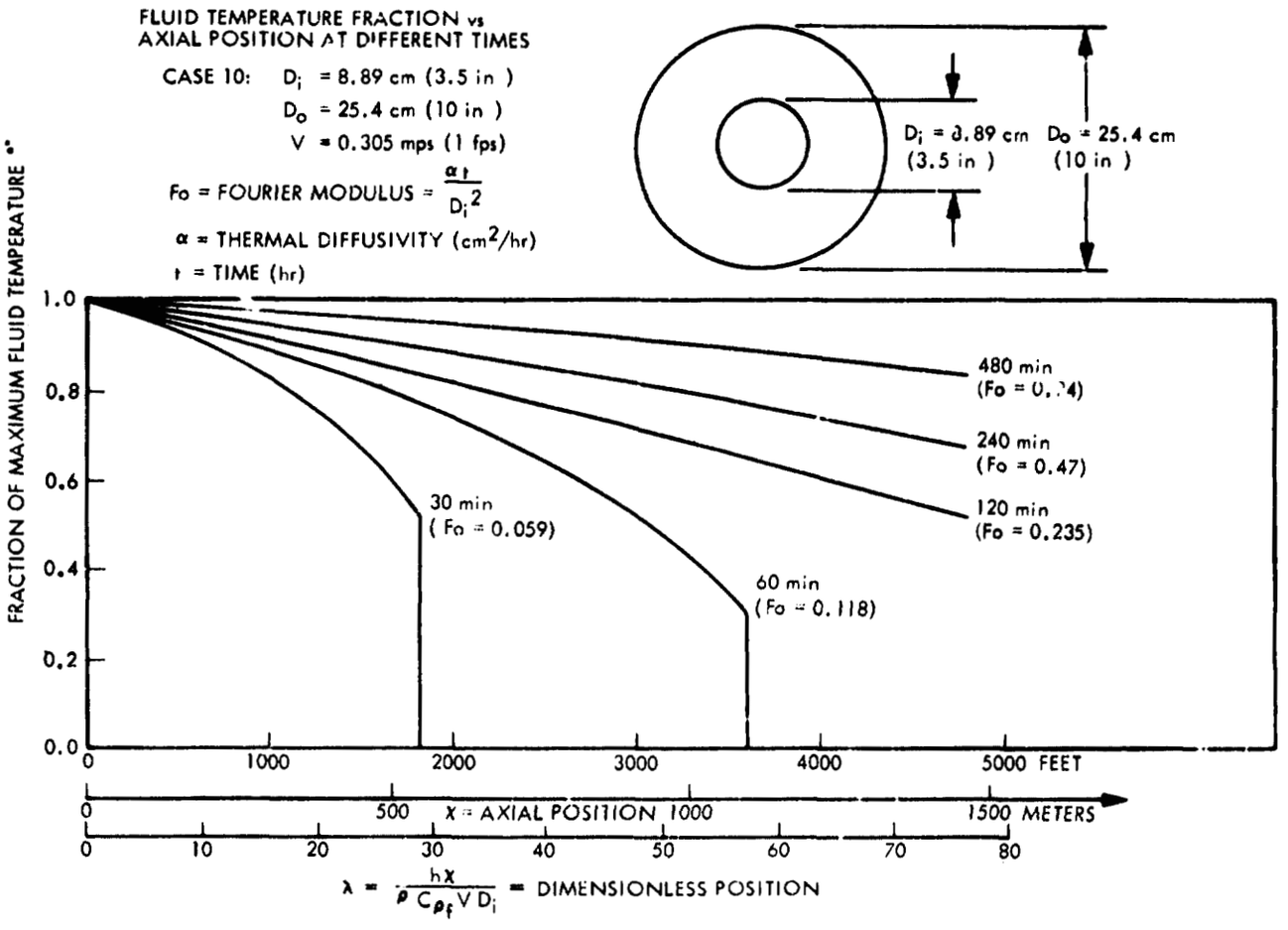

Figure 4.14. Fluid Temperature Fraction vs Axial Position at Different Times, Case 10

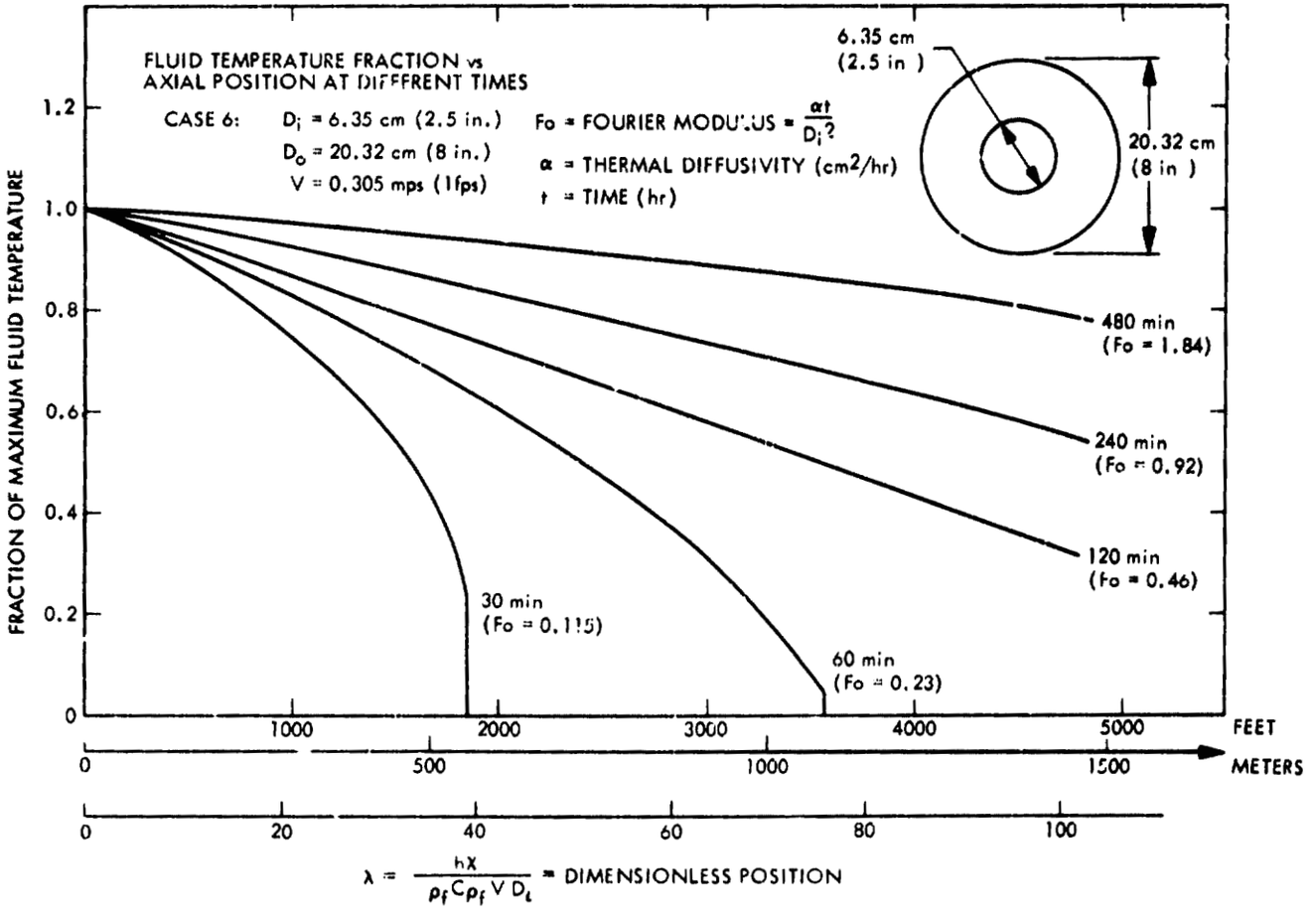

Figure 4.15. Fluid Temperature Fraction vs Axial Position at Different Times, Case 6

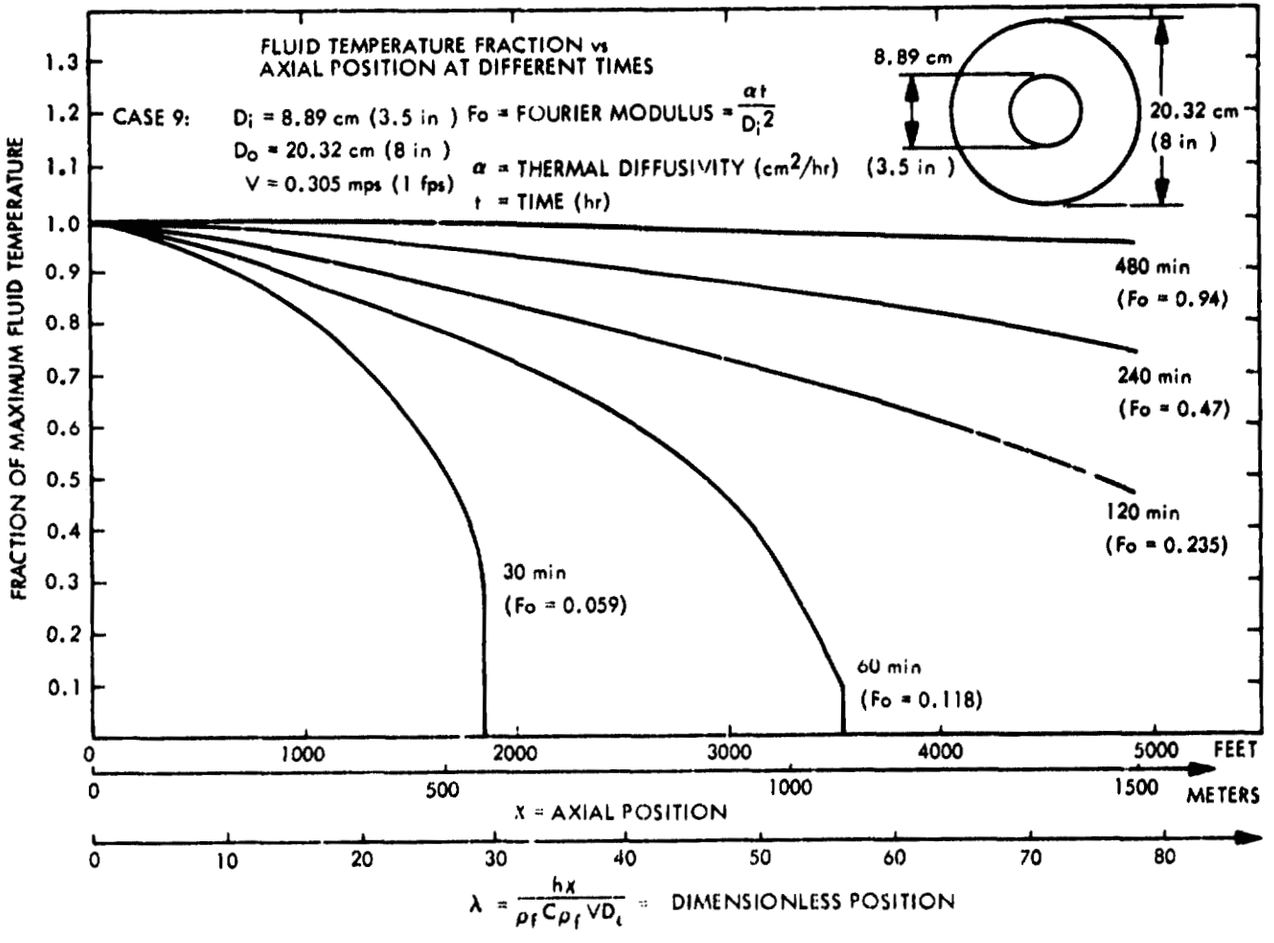

Figure 4.16. Fluid Temperature Fraction vs Axial Position at Different Times, Case 9

versus axial location at various time intervals for Case 10 is indicated in Figure 4.12. From a practical system design basis, curve sets such as Figure 4.12 are useful because they inform us what parts of the system require continued exposure to charging fluid and which parts do not. For example, during the first 35 minutes in all systems where fluid velocity is 0.3 m/sec (1 fps), we would close valves so only the first 510 m (2000 ft) or less of flowpath is exposed to the fluid, because pumping the cold water ahead of the advancing hot-cold water front would not promote system charging and would cost pressure drop and pumpwork. A striking feature of Figure 4.12 is the relative flatness of the temperature curves after 2 hours (120 min). Even at 8 hours (480 min), the average system temperature at the inlet (x = 0) is 0.91, despite the fact that the water temperature has been at 1.0 for the entire time (see Figure 4.13). This long charge time is a consequence of the low thermal diffusivity of the sand, which means that a long time is required for the heat to conduct into the sand. As shown in Table 4.1, 69% of the heat is stored in the sand for Case 10 when fully charged, and the low sand thermal diffusivity manifests as long charge times which will be compensated from economic considerations when long charge and discharge times are available.

Figure 4.13 shows the system average temperature versus position for Case 9 (D_i = 8.9 cm = 3.5 in, D_o = 20 cm = 8 in). A series of comparisons is obtained by comparing Figure 4.13 to Figure 4.12 (for Case 10 with D_i = 8.9 cm = 3.5 in, D_o = 25 cm = 10 in). It is immediately obvious that the closer tube spacing case (Case 9) charges faster, as we would expect. Another very important feature of closer spacing is the increased separation of temperature during charging along the system length. For example, at time 60 minutes, when the advancing hot-cold front fluid has reached 3600 ft, Case 9 has a maximum and minimum dimensionless temperature of 0.70 and 0.08, whereas Case 10 has 0.50 and 0.06. At 120 minutes, the axial system temperature gradient remains steeper for the closer spacing condition. This hot-cold separation is important from a storage standpoint because if heating were suddenly stopped at a given charge condition, the system temperature would equilibrate to an intermediate level to that of the sand and water, with resulting deterioration of heat availability. Then, when water flow were reversed, the axial temperature separation would impact upon the fluid recovery temperature, thus, the higher the better. This advantage of heat separation achieved by closer tube spacing is bought by increased system cost, and so again the tradeoff between system performance and cost becomes obvious. If long charge and discharge times are available, the large tube spacings become practical (and probably economically necessary).

A comparison curve to Figure 4.12 is Figure 4.14. And for Case 10, Figure 4.14 plots the fluid temperature (not system locally averaged temperature) against axial position for different times, and is useful for determining charge and discharge conditions from a system level. For example, although the fluid always enters the system at temperature T = 1, after 240 minutes (4 hr) its exit

temperature is T = 0.68 at flow length of 1463 m (4800 ft), and increases with time. This may impact on the source of heat (fossil, solar, etc.), because for the first 90 minutes the heat source could conceivably accept water at temperature T = 0 and heat it to temperature T = 1. When the ratio of inlet water temperature to the heat source begins to rise, then conditions within the heat source system become time variable. The fluid temperatures at flow length L = 1524 m (5000 ft) for different times, taken from the computer outputs or alternatively from graph sets like Figure 4.14, provide the data points for Figure 4.11, previously discussed. The effect of varying the input fluid velocity can be estimated in Figure 4.14 by use of dimensionless parameter α and Fo. In the calculations, a convective heat transfer coefficient h = 488 cal/hr-cm^{2}-^{o}C (1000 Btu/hr-ft^{2}-^{o}F) was used as a precalculated input, because turbulent flow inside a pipe h is relatively insensitive to velocity (h varies approximately as $V^{0.2}$). Appendix D shows the derivation of a dimensionless parameter

$$\lambda = \frac{hx}{C_p V D_i}$$

and explains each symbol. In Figure 4.14, dimensionless λ is used as an alternative abscissa to axial position (ft). λ has the practical effect of making a given graph independent of velocity V, since V is contained in λ. Therefore, if the λ abscissa is used in Figure 4.14, then the V = 0.3 m/sec (1 fps) restriction in the title should be disregarded. If Figure 4.14 is to be expressed in terms of dimensionless parameters, then the dimensionless time would be the Fourier Modulus, Fo, based on pipe diameter D_i, or

$$Fo = \frac{\alpha t}{D_i^2}$$

where

Fo = Fourier Modulus (dimensionless)

α = thermal diffusivity of sand (m^2/hr)

t = time (hr)

D_i = pipe diameter (m)

An attempt was made to generate universal graphs which would display the general case in terms of dimensionless parameters for all geometries and operating conditions, but comparisons with the computer outputs were in vain. Figure 4.1, limited to fixed radial geometry, is the most general type of graph which correlates with the data. Figure 4.15 and 4.16, both of which plot fluid temperature against axial locations at various time intervals for Cases 6 and 9,

respectively, are two other configurations which might be considered for 6 or 8 hour storage. The effect of different geometries on fluid axial temperature distribution for different times can be observed by comparison of Figures 4.14, 4.15, and 4.16.

In terms of charging and discharging performance, generally the smallest tube spacing and largest pipe diameters are desirable, but both of these conditions results in larger cost, as the pipe density (pipes per volume) is higher. Large spacing and small pipes yield the least system cost, because the sand increases its share of the heat stored and is far cheaper than the pipes, but the response performance decreases. Therefore, tradeoffs are necessary between cost and required performance. In designing a thermal storage system, a rapid charging or discharging rate may not always be necessary in certain applications (long-term storage, for example), and the designer may opt to select a system with slower charge/discharge rate to reduce costs. Table 4.1 summarizes costs for the various system plus charging performance data in the form of percent of charge at 6 and 8 hours. Six and 8 hour charge times were arbitrarily chosen as a representative interest for a power plant which may have this amount of time to charge or discharge a thermal storage unit on a diurnal cycle. The system cost calculations presented in Table 4.1 includes the pipe installed cost (including welding and materials, inspection, testing, etc.) and sand costs. Valves and controls were assumed to be a small cost, as was the containing structure. The present value of all future operation and maintenance costs are not considered in Table 4.1. Appendix E presents a sample cost calculation and pipe installation cost tables which are used here. The general methodology is described below.

In each case, a 1524 m (5000 ft) length of pipe and surrounding sand are considered, the pipe being filled with pressurized water. From geometry and heat capacities it is possible to estimate how much heat will be contained by both the sand and water when each undergoes the maximum possible temperature swing. The total heat stored for 100% charge conditions is listed in Table 4.1, for sand alone, water alone, and the sum of the two which comprises the system heat storage. The percent of heat storage in sand is also listed in Table 4.1. Knowing the cost of 1524 m (5000 ft) of pipe (from Appendix E) and the cost of sand at 2.2¢/kg ($20/ton), the system cost is estimated for 100% charge, subject to the assumptions previously discussed. In Table 4.1 the temperature swing was assumed to be 222°C (400°F) and averaged thermal and fluid properties were used for the water. For example, if the average input temperature is 315°C (600°F) and output is 93°C (200°F), then properties were evaluated at 205°C (400°F). The pipe installation and material costs were obtained from a survey of major contractor engineering firms. Sand costs were assumed to be 2.2¢/kg ($20/ton) based upon freight bulk carrying charges. This figure is judged to be conservatively high, and there are indications of a low cost of 0.2¢/kg ($2/ton) for concrete grade sand if transportation is provided by the customer. However, sand costs are generally a small portion of the total system cost for every case in Table 4.1 even assuming sand

at 2.2¢/kg ($20/ton). The pipe installed cost dominates the system cost. Therefore, having determined the pipe and sand cost, and the system cost (which is obtained by multiplying the pipe and sand cost by 2.22 as discussed in Section 3), the total TSU capital cost is estimated. From these data, the system cost is divided by the total heat capacity (kWhr-t) and again by 3.0, as discussed in Section III, to obtain the system energy storage cost estimate for 100% charge (Table 4.1).

However, as is apparent from the thermal analysis, the charging (and discharging) of the sand thermal storage unit is a dynamic operation, and a system may not be able to accept its total possible charge in a given length of time. A system which receives less than 100% of its possible charge during a cycle has an unused capability, and this must be considered in the cost analysis. The costing technique applied to System 10 in Table 4.1, features 1524 m (5000 ft) of 8.9 cm (3.5 in) O.D. tubing and a 25 cm (10 in) tubing spacing. The pipe cost $20,100 and the sand cost $2393, so the subtotal TSU cost is $22,493, and the total TSU cost is multiplied by 2.22 to total $49,934. For a fully charged system, 69% of heat would be stored in the sand and the remaining 31% in water (neglect pipe heat capacity). Since the system contains 7926 kWhr-t with a temperature swing of 204°C (400°F) when 100% charged, the energy cost for a 100% charged system would be

$$1/3\ (\$49,932/7926\ \text{kWhr-t}) = \$2.10/\text{kWhr-t}$$

Assuming flow paths of 1524 m (5000 ft) after 6 hours of charging, the percent charge is only 71.5% of maximum possible (see Figure 4.6 and Table 4.1). Therefore, instead of storing the full 7926 kWhr-t of energy, the system has only been able to absorb 5667 kWhr-t, and the energy unit storage cost for this condition is 1/3 ($49,934/5667 kWhr-t) = $2.94/kWhr-t, which value is reported in Table 4.1 for 6 hours of charge time. If we allow 8 hours for the same system to charge, then the energy unit storage costs drops to $2.62/kWhr-t, because 80% of the system becomes charged (reported in Table 4.1). The point is that energy unit storage cost is dependent upon the operating conditions, which involve rates and Second Law of Thermodynamics considerations, and not only on static First Law calculations. Otherwise stated, it is not possible to predict which of a set of possible system configurations will provide the lowest energy cost by calculation of heat capacities only, unless an infinite time is available for each half-cycle. In Case 4 (Table 4.1 and Figure 4.5) (Di = 6.35 cm = 2.5 in, D_o = 10 cm = 4 in), 6 hours constitutes an "infinite time," because after 4 hours the Case 4 system is 100% charged.

The system energy cost ($/kWhr-t) for 100% charging and limited time (6 and 8 hr) charging previously described and reported in Table 4.1 is a straightforward and unambiguous calculation. Although the energy cost is important, it is only one of two significant cost indicators which characterize a system. The other cost criterion is system power cost ($/kW-t), and for the considered sand and water

system which features variable power rates, this power cost is open to some interpretation. Generally the system initial power cost is determined by dividing the TSU system power related costs by rated system power. The system cost, with limitations defined above, for each configuration is listed in Table 4.1; for Case 10 it is $49,934 for a 1524 m (5000 ft) length. The maximum system power input rate for assumed conditions depends on the velocity of water and tube diameter, and water temperature swing. This is the same for all configurations with a given tube diameter; for Cases 8, 9 and 10 it is 1767 kW-t for water velocity of 0.3 m/sec (1 fps) (see Table 4.2). For these conditions the system power cost is

$$\text{TSU Power Related Cost Ratio } (C_p) \text{ (Maximum Power Rate)} = \frac{\text{Power Related Cost (\$)}}{\text{Maximum Power Capability (Kw-t)}} \tag{4.8}$$

Using Equation 4.8, the System Power Cost for Maximum Power Condition for Case 10 is (2/3) ($49,934/1767 kW-t) = $18.84/kW-t. But increasing the water velocity would increase the maximum power input and thus proportionately decrease the System Power Cost. Thus, for Case 12 (same tube diameter as Case 10 but with water velocity 3 m/sec (10 fps) the maximum power would be 10 times greater and the Power Cost would be 10 times less, or $1.88/kW-t. Although Case 12 (3 m/sec) (10 fps) has a low apparent power cost, it is apparent from Figure 4.11 that the high power capability can only be sustained for 1524 m, 3 m/sec (5000 ft/10 fps) = 500 sec or 8.3 min, after which the power capability plummets. Furthermore, it is apparent that the sand packing does not influence the maximum power rating. When water is introduced into a TSU which has stood dormant for awhile, the exit water is uniform at the saturated TSU temperature for the time it takes the introduced water alone to reappear at the other end. Thus, Equation 4.8 clearly has a major deficiency which disqualifies it from application when wide variations of power can occur during a given cycle. Note that these problems were secondary when we considered energy cost, becuase the energy capacity is an intrinsic property of the considered configuration. Dynamic and transient effects appeared on a small scale when less than 100% charging was considered, but there was no impact on the System Energy Cost order of magnitude. It is clear that costing the sand-pipe thermal energy storage system on an energy basis is primarily a First Law of Thermodynamics problem and relatively unambiguous. Costing per unit power involves the Second Law and is open to interpretation.

It is clear that any cost per unit power criterion should include both the water and sand elements of the system and include a significant duration of a charging or dischargine cycle. The device adopted here is to consider the amount of time a given system requires to achieve 80% of maximum charge and then to divide 80% of the full charge (kWhr-t) by this time. Times are found from Figures 4.4 through 4.7.

Thus,

ASP = Average System Power

$$= \frac{\text{0.8 Total Energy Capacity in kWhr-t).}}{\text{Time to Achieve 80\% of Full Charge}} \quad (4.9)$$

Then the System Power Cost (SPC) is

$$SPC = \frac{\text{System Power Related Cost in \$}}{\text{ASP}} \quad (4.10)$$

Table 4.2 shows the SPC using equations from 4.9 and 4.10. Comparing the results for Cases 10 and 12, both for the same geometry of D_i = 8.9 cm (3.5 in) and D_o = 20 cm (8 in), it can be seen that the SPC for water velocity of V = 0.3 m/sec (1 fps) is \$42.93/kW-t, and for V = 3 m/sec it is \$13.00/kW-t. In this case, increasing the velocity by a factor of 10 results in an order of magnitude power unit storage cost reduction of approximately 3, rather than 10 as would have been computed by Equation 4.8. Thus, the way the system is operated impacts upon the cost per unit power, but the result also takes into account the entire system response, as should be the case.

In selecting a storage system to integrate into a specific storage requirement, three columns in Table 4.2 are of interest; these are: (1) System Energy Cost Ratio (C_t) (\$/kWhr-t), (2) System Power Cost Ratio (Cp) (\$/kW-t), and (3) the Time to accept a given percentage of maximum system heat (hr). When comparing Cases 2 and 3, both costs are slightly less for Case 3 than for Case 2, but the 80% charge time for Case 3 is 12.8 hours compared to 9.2 hours for Case 2. Therefore, if we could afford the longer charge time, we would probably select Case 3 over Case 2, and vice versa.

An interesting observation regarding Table 4.2 System Power Costs is that, regardless of configuration, for velocity of 0.3 m/sec (1 fps) the SPC ranges from \$19/kW-t to \$55/kW-t, with an average of about \$25/kW-t, and the system likely to be selected may cost less than \$30/kW-t. The general result for a velocity of 0.3 m/sec (1 fps), the SPC is about \$30/kW-t, and could drop to \$15/kW-t for higher water velocities (Cases 11 and 12).

Because it has been demonstrated that higher water velocities are consistent with lower system costs and improved system response, it is necessary to determine what is the effect of velocity on pressure drop and also parasitic pump work. The well known equation for friction pressure drop inside a pipe of given internal diameter D_i and length L is

$$P = \frac{fL\rho V^2}{2g_c D} \quad (4.11)$$

where the friction factor f is obtained by first calculating the Reynold's Number,

$$Re = \frac{VD}{\tau} \quad (4.12)$$

where τ is the kinematic viscosity (m^2/sec). For turbulent flow (Re is greater than 10^4) Equation 4.13 is used to calculate f from Re for a smooth pipe

$$f = 0.184\ Re^{-0.2} \tag{4.13}$$

Assume average water temperature at 205°C (400°F), for which τ = 1.76×10^{-7} m^2/sec (1.89×10^{-6} ft^2/sec) and ρ = 913 kg/m^3 (57 lb/ft^3). Then, using Equations 3.11, 3.12 and 3.13, it is possible to generate Table 4.3 for L = 1524 m (5000 ft).

The pump power (PP) necessary to impel the water flow against a given pressure drop is

$$PP = \frac{M\ P}{\rho \eta_p}$$

with

$$M = \rho AV = \frac{\pi}{4} D^2 \rho V$$

so $$PP = \frac{\pi D^2 V \Delta P}{4\eta_p} = \frac{\pi f L D \rho V^3}{8 g_c \eta_p} \tag{4.14}$$

where

η_p = pump efficiency (η_p = 0.8 in this study)

g_c = dimension constant

The pressure drop using Equations 4.11, 4.12 and 4.13 and also the pump power (Equation 4.14) required to overcome the pressure drop for water at 205°C (400°F) flowing through 1524 m (5000 ft) of pipe are presented in Table 4.3. Parameters are pipe diameter and water velocity. Note that the pump power in the last column has units of kW-e (not thermal). The high grade mechanical pump power input to the system manifests as heat, so it is not completely lost, only degraded. The percentage of pump work recoverable is dependent upon the conversion efficiency of the machine which the storage unit will drive. The Real Work Lost is,

$$\text{Real Work Lost} = W_1 (1 - \eta) \tag{4.15}$$

where W_1 is pump work (power times time) expended and η is the thermal-to-mechanical conversion efficiency as heat from storage. This recovery availability suggested by Equation 4.15 can be a small quantity which will not change any order of magnitude calculations, but should be considered in a detailed system design.

The system average power (kW-t) capability varies with considered configuration and flow velocity (Tables 4.1 and 4.2)

Table 4.2. Economic Relationships

Case	D_i cm (in)	D_o cm (in)	V m/sec (fps)	TSU System Cost $	TSU System Heat Capacity kWhr-t	Time to Accept 80% of maximum System Heat hr	Average TSU System Power kW-t	Maximum Charge Rate kW-t	Average TSU System Power Cost Ratio $/kW-t	TSU Energy Cost Ratio for 8 hr Charge $/kWhr-t
1	3.8 (1.5)	10 (4)	0.30 (1.0)	17,816	1324	4.0	282	324	42.12	4.49
2	3.8 (1.5)	15 (6)	0.30 (1.0)	19,025	2578	9.2	224	324	56.62	3.26
3	3.8 (1.5)	20 (8)	0.30 (1.0)	20,721	4294	12.8 (est)	268	324	51.54	3.22
4	6.35 (2.5)	10 (4)	0.30 (1.0)	29,673	1875	1.75	357	901	55.41	5.28
5	6.35 (2.5)	15 (6)	0.30 (1.0)	30,882	3128	4.2	596	901	34.54	3.56
6	6.35 (2.5)	20 (8)	0.30 (1.0)	32,579	4856	8.0	486	901	44.69	2.77
7	6.35 (2.5)	25 (10)	0.30 (1.0)	34,759	7126	10.7 (est)	533	1767	43.48	2.69
8	8.9 (3.5)	15 (6)	0.30 (1.0)	46,061	3963	2.0	1586	1767	19.36	3.87
9	8.9 (3.5)	20 (8)	0.30 (1.0)	47,754	5756	4.0	1194	1767	26.66	2.89
10	8.9 (3.5)	25 (10)	0.30 (1.0)	49,934	7926	8.0	792	1767	42.03	2.63
11	8.9 (3.5)	25 (10)	0.90 (3.0)	49,934	7926	2.5	1842	5300	18.07	2.80
12	8.9 (3.5)	25 (10)	3.0 (10.0)	49,934	7926	1.8	2560	17670	13.00	2.77

whereas in Table 4.3 we observe that the pumpwork order of magnitude is influenced more by water velocity than pipe diameter. It is emphasized that the power levels in Tables 4.1 and 4.2 are in kW-t, and in Table 4.3 it is expressed in kW-e. Therefore, to compare orders of magnitude of parasitic pump power from tables 4.3 with storage power input levels in Tables 4.1 and 4.2, it is necessary to divide the electric power value in Table 4.3 by the conversion efficiency, which will generally increase the value by at least a factor of three. Table 4.3 indicates that the power to pump water in a 1524 m (5000 ft) long pipe can be significant for velocities in the range of 3 m/sec (10 fps), whereas for 0.3 m/sec (1 fps) it is negligible and for 0.9 m/sec (3 fps) it is probably acceptable.

Another important consideration is the water pressure drop through the pipe section. Table 4.3 indicates that for 3 m/sec (10 fps)the pressure drop will be order of magnitude of hundreds of psi, for 0.9 m/sec (3 fps) it will range in the tens of psi, and for 0.3 m/sec (1 fps) it may vary between 14 to 35 kPa (2 to 5 psi), depending upon pipe diameter and perhaps pipe roughness characteristics. The low pressure drop and pump power associated with flow velocity of 0.3 m/sec (1 fps) has determined why much of the analysis in this section was done for 0.3 m/sec, although 0.9 m/sec could have been considered. Also, the effect of bends and elbows in the convolutional geometry has been ignored in the previous order of magnitude calculation, although this would increase both pressure drop and pump work in every case.

Table 4.7. Friction Pressure Drop and Pump Work

205°C (400°F) water in 1524 m (5000 ft) long smooth pipe

Parameters used: ρ = 913 kg/m^3 (57 lb/ft^3)
τ = 1.76 x 10^{-7} m^2/sec (1.89 x 10^{-6} ft^2/sec)
Pump efficiency η_p = 0.8

Pipe Diameter cm	Pipe Diameter (in)	Water Velocity mps (fps)	Reynold's Number (-)	Friction Factor (-)	Pressure Drop kPa (psi)	Pump Power (kW-e)
3.9	1.5	0.3 (1)	66,000	0.02	33.78 (4.9)	0.015
6.35	2.5	0.3 (1)	110,000	0.018	18.34 (2.66)	0.022
8.9	3.5	0.3 (1)	154,000	0.0169	12.41 (1.8)	0.029
3.9	1.5	0.9 (3)	198,000	0.016	244.74 (35.5)	0.32
6.35	2.5	0.9 (3)	330,000	0.0145	132.36 (19.2)	0.48
8.9	3.5	0.9 (3)	462,000	0.0135	88.24 (12.8)	0.63
3.9	1.5	3 (10)	660,000	0.0126	2137.14 (310)	9.3
6.35	2.5	3 (10)	1,100,000	0.0114	1158.19 (168)	14.0
8.9	3.5	3 (10)	1,540,000	0.0106	772.13 (112)	18.3

SECTION V

ECONOMICS AND THE SAND-PIPE THERMAL STORAGE UNIT

A. GENERAL CONSIDERATIONS

When designing a thermal storage unit (TSU) it is convenient to separate the costs into two components, energy related cost and power related costs. Energy related components include the storage medium, containment costs, transportation of energy related materials to the site, insulation, and generally any items related to the storage of heat, but not to the input or extraction of heat from the system. The power related components are all parts of the system which relate to the input or extraction of heat to the system and normally include any heat exchangers, pumps, most plumbing, intermediate transport fluids and their subsystems, most controls, and generally any device pertaining to system heat transfer. System heat loss is an energy related penalty, whereas pump work and pressure drop are power related.

The bifurcation of TSU system expenses into energy related and power related costs stimulates a search for a technique to categorize candidate TSUs on a systematic economic bases. Power is the time derivative of energy. Compare here the ratio of energy related costs to power related cost or

$$\text{Proposed Cost Ratio} = \frac{\text{TSU Energy Related Cost}}{\text{TSU Power Related Cost}} \qquad (5.1)$$

where

$$\text{TSU Total Capital Cost} = \text{TSU Energy Related Capital Cost} + \text{TSU Power Related Capital Cost} \qquad (5.2)$$

Figure 5.1 explains why the above proposed cost ratio is deficient because the same TSU storage concept employed in two different applications will have an entirely different cost ratio. Consider, for example, a large body of sand poured in place around pipes so that heat transport fluid is contained by the pipes and brought into contact with the sand to allow heat to diffuse between the fluid and the sand. Here, the sand and container comprise the energy related cost and the pipes and pump constitute the power related cost. For a given energy storage capacity, disregarding the heat capacity of fluid filling the pipes, the sand volume and thus cost is the same regardless of the pipe packing density, and so may be considered a constant, as indicated by the dashed path a-b in Figure 5.1. If, for example, in a very large sand volume only one pipe is provided for thermal power input or recovery, then the power related cost will be very low (path c-d in Figure 5.1) and the power capability of the TSU will be correspondingly low. It may take a year to charge or discharge the sand volume with thermal energy. For some applications, this enormous energy-to-power ratio might be acceptable. However, if a considered application demands a higher charge and discharge rate, then many more tubes must be embedded within the sand pile at a higher

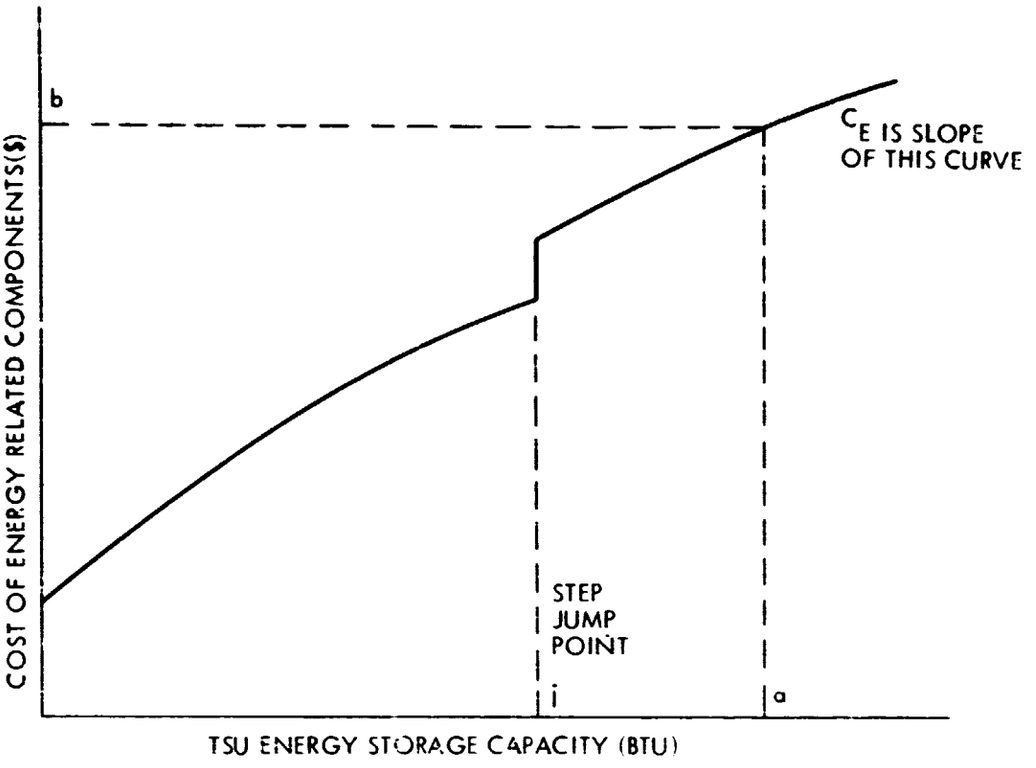

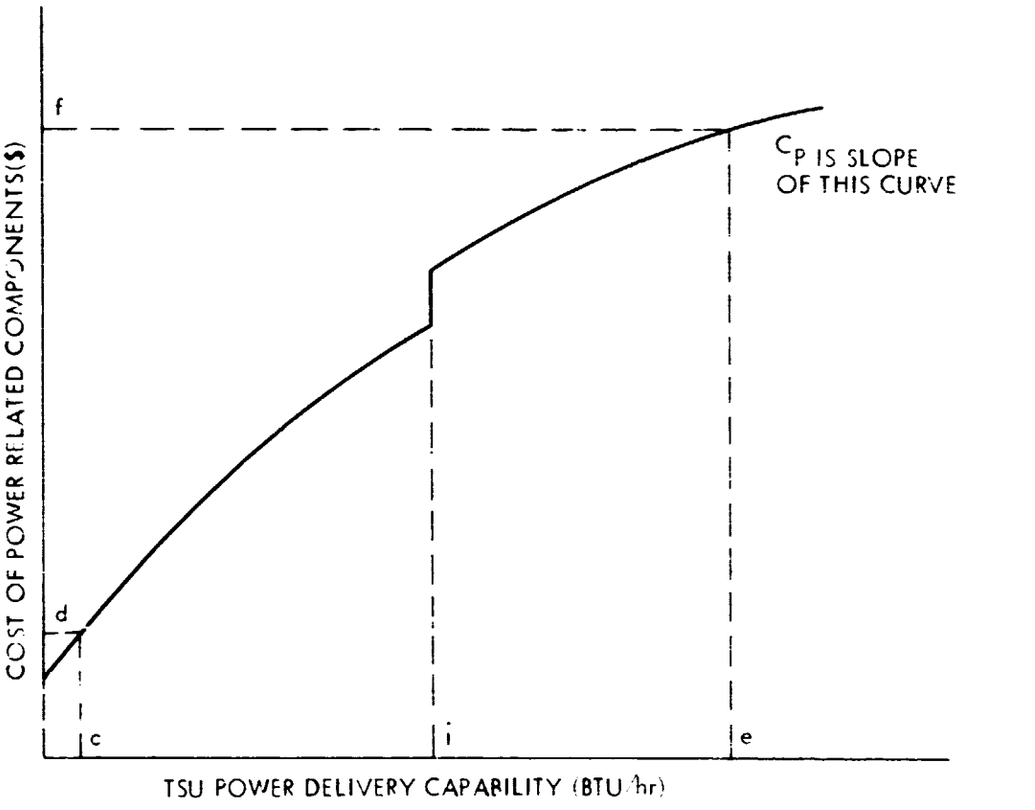

Figure 5.1. TSU Energy and Power Related Costs vs System Capabilities

power cost (path e-f in Figure 5.1). It is clear that applying Equation 5.1 to the pipes-embedded-in-sand TSU will yield a "Proposed Cost Ratio" which is dependent upon application, with perhaps a high ratio for low power extraction capability and low ratio for high power capability. Equation 5.1 thus fails to provide a TSU classification parameter which is independent of specific application.

Calculation relevant to several TSU systems have all indicated that both curves in Figure 5.1 can be qualitatively represented as indicated, with the curve intersecting the ordinate at a postive value for a zero value of the abscissa. This zero displacement represents the fact that even a small performance requires some equipment and installation labor. The characteristic of gradual slope decrease with increasing size is generally due to economy of scale, although either curve can take sudden jumps, as point j on each curve, to indicate a size threshold above which additional equipment in many systems must be specified, such as another heat exchanger or storage tank.

Although economy of size can cause the slopes of the two curves in Figure 5.1 to decrease somewhat with increasing system size, all calculations indicate that the slope retains its order of magnitude regardless of the absciss value, and that variations of the slope value are not large throughout the likely range of the abscissa. The slope of the energy curve at a location of interest in Figure 5.1 is the Energy Unit Storage Cost (C_E). C_E has dimensions of \$/energy and is defined as

$$C_E = \text{Slope of Energy Cost Versus Energy Curve (Figure 5.1)}$$

$$= \left| \frac{d\ (\text{Energy Related Costs})}{d\ (\text{Energy Storage Capacity})} \right| d\ (\text{Abscissa}) \to 0 \qquad (5.3)$$

Similarly, the slope of the power curve in Figure 5.1 is defined as the Power Unit Storage Cost (C_P), with dimension of \$/power, and is defined as

$$C_P = \text{Slope of Power Cost Versus Power}$$

$$= \left| \frac{d\ (\text{Power Related Costs})}{d\ (\text{Power Input or Extraction Capabilities})} \right| d\ (\text{Abscissa}) \to 0 \qquad (5.4)$$

where only the power input or the extraction capability is considered for the abscissa, whichever is smaller. The sum of input and extraction power costs is used for the ordinate. In many systems the same power related equipment is used for heat insertion and removal, but in some systems different heat exchangers may be used for the two functions.

Because the C_E and C_P vary slightly with the value of either energy or power capacity levels, the ratio of the two should be almost independent of abs issa in Figure 5.1. This ratio can serve as an application independent parameter useful for cataloging TSUs on a consistent economic basis. Thus, we define the Energy Power Cost

Ratio (EPCR) as

$$EPCR = \frac{C_E}{C_P} \tag{5.5}$$

For small systems, with a low abscissa value on both curves in Figure 5.1, two points on each curve must be taken to determine the C_E and C_P slopes in order to determine the EPCR characterizing parameter in Equation 5.5. But because both the energy and power components of large systems will cost considerably more than small systems, the ordinate intercept for zero abscissa will generally be relatively small. For large systems, one of the points for computing slopes in both curves in Figure 5.1 can be taken as the origin (0,0) without incurring serious error. This is a decided convenience for quickly determining the EPCR of a large system with known characteristics at a single point design, because the EPCR becomes

$$EPCR = \frac{\dfrac{\text{Energy Related Cost (\$)}}{\text{Energy Storage Capacity (kWhr)}}}{\dfrac{\text{Power Related Cost (\$)}}{\text{Power Transfer Capability (kW)}}} \tag{5.6}$$

Thus, either Equation 5.5, (which is general for any size TSU), or Equation 5.6, (valid for large TSU systems), can be used to determine the EPCR. Equation 5.2 is generally applicable to determine the total capital TSU cost.

The C_E, C_P, and EPCR parameters defined above were developed to allow economic classification of various TSU concepts on a nearly application independent basis. One problem with the technique is that often only the total TSU first cost is known, and in some applications it is difficult to bifurcate a component cost into a solely energy related or power related item. Frequently useful are the System Cost of Energy Storage (CES) and the System Cost of Power Storage (CPS) where

$$\text{System Cost of Energy Storage (CES)} = \frac{\text{TSU Total Cost (from Equation 5.2)}}{\text{Useful Stored Energy When System is Fully Charged}} \tag{5.7}$$

and

$$\text{System Cost of Power Storage (CPS)} = \frac{\text{TSU Total Cost (from Equation 5.2)}}{\text{Maximum Power Extraction Capability}} \tag{5.8}$$

The simplicity of formulating the CES and CPS, plus the ease of comparing different TSU approaches on a consistent economic basis for given applications, make them advantageous in some analysis.

Sizing a TSU relative to the larger system of which the TSU is a part is a matter of application and economics. The "TSU Time Factor" τ, defined as

$$\tau = \frac{\text{TSU Energy Storage Capacity}}{\text{TSU Power Transfer Capacity}} \quad \text{(hours)} \qquad (5.9)$$

is a useful ratio which can normalize the energy related costs to the power related costs. The dimension of τ is time. If a given TSU can store 600 MWhr-t and the average power extraction capability is 100 MW-t, then τ = (600 MWhr-t)/(100 MW-t) = 6 hr, and in this case τ is the length of time which a system can be operated from the storage mode. However, if 12 hours of operation from storage at the 100 MW-t extraction level are required from the same kind of storage system, then supplying two identical 6 hour units at double the cost will obviously satisfy the energy requirement. But it will be more than adequate to supply the power extraction requirement, because there is also twice as much heat transfer surface, the power extraction capability is 200 MW-t so the TSU Time Factor τ remains 6 hours. Because we generally have to pay for additional heat transfer capability, a large τ is associated with smaller power related costs, and vice versa. A certain amount of heat transfer surface is required to achieve 100 MW-t of power, whether or not the heat for 6 hours or 12 hours is withdrawn. It is clear that a system such as the sand-pipe TSU designed to produce 100 MW-e for 12 hours will cost less than one for 6 hours at the same power recovery level, provided the power related cost is significant compared to energy related cost. For example, if the tube-intensive sand-sensible heat storage system must have a tube spacing of 12.6 cm (5.0 in) in order to achieve a given τ, then for double energy capacity with the same power capability (2τ) the sand volume and containment costs might be twice as great. But the tube spacing for the same power might be only 17.8 cm (7.0 in), hence the tubes would not cost twice as much. Because in the sand heat exchanger design the tubes represent a significant portion of the overall cost, this saving is important.

For long-term storage or even seasonal storage we normally have a high τ, perhaps measured in months. In this case we can afford an expensive (power related) extraction device (i.e., heat exchanger) because it will be relatively small in cost. But we require an inexpensive energy related cost (storage medium, containment, insulation, etc.) because this will be the bulk of the system. For example, for long-term storage, the sand and pipes approach might be appropriate because the energy related costs are low. However, for short-term storage requirements (defined as low τ in Equation 5.9) a system must have the capacity to discharge very rapidly (high power) hence, the power related costs for the selected TSU approach should be inherently low and we can afford greater energy related costs. An adequate short-term storage device might be the pressurized water TSUs because little or no heat exchanger is needed, and so the pipes buried in sand TSU could be suboptimal.

Personnel safety and the proclivity of the storage system to fire, leaks, explosions or other self-destruction are intangible factors which are difficult to quantify, but nevertheless, they would detract from the system attractiveness. System resistance to damage from natural disasters, sabotage, and vandalism also possesses unquantifiable appeal.

Development risk is another factor to which it is difficult to assign a dollar value. Although an untried system concept may appear to have promising potential on paper, it may contain certain elements requiring new technology development. If this new technology proves to be either very expensive or impractical to implement, then the entire conceptual system may either by unusable or more expensive to install and operate than the original estimate. But such a determination is, in some cases, possible only after considerable expenditure of time and money. As an example of development risk, a new storage medium may have many desirable properties, but its long-term interaction with other parts of the system may be unknown or the medium may tend to degrade with time. Low-development risk systems are fabricated from off the shelf technology using materials and techniques which have been previously used successfully in similar environments where operating experience is available.

In most thermal storage units, it is necessary to input some initial energy to heat or change the system to some minimum energy level to prepare the system to receive energy for storage which can be usefully extracted. As an illustration, if a thermal storage system has a cyclical temperature swing between 315°C (600°F) and 205°C (400°F), then before the system can usefully store heat it must be heated from ambient temperature to 205°C (400°F). This leads to the concept of Initial Energy Investment (IEI) as a prerequisite for useful thermal storage. The IEI is normally nonrecoverable, although with good insulation and design the IEI may have to be paid occasionally, especially for large systems. If a major part of the IEI must be invested at the beginning of every storage cycle (i.e., daily) this could manifest as a severe performance penalty.

In estimating the installed cost of a thermal storage system several items must be considered. From the First Law of Thermodynamics, it is usually possible to calculate the required charge of the thermal storage medium, and thus its cost. The volume of charge is then used to determine the containment volume and costs; these are energy related costs. Second Law considerations are used to determine the necessary heat exchanger capacity, which is an indication of heat exchanger (power related) cost. A multitude of miscellaneous cost items must be considered, including labor, foundation and site preparation, transportation of materials to site, plumbing, controls, monitoring devices, regulation valves, insulation, weatherproofing, perhaps a charge protection and purifier system, and pumps. These items may have minor cost impact in many systems, but in some these costs may be significant.

An economic analysis which computes only the initial capital cost of energy storage (C_T) of a system is not complete without considering factors such as throughput efficiency, reliability, operation and maintenance, cost of parasitic power and heat loss, system efficiency from storage relative to direct operation from the heat source, etc. The storage system first cost is only one of several important indicators of economic performance. For example, a thermal storage system characterized by relative low first cost may be afflicted with frequent unscheduled outages which could cripple the performance of a very expensive power plant.

It is difficult to estimate recurring costs such as operation and maintenance, degradation and replenishment of charge, deterioration and replacement of various components, taxes, insurance, etc. But a comparative cost estimate is more meaningful if all recurring costs expended over the lifetime of the installation can be estimated and expressed as a present value or initial capital cost. Unfortunately, this requires knowledge of future economic conditions including interest rates. The nuisance and lost revenue due to scheduled and unscheduled shutdowns caused by the storage subsystem should also be part of the capitalized first cost. It is therefore apparent that, although the C_T ($/kW) of a storage system is an important parameter which may be relatively straightforward to approximate, the actual owning cost stated as a present value is an even more useful parameter and is also more difficult to estimate.

B. ECONOMICS OF A SAND-PIPE THERMAL STORAGE UNIT

The results from Section IV, which analysis was done in every case for a single 1524 m (5000 ft) flow length of pipe and surrounding sand, are applied here to estimate the costs relating to a large TSU of such size that might be integrated into a power plant. Although 1524 m (5000 ft) flow lengths were previously considered, it is recognized that the flow path will serpentine, with straight flow lengths of perhaps 15 to 30 m, (50 to 100 ft), after which headers reverse the flow direction back into the sand system. It is obvious that to form a large TSU many flowpaths will be arranged in parallel. The question of how many and what configuration depends upon expected performance, which in turn impacts on cost.

An example will illustrate how a large TSU might be designed from the data presented in Section IV, for flow velocity of 0.3 m/sec (1 fps) and flow length of 1524 m (5000 ft). Suppose we require a TSU which will accept 333 MW-t average thermal power and have a capacity of 2000 MWhr-t, from Equation 5.9 it is apparent that the TSU Time Factor τ will be

$$\tau = \frac{\text{TSU Energy Storage Capacity}}{\text{TSU Power Transfer Capacity}} \quad \frac{2000 \text{ MWhr-t}}{333 \text{ MW-t}} = 6 \text{ hr}$$

so it will require 6 hours to charge up the system. It is necessary to select a geometry from Table 4.2 which has approximately the same time to accept a significant amount of the system heat, about 80%. From Table 4.2, the following data can be observed:

Case	D_i (in)	D_o (in)	V	Time to Accept 80% of Maximum System Heat	System Power Cost ($/kW-t)	System Energy Cost ($/kWhr-t)
1	3.8cm (1.5)	10cm (4)	0.3m/sec (1 fps)	4.0 hrs	42.12	4.49
2	3.8cm (1.5)	15cm (6)	0.3	9.2	56.62	3.26
5	6.35cm (2.5)	15cm (6)	0.3	4.2	34.54	3.56
6	6.35cm (2.5)	20cm (8)	0.3	8.0	44.69	2.77
9	8.9cm (3.5)	20cm (8)	0.3	4.0	26.66	2.89
10	8.9cm (3.5)	25cm (10)	0.3	8.0	42.03	2.63
11	8.9cm (3.5)	25cm (10)	0.9/m/sec (3 fps)	2.5	17.28	2.80

In an 8 hour charge period, Cases 2, 6, and 10 can be selected and in practice, Case 10 would be selected because both system power cost and also system energy cost are less for Case 10 than for the other candidates. Also, because Case 10 features greater spacing 25 cm (10 in) than the other two 15 cm (6 in) and 20 cm (8 in) for Cases 2 and 6, respectively, there will be fewer pipes, headers, controls, and therefore less maintenance cost. Fewer tubes also mean lower operational costs because parasitic pump power is less. For the 6 hour charge period we would interpolate between Case 1 and Case 2, Cases 5 and 6, and Cases 9 and 10; the likely result would be a "Case 9 1/2" with D_i = 8.9 cm (3.5 in), D_o = 23 cm (9 in) tube spacing, system power cost of $24/kW-t, and system energy cost of $2.75/kWhr-t. In the preceding example where interpolation between cases is used, it is recognized that all interpolations may not be linear. However, they will provide a reasonable order of magnitude estimate. To determine how large the 2000 MWhr-t system with 6 hour charge must be, consider that each 1524 m (5000 ft) flow length with D_i = 8.9 cm (3.5 in) and D_o = 23 cm has an average power input capability (from Table 4.2, Cases 9 and 10) of 1/2(1194 + 792) = 993 kW-t, so for 6 hour the total heat capacity is 6(993) = 5958 kWhr-t. Then,

$$N = \frac{2000 \text{ MWhr-t}}{5.96 \text{ MWhr-t/flowlength}} = 336$$

flow paths in parallel are required. The TSU volume will be

$$\text{TSU Volume} = 336 \frac{\pi}{4} (9/12 \text{ ft})^2 (5000 \text{ ft}) = 742{,}000 \text{ ft}^3$$

$$= 21{,}000 \text{ m}^3$$

and the cost for pipes and sand will be (assuming average system energy cost of $2.75/kWhr-t from Cases 9 and 10 Table 4.2)

Pipe and Sand Cost = ($2.75/kWhr-t) (2000 MWhr-t) (1000 kWhr/MWhr)

= $5.5 Million

The parasitic power losses are estimated from information on Table 4.3. The TSU pressure drop is 12.4 kPa (1.8 psi), because all tubes are in parallel. The TSU pump power requirement is

TSU Pump Power = (3336) (0.029 kW-e) = 9.7 kW-e

= 32.5 kW-t (conversion efficiency = 0.3)

which is about 0.1% of the total power being inputted.

Table 5.1 was prepared to determine the effect of tube spacing on the technical and economic performance of a system with given tube diameter, and also the effect of water velocity for a given geometrical configuration. Systems 1, 2, and 3 vary tube spacing for a given tube diameter and water velocity of 0.3m/sec (1 fps). As tube spacing increases, the system response becomes more sluggish, as expected, because a greater percentage of the total stored heat must transfer to sand which is characterized by a low thermal diffusivity. To input the same quantity of heat requires a longer time, consequently the average power capability is lessened. Because more heat is stored in sand for larger spacing, less pipe length is required which is manifested as lower system cost and marginally less pump power requirement, although the system volume is greater because the energy storage density is less for sand than water. Therefore, the TSU energy cost is less as the tube spacing increases. However, the TSU power cost is greater for larger tube spacing because the magnitude of power input (output) is less. Thus, the tube embedded in sand TSU will show best performance when long system charge and discharge times are available.

The effect of water velocity on a given system geometry can be appreciated by comparing Systems 3 and 4 of Table 5.1. System 3 features water velocity of 0.3 m/sec (1 fps) and System 4 has 0.9 m/sec (3 fps). But System 4 charges faster (2.5 hr compared to 4 hr), as expected, because the average power charge capability is greater. Because there is not a great difference in the cost of the two systems, the TSU power cost is less for the faster velocity. There is less time for the heat to transfer into the sand for the faster velocity, so the system is a little larger and costs more, therefore the TSU energy cost is marginally higher. The high velocity generally performs better technically and economically except for pressure drop and pump work, which increases very quickly with flowrate or velocity. Therefore, in a practical system design, the velocity will be consistent with acceptable pressure drop and pump work losses.

The direct costs compiled in Tables 5.1, 4.1 and 4.2 are those for pipe and sand only, which is the largest single expense. However, in Section III it was estimated for a large system that in order to account for the additional total system components, it is necessary to multiply the base pipe and sand figure by a factor of 2.22. For example, in Table 5.1 for System 1, where the pipe and sand cost is estimated at \$7.1 million, the TSU system captial cost is estimated at (\$7.1 x 106 x 2.22 =) \$15.8 x 106. The energy unit storage cost (C_E) is

$$C_E = (1.3)\ (\$15.8 \times 10^6)/(2 \times 10^6\ \text{kWhr-t}) = \$2.63/\text{kWhr-t}.$$

The power unit storage cost (C_P) is

$$C_P = (2/3)\ (\$15.8 \times 10^6)/(250{,}000\ \text{kW-t}) = \$42.03/\text{kW-t}.$$

The same applies to the rest of Table 5.1, which gives an indication of how much a large sand and pipe system might cost, although the system design is not optimized.

Table 5.1. Large TSU Technical and Economic Performance Estimates
TSU Usable Capacity = 2000 MWhr-t
Temperature Swing 222°C (400°F)
1525 m (5000 ft) Flowlength

FEATURE OR DESCRIPTOR	SYSTEM 1 (Case 10)	SYSTEM 2 (Interpolate between Cases 9 and 10)	SYSTEM 3 (Case 9)	SYSTEM 4 (Case 11)
Tube D_i, Tube Spacing D_o	8.9cm, 25cm (3.5in, 10in)	8.9cm, 22.8cm (3.5in, 9in)	8.9cm, 20cm (3.5in, 8in)	8.9cm, 20cm (3.5in, 8in)
Water Velocity	0.3 m/sec (1 fps)	0.3 m/sec (1 fps)	0.3 m/sec (1 fps)	0.9 m/sec (3 fps)
Time for System to Achieve 80% of maximum charge	8 hr	6 hr	4 hr	2.5 hr
Number of Flowpaths in Parallel	316	336	419	434
Average Charge Power Capability	250 MW-t	333 MW-t	500 MW-t	800 MW-t
TSU Volume m^3 (ft^3)	24,400 (862,000)	21,000 (742,000)	20,700 (731,000)	21,500 (758,000)
TSU Pressure Drop	12.4 kPa (1.8 psi)	12.4 kPa (1.8 psi)	12.4 kPa (1.8 psi)	88.2 kPa (12.8 psi)
TSU Pump Power Requirement (Conversion Efficiency = 0.3)	30.5 kW-t	32.5 kW-t	40.5 kW-t	272 kW-t
Pipe and Sand Cost ($ Million)	$7.1	$7.5	$9.0	$9.3
TSU System Cost*	$15.8	$16.7	$20.0	$20.6
C_p, TSU Power Cost** ($ Million)	$42.03/kW-t	$33.43/kW-t	$26.67/kW-t	$17.17/kW-t
C_E, TSU Energy Cost** ($/kWhr-t)	2.63	2.78	3.33	3.43

*Multiply total pipe and sand cost by 2.22 to estimate the total storage system cost, which includes insulation, containment, etc. The factor 2.22 is discussed and documented in Section III.

**TSU Power Cost and TSU Energy Cost estimates in Table 5.1 include the effect of the 2.22 multiplication factor and assumes power related equipment costs 2/3 of total TSU capital cost and energy related components cost 1/3.

SECTION VI

RESULTS AND DISCUSSION OF RESULTS

It was originally believed that a hollow steel ingot could be produced for 33¢/kg (15¢/lb), and this would provide a pressure containing TSU with fast response time, no heat exchanger nor intermediary transport fluid requirement, and a low maintenance unit (see Figure 2.1). However, it was found that production of such a unit would cost $1.32/kg (60¢/lb) and that lengths would be restricted to 6 m (20 ft) instead of 18.3 m (60 ft), necessitating more heater welds, system complexity, and cost. To overcome these limitations thick large diameter pipes and square welded slabs (both described in Section II) were considered, which had the advantage over the hollow steel ingot in that a significant weight of water could also be contained, substantially assisting in the storage of heat (and thereby reducing the cost for steel). A preliminary materials cost, which did not account for all systems costs, indicated that each system would have an energy unit storage cost (C_E) around $14/kWhr-t.

An alternative approach was considered using poured concrete around closely spaced tubes. The tubes would contain pressurized water or steam, and the heat would transport into and out from the concrete by conduction. Because a large concrete unit would hold its own shape, no external containment would be necessary, reducing cost for this item. However, a thermal stress analysis revealed that differential thermal stresses would cause tube separation from the concrete, resulting in severe thermal conduction resistance between the tubes and concrete. This would severely reduce thermal performance and disqualify the concrete approach from further consideration. The approach which was successfully adopted was to replace the concrete with loose sand and provide external containment for the sand. The sand has a somewhat lower thermal diffusivity than does the concrete, but being loose it should stay pressed against each pipe due to overpressure from sand above. But the sand requires external containment at added complexity and expense (over the concrete concept). However, there is no obvious reason why the sand-pipe system should not work well, and the energy unit storage cost C_E was estimated at $3/kWhr-t for a large TSU, which includes costs for all parts of the system including 30% contingency penalty in addition to subtotal costs (see Table 3.1).

Because the sand-pipe TSU is characterized by a substantially lower cost than the two steel and water TSUs, the sand-pipe TSU was selected for closer technical and economic evaluation, and the two steel concepts were discarded from further study. A computer model was developed to evaluate transient thermal response of the sand-pipe TSU for given conditions, and to evaluate the effect of varying tube diameter and tube spacing on system technical and economic performance. For a large TSU with maximum temperature in the 343°C (650°F) range, a tube diameter of 8.9 cm (3.5 in) and tube spacing inside the sand volume of approximately 25 cm (10 in) appears to be

associated with minimal cost consistent with 6 to 8 hour charge or discharge time. The results of different TSU configurations are displayed in Tables 4.1 and 4.2. In each case pressurized liquid water was assumed to be contained within the tubes, because very long flow lengths would give rise to unacceptable pressure drops and pump work expenditure if lower density steam were used. But with liquid water, the velocity (and hence the possible system charge rate) cannot be too great, as indicated in Table 4.3.

The economic results for some of the better cases are assembled in Table 5.1, where a TSU with usable energy capacity of 2000 MWhr-t, 222°C (400°F) water temperature cyclic swing, and 1524 m (5000 ft) flow length is considered. For an average thermal power charge rate of 333 MW-t the TSU system capital cost is estimated at $16.7 million, the power unit storage cost (C_P) is $33.43/kW-t, and the energy unit storage cost (C_E) is $2.78/kWhr-t.

In this study, maintenance costs have not been considered in the economic evaluations. If the results of this study appear applicable to some applications, then a test module should be built and evaluated in the field to gain operational experience. This appears to be the only way to better understand what maintenance costs will be and to assess other possible problems, as well as to test technical performance. This would provide a practical capital cost comparison to the estimates made in this study.

APPENDIX A

NUMERICAL DIFFERENCING OF THE TRANSIENT HEAT CONDUCTION EQUATION IN CYLINDRICAL COORDINATES; DERIVATION OF EQUATION 4.1

The thermal analysis of the sand around pipe thermal storage unit described in Section IV is dependent upon a numerical finite differencing of the appropriate transient conduction equation.

If we neglect axial (z coordinate) conduction effects and consider radial symmetry in the cylinder in Figure 4.2 and 4.3 the transient heat conduction equation in radial coordinates becomes:

$$(a)\quad \frac{\partial T}{\partial t} = \alpha\left(\frac{\partial^2 T}{\partial r^2} + \frac{1}{r}\frac{\partial T}{\partial r}\right), \qquad \begin{array}{l} T = \text{temperature} \\ t = \text{time} \\ r = \text{radial coordinate} \end{array}$$

where

$$\alpha = \frac{K}{\rho C_p} \quad \text{(thermal diffusivity)}$$

Replacing the terms on right hand side of equation (a) with their central difference analogs,

$$\left(\frac{\partial^2 T}{\partial r^2}\right)_n = \frac{T_{n+1} - 2T_n + T_{n-1}}{(\Delta r)^2}, \qquad \left(\frac{\partial T}{\partial r}\right)_n = \frac{T_{n+1} - T_{n-1}}{2\Delta r}$$

and replacing the time term with a forward difference term,

$$\left(\frac{\partial T}{\partial t}\right)_n = \frac{T_n^{m+1} - T_n^m}{\Delta t}$$

and the partial differential equation becomes,

$$\frac{T_n^{m+1} - T_n^m}{\Delta t} = \left(\frac{T_{n+1} - 2T_n + T_{n-1}}{(\Delta r)^2} + \frac{T_{n+1} - T_{n-1}}{2r\,\Delta r}\right)$$

Some rearranging results in,

$$T_n^{m+1} = T_n^m (1 - 2F) + F\left[T_{n+1}\left(1 + \frac{\Delta r}{2r_n}\right) + T_{n-1}\left(1 - \frac{\Delta r}{2r_n}\right)\right]$$

where F is the Fourier modulus $(\alpha\Delta t/(\Delta r)^2)$. F = 1/2 represents the upper limit of stability from error damping criteria. Therefore,

$$T_n^{m+1} = \tfrac{1}{2}\left[T_{n+1}^m \left(1 + \frac{\Delta r}{2r_n}\right) + T_{n-1}^m \left(1 - \frac{\Delta r}{2r_n}\right)\right]$$

where

$$\Delta t = \frac{F(\Delta r)^2}{\alpha} = \frac{(\Delta r)^2}{2\alpha}$$

equals the time step.

This is Equation 4.1. The geometry for this finite differencing scheme is shown in Figure 4.2. The superscript refers to time accounting, while the subscript refers to radial location in Figure 4.2.

APPENDIX B

HEAT CAPACITY WEIGHTED AVERAGE TEMPERATURE FOR A CYLINDRICAL SECTION

At any given time the average temperature within a cylindrical section, illustrated in Figure 4.2, is related to the amount of thermal charge which has been accepted by that element. Since generally the temperature distribution within the element is changing with time, the percent of total possible thermal charge is also changing. The average temperature of the section, $\bar{T}_s$, is defined as

$$\bar{T}_s = \frac{\sum_{i=1}^{N} \rho_i A_i L_i C_{p_i} T_i}{\rho A L C_p}$$

Assuming density (ρ_i) and heat capacity (C_{pi}) are constant throughout the volume of thick wall cylinder, then

$$\bar{T}_s = \frac{\sum_{i=1}^{N} A_i T_i}{\sum_{i=1}^{N} A_i}, \text{ where } A_i \text{ for } i = 1 \text{ is } \frac{\pi}{4}\left[\left(r_1 + \frac{1}{2}\Delta r\right)^2 - r_i^2\right]$$

$$A_i \text{ for } 1 < i < N \text{ is } \frac{\pi}{4}\left[\left(r_i + \frac{1}{2}\Delta r\right)^2 - \left(r_i - \frac{1}{2}\Delta r\right)^2\right]$$

$$A_i \text{ for } i = N \text{ is } \frac{\pi}{4}\, r_N^2 - \left[\left(r_N - \frac{1}{2}\Delta r\right)^2\right]$$

$\bar{T}_s$ is then

$$\bar{T}_s = \frac{T_1\left[r_1 + \frac{1}{2}\Delta r\right)^2 - r_1^2] + \ldots T_I[r_I + \frac{1}{2}\Delta r)^2 - (r_1 - \frac{1}{2}\Delta r)^2 + \ldots T_N[r_N - \frac{1}{2}\Delta r)^2]}{[(r_1 + \frac{1}{2}\Delta r)^2 - r_1^2] + \ldots [(r_1 - \frac{1}{2}\Delta r)^2 - (r_1 - \frac{1}{2}\Delta r)^2] + \ldots [r_N^2 - (r_N - \frac{1}{2}\Delta r)^2]}$$

then

$$\bar{T}_s = \frac{\frac{1}{2}T_1(r_1 + \frac{1}{4}\Delta r) + \ldots + T_1 r_I = \ldots + \frac{1}{2}T_N(r_N - \frac{1}{4}\Delta r)}{\frac{1}{2}r_1 + \ldots + r_1 + \ldots + \frac{1}{2}r_N}$$

The heat capacity weighted average temperature including the flowing fluid is

$$\bar{T} = \frac{\rho_{sand} (B^2 - A^2) C_{p_{sand}} \bar{T}_s + \rho_{water} A^2 C_{p_{water}} T_{water}}{(B^2 - A^2) \rho_{sand} C_{p_{sand}} + A^2 \rho_{water} C_{p_{water}}}$$

A = pipe radius

B = sand thermal influence radium

which is Equation 4.5.

APPENDIX C

COMPUTER CODE LISTING OF THE THERMAL ANALYSIS IN SECTION IV.

```
      REAL      MDOT,AXIAL(999),RADIUS(15)
      REAL T(999,15),Q(999),TFLUID(999),TNEW(999,15),TFLNEW(999)
      REAL TSYSTM(999),RDIFSQ(15)
C     INPUT RADIAL SPACE STEPS(I),  KOUNT DECIDES HOW OFTEN RESULTS
C     WILL BE PRINTED
C     NFIRST IS NUMBER OF INITIAL TIME STEPS WHICH WILL BE PRINTED
      READ(5,130)I,KOUNT,NFIRST
C     INPUT INNER AND OUTER RADII    (INCHES)    A  AND B
C     INPUT TIME LIMIT(MINUTES)   TIMAX
C     INPUT AXIAL FLOW LENGTH(FEET), ZLONG
C     INPUT CONVECTION HEAT TRANSFER COEFFICIENT (BTU/HR-FT2-F)    H
C     INPUT FLOW VELOCITY (FT/SEC)   V
C     INPUT INITIAL FLUID TEMPERATURE (DEGREES F)    TF
C     INPUT INITIAL SOLID TEMPERATURE(DEGREES F)     TS
      READ(5,120) A,B,TIMAX,ZLONG,H,V,TF,TS
C     INPUT SOLID PROPERTIES (THERMAL CONDUCTIVITY(BTU/HR-F--F
C         DENSITY(LB/FT3),HEAT CAPACITY(BTU/LB-F))
      READ (5,150) TC,D,CP
C     INPUT FLUID PROPERTIES(HEAT CAPACITY(BTU/LB-F),DENSITY
C     VISCOSITY(LB/FT-SEC)
      READ (5,160) CPF,DF,VISCO
C     VERIFY INPUTTED DATA
      WRITE (6,170) A
      WRITE (6,180) B
      WRITE (6,190) I
      WRITE(6,195)KOUNT
      WRITE(6,196)NFIRST
      WRITE (6,200) ZLONG
      WRITE (6,310) TIMAX
      WRITE (6,220) H
      WRITE (6,230) V
      WRITE (6,240) TF
      WRITE (6,250) TC
      WRITE (6,260) D
      WRITE (6,270) CP
      WRITE (6,280) TS
      WRITE (6,290) CPF
      WRITE (6,300) DF
      WRITE (6,80) VISCO
      CONST1=(B*B-A*A)*CP*D/144.
      CONST2=A*A*CPF*DF/144.
      CONST3=CONST1*CONST2
      J=I+1
      PI=3.14159
      TMAX=TF
      C=I
      DELR=(B-A)/(2.*C)
      RADIUS(1)=A
      DR=DELR*2.
      DO 400 II=2,J
      FLOAT=II-1
  400 RADIUS(II)=A+FLOAT*DR
      DENOM=0.5*(RADIUS(1)+RADIUS(J))
      DO 500 JJ=2,I
  500 DENOM=DENOM+RADIUS(JJ)
      ALPHA=TC/(D*CP)
      DELT=DELR*DELR/(2.*ALPHA)
```

```
      DTIME=DELT*60.
      DELX=DELT*V*3600.
C     CALCULATE NUMBER OF AXIAL SPACE STEPS, NAXIAL
      DUMMY=ZLONG/DELX
      NAXIAL=DUMMY
      XLONG = NAXIAL
      WRITE(6,129)NAXIAL
      WRITE (6,210) DELX,DELT,ALPHA,DELR
      MDOT=DF*PI*A*A/144.*V
      WRITE(6,995)MDOT
C     WRITE OUT RADII FOR WHICH TEMPERATURE WILL BE CALCULATED
      WRITE(6,999)
      WRITE(6,998)(RADIUS(JPL),JPL=1,J)
C
C     WRITE OUT PUMP WORK,PRESSURE DROP AND RELATED PARAMETERS
      RE=DF*V*2.*A/VISCO/12.
      F=0.184*RE**(-0.2)
      DP=(F*ZLONG*12.*DF*V*V)/(2.*A*2.*32.2)
      PUMP=(MDOT*DP)/(0.85*DF)/778.*3600.
      PWKW=PUMP/3413.
      WRITE(6,110)PUMP,RE,F,DP
      WRITE(6,198)PWKW
      QSOLID = CONST1*PI*XLONG*(TF-TS)*DELX
      QFLUID = CONST2*PI*XLONG*(TF-TS)*DELX
      QCHARG = QSOLID + QFLUID
      QKWHRT=QCHARG/3414.
      WRITE(6,85)QSOLID,QFLUID,QCHARG,QKWHRT
C     INITIALIZE FLUID AND CYLINDER TEMPERATURES AND CALCULATE AXIAL LOC
      AXIAL(1)=0.0
      DO 10 JPL=1,NAXIAL
        Q(JPL)=0.0
        TFLUID(JPL)=0.0
      IF(JPL.EQ.1)GO TO 9
      AXIAL(JPL)=AXIAL(JPL-1)+DELX
    9   DO 10 L=1,J
      TNEW(JPL,L) = 0.0
   10     T(JPL,L)=0.0
      TFLUID(1)=1.0
      TFLNEW(1)=1.0
C     WRITE OUT INITIAL CONDITIONS
      TIME=0.0
      QTOTAL=0.0
      HEATIN=0.0
      AVG = 0.0
      WRITE (6,90) TIME,QTOTAL,HEATIN
      WRITE(6,340)
      NPRINT=0
      KOUNTR=0
C
CALCULATE PRELIMINARY CONSTANTS
      CON1=PI*DF*A*A*DELX*CPF/144.
      CON2=2.*PI*A*DELX*H*DELT/12.
      CONQ=0.5*D*PI*CP*DELX/144.
      CONRAD=2.*A*DR*DR*DR
      CONK1=CONQ*CONRAD
      DO 20 JPL=2,I
      LPJ=JPL-1
```

```
      20    RDIFSQ(JPL)=RADIUS(LPJ)*RADIUS(LPJ)-RADIUS(JPL)*RADIUS(JPL)
      C
            LENGTH = 3
      30    QTOTAL=0.0
            LENGTH = LENGTH + 1
            IF(LENGTH.GT.MAXIAL) LENGTH = MAXIAL
            DO 50 L=1,LENGTH
      C  SOLID TEMPERATURES  FOR THE NEXT TIME STEP CAN BE EXPLICITLY DETER
      C  MINED FROM THOSE OF THE PRECEEDING TIME STEP, EXCEPT FOR THE INNER
      C  SURFACE TEMP WHICH MUST BE DETERMINED FROM A CONDUCTION CLOSURE COND
            DO 95 K=2,J
                IF (B(L).EQ.(I+1)) GO TO 90
                VAR1=C+1
                VAR=DELR/(2.*(A/12.*(VAR1+DELR)))
                TNEW(L,K)=0.5*(T(L,K+1)*(1.+VAR)+T(L,K-1)*(1.-VAR))
            GO TO 95
      C     NO FLUX BOUNDARY CONDITION
      90        TNEW(L,K)=TNEW(L,K-1)
      95    CONTINUE
      C
      CALCULATE HEAT CONSTANT QSET WHICH DESCRIBES HEAT WHICH HAS CONDUCTED
      C  INTO THE SOLID INTERIOR DURING TIME STEP.  THIS EXCLUDES HEAT INTO TH
      C  FIRST ELEMENT
            QSET=0.0
            DO 96 JPL=2,I
            LPJ=JPL+1
      96    QSET=QSET+RDIFSQ(JPL)*(TNEW(L,LPJ)+TNEW(L,JPL)-
           1(T(L,LPJ)-T(L,JPL))
            CONRT=CONRAD*(TNEW(L,2)-T(L,2)-T(L,1))
            CONK2=CONQ*(CONRT+QSET)
      C
      C  DETERMINE NEW SURFACE TEMPERATURES TNEW(L,1)
            IF(L.EQ.1)GO TO 98
            LLLL=L-1
            TOP=TFLUID(LLLL)*CONK2/CON1+CONK2/CON2
            BOTTOM=1.0+CONK1/CON1+CONK1/CON2
            TNEW(L,1)=TOP/BOTTOM
            TFLNEW(L)=TNEW(L,1)*(1.0+CONK1/CON2)+CONK2/CON2
            Q(L)=CONK1*TNEW(L,1)+CONK2
            GO TO 50
      98    Q(1)=CONK1+CONK2
            TNEW(1,1)=1.0
            TFLNEW(1)=1.0
      50    QTOTAL=QTOTAL+Q(L)
      C
      C  QTOT IS HEAT INTO SOLID DURING TIME STEP (BTU)
            QTOT = QTOTAL * (TF (S)
            HEATIN=HEATIN+QTOT
      C     REPLACE OLD TEMPS WITH NE  EMPS
            DO 52 L=1,LENGTH
            DO 51 K=1,
      51    T(L,K)=TNEW(L,K)
      52    TFLUID(L)=TFLNEW(L)
            TIME=TIME+DTIME
      C
      C     PRINT RESULTS
            NPRINT=NPRINT+1
```

```
      IF(NPRINT.LE.NFIRST)GO TO 55
C     DECIDE IF THIS TIME STEP SHOULD BE REPORTED
      KOUNTR=KOUNTR+1
      IF(KOUNTR.LT.KOUNT)GO TO 30
      KOUNTR=0
55    CONTINUE
C
      TSSUM = 0.0
      FLSUM = 0.0
      DO 70 L=1,LENGTH
      FNUM=0.5*.(RADIUS(1)*DR/4.)*T(L,1)*(RADIUS(J)-DR/4.)*T(L,J))
      DO 600 J.=2,I
600   FNUM=FNUM+T(L,JJ)*RADIUS(JJ)
      TAVGSD=FNUM/DENOM
C     TAVGSD IS WEIGHTED AVERAGE TEMPERATURE FOR SOLID ONLY
      TSYSTM(L)=(CONST1*TAVGSD+CONST2*TFLUID(L))/CONST3
C     TSYSTM IS WEIGHTED AVG TEMPERATURE FOR SOLID AND FLUID CONTAINED
      TSSUM = TSSUM + TAVGSD
      FLSUM = FLSUM + TFLUID(L)
   70 CONTINUE
C
      SOCHRG = TSSUM/XLONG
      FLCHRG = FLSUM/XLONG
      HEATFL = FLCHRG * QFLUID
      HEATSO =SOCHRG*QSOLID
      HEATSY = HEATFL + HEATSO
      AVG = (HEATSO + HEATFL) / QCHARG
      PBTUHR = MDOT*CPF*(TF-TS)*(TFLUID(1)-TFLUID(NAXIAL))*3600.
      PKWT = PBTUHR/3414.
C
C  REPORT RESULTS OF THIS TIME STEP
      WRITE(6,90)TIME,QTOT,HEATIN
      WRITE(6,91) HEATFL, HEATSY, AVG
      WRITE(6,330) PBTUHR,PKWT
      WRITE(6,350)(TFLUID(L),L=1,LENGTH)
      WRITE(6,350)(TSYSTM(L),L=1,LENGTH)
C     IF THE SYSTEM IS 98 PER CENT CHARGED, GO ONTO NEXT CASE
      IF(AVG.GE.0.98)GO TO 75
      IF (TIME.LE.TIMAX) GO TO 30
 75   STOP
C
 80    FORMAT (1X,'FLUID VISCOSITY(LB/FT-SEC) = ',2X,E13.5)
   85 FORMAT(/,' HEAT SOLID CAN ACCEPT (BTU) = ',F12.2,' HEAT FLUID CA
     1 ACCEPT (BTU) = ',F12.2,/,' HEAT SYSTEM CAN ACCEPT (BTU) =',F12.2
     2'      = ',F10.2,' KW-HR-T')
 90    FORMAT(//,1X,'TIME(MINUTES)=',F10.3,5X,'TOTAL HEAT TO WALL(BTU) =
     C',F10.2,5X,'HEAT TO WALL FROM TIME ZERO (BTU) = ',F12.1)
   91 FORMAT( ' HEAT CONTAINED IN FLUID (BTU) =', F12.1, '  HEAT CONTAI
     1ED IN SYSTEM(BTU) = ', F12.1,'    SYSTEM AVERAGE CHARGE = ',F9.4)
110    FORMAT(//,1X,'PUMPWORK(BTU/HR)  ',E13.5,/,1X,'REYNOLDS NUMBER = '
     CE15.5,/,1X,'THE FRICTION FACTOR IS ',E15.5,/,1X,'THE PRESSURE DRO
     C(LB/FT2)  IS ',E15.5)
  120 FORMAT (8F10.3)
129    FORMAT(1X,'NUMBER OF AXIAL STEPS CALCULATED IS',2X,I7)
130    FORMAT(8I10)
190    FORMAT (F10.2)
150    FORMAT (3F10.3)
```

```
230•      160   FORMAT (2F10.3,E13.6)
231•      170   FORMAT(1H1,'INNER RADIUS,INCHES',2X,F10.4)
232•      180   FORMAT (1X,'OUTER RADIUS,INCHES=',2X,F10.4)
233•      190   FORMAT (1X,'NUMBER OF SPACE STEPS IN RADIAL DIRECTION =',2X,I6)
234•      195   FORMAT(1X,'RESULTS WILL BE REPORTED EVERY ',I6,'  -TH TIME STEP')
235•      196   FORMAT(1X,'THE FIRST ',I8,'  -TH TIME STEPS WILL BE REPORTED AS
236•           C DEBUG AID')
237•      198   FORMAT(1X,'PUMPWORK(ONE FLOW LENGTH) IN KILOWATTS IS  ',E15.5)
238•      200   FORMAT (1X,'SYSTEM LENGTH(FEET)  = ',2X,F10.3)
239•      210   FORMAT(1X,'AXIAL STEP SIZE,FEET =',2X,F10.2,/,1X,
240•           C'TIME STEP,HOURS =',F10.5,/,1X,'THERMAL DIFFUSIVITY,FT2/HR =',
241•           CF10.5,/,1X,'RADIAL SPACE STEP,FEET = ',F10.5,/)
242•      220   FORMAT (1X,'CONVECTION HEAT TRANSFER COEFFICIENT(BTU/HR-FT2-F) ='
243•           12X,F10.2)
244•      230   FORMAT (1X,'FLOW VELOCITY(FT/SEC) =',2X,F10.2)
245•      240   FORMAT (1X,'FLUID TEMPERATURE INPUT(DEGREES F) =',2X,F10.2)
246•      250   FORMAT (1X,'THERMAL CONDUCTIVITY OF SOLID(BTU/HR-FT-F) =',2X,F10.2
247•           1)
248•      260   FORMAT (1X,'DENSITY OF SOLID(LB/FT3) =',2X,F10.2)
249•      270   FORMAT (1X,'HEAT CAPACITY OF SOLID(BTU/LB-F) =',2X,F10.3)
250•      280   FORMAT (1X,'INITIAL SOLID TEMPERATURE(F) =',2X,F10.2)
251•      290   FORMAT (1X,'FLUID HEAT CAPACITY(BTU/LB-F) =',2X,F10.3)
252•      300   FORMAT (1X,'FLUID DENSITY(LB/FT3) =',2X,F10.3)
253•      310   FORMAT (1X,'MAXIMUM TIME(MINUTES) = ',2X,F10.3)
254•      320   FORMAT(1X,F8.2,1PE7.4,F15.2)
255•        330 FORMAT('    THERMAL POWER TO SYSTEM DURING TIME STEP = ',F14.1,
256•           1 ' BTU/HR    = ',F12.1,' KW-T')
257•      340   FORMAT(/,1X,'FLUID TEMPS WILL BE PRINTED IN GROUPS OF SIXTEEN
258•           CSTARTING FROM THE HOTTEST,ENDING WITH THE COOLEST ',/,1X,
259•           C'THEN THE VOLUME WEIGHTED AVERAGE TEMPS WILL BE PRINTED IN GROUPS
260•           COF SIXTEEN')
261•       350  FORMAT(1X,16F7.4)
262•      995   FORMAT(1X,'MASS FLOW RATE(MDOT-LB/SEC) IS  ',F6.3)
263•      998   FORMAT(15F8.3)
264•       999  FORMAT(/,1X,'RADII FOR WHICH TEMPERATURES ARE CALCULATED(INCHES)')
265•            END

ND OF COMPILATION:        NO  DIAGNOSTICS.
9   CTP:.086   SUPS:6.968
```

APPENDIX D

DERIVATION OF DIMENSIONLESS PARAMETER λ

In an attempt to find correlation parameters which would apply to all of the system thermal dynamic curves in Section III, different dimensionless parameters were considered. No general parameters were found which would be generally applicable in all cases, although the dimensionless parameter, which is used in Figure 4.14, does provide a dimensionless flowlength which may be useful in some circumstances. A heat valance on a differential element dx of pipe is described below.

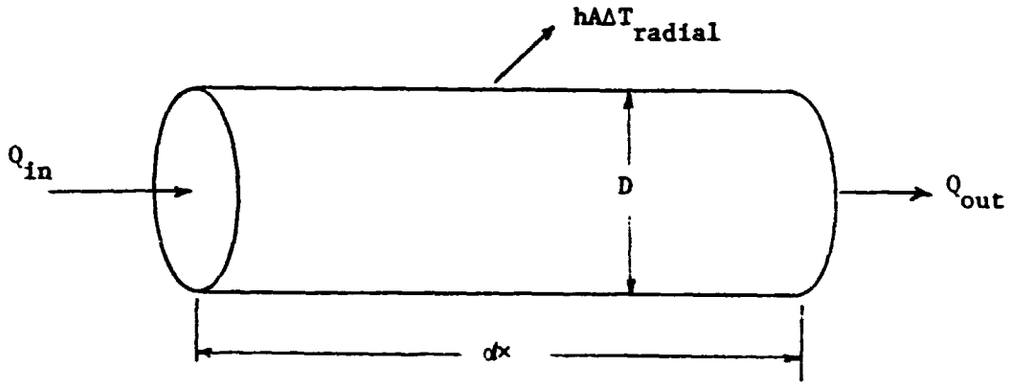

where the following definitions follow,

$Q_{out} = \dot{M} C_p T_{out}$

$Q_{in} = \dot{M} C_p T_{in}$

$\dot{M}$ = mass flow rate through pipe

C_p = heat capacity of fluid

ρ = density of fluid

T_{out} = temperature of fluid at outlet

T_{in} = temperature of fluid at inlet

h = convective heat transfer coefficient (fluid to pipe wall)

A = pipe wall area in element dx

$\Delta T_{radial} = T_f - T_w$

T_f = bulk fluid temperature

T_w = wall temperature

The heat balance is,

$$Q_{out} - Q_{in} = \dot{M} C_p (T_{out} - T_{in}) = hA \Delta T_{radial} = hA (T_f - T_w)$$

Differentially,

$$\dot{M} C_p \, dT_f = hA (T_f - T_w)$$

The mass flow rate can be written in terms of fluid velocity and the areas in terms of pipe diameter,

$$\rho V \frac{\pi D^2}{4} C_p \, dT_f = h \pi D \, dx (T_f - T_w)$$

If we group temperature terms together,

$$\frac{dT_f}{T_f - T_w} = \frac{4h dx}{\rho V D C_p}$$

integrating,

$$\int \frac{dT_f}{T_f - T_w} = \frac{4hx}{\rho V D C_p} = \lambda$$

In English units

h = BTU/hr ft^2 °F

x = ft

f = lb/ft^3

V = ft/hr

C = ft

C_p = BTU/lb°F

$$\frac{hx}{\rho V\ D\ C_p} = \frac{\left(\frac{BTU}{HR\ FT^2\ °F}\right)\left(FT\right)}{\left(\frac{LB}{FT^3}\right)\left(\frac{FT}{HR}\right)\left(FT\right)\left(\frac{BTU}{LB\ °F}\right)} = \frac{\frac{BTU}{HR\ FT\ °F}}{\frac{BTU}{HR\ FT\ °F}} = \text{DIMENSIONLESS}$$

λ is then the dimensionless parameter which relates several transport variables to each other and serves as a dimensionless flow distance from the system entrance.

APPENDIX E

PIPE AND SAND COST SAMPLE CALCULATION

In this report the cost of installed carbon steel pipes capable of containing pressurized water to 2000 psia in the sand-around-pipe thermal storage unit (TSU) is taken from the following table, which was generated from surveys of engineering construction firms.

Pipe Diameter (inch)	Material Cost $/ft	Welding Cost $/ft	Installation $/ft	Total $/ft
1.5	1.29	.12	.12	1.53
2	1.62	.12	.12	1.86
2.5	---	---	---	2.62*
3	2.60	.64	.13	3.37
3.5	---	---	---	4.02*
4	3.65	.87	.14	4.66

*Interpolated costs

Sample Calculation of Sand and Pipe Cost

Consider a sand-around-pipe thermal storage unit (TSU), such as described in Section II and III, which has 1.5 inch O.D. pipes on 4 inch centers. In Section III the thermal performance of such a system is calculated for different conditions, and the cost of a 5000 foot section of such pipe and sand is estimated here. From the above we see that the installed pipe will cost about

$$\text{Pipe Cost} = (\$1.53/\text{foot})\ (5000\ \text{feet}) = \$7650$$

The area within the boundaries of an annulus defined by 4 inch outer circle and 1.5 inch inner circle and is 0.075 square feet, and so the sand volume in a 5000 foot length is 375 cubic feet, which at 100 lb/ft^3 weighs 37,500 pounds or 18.75 tons. Delivered sand at $20/ton would then cost

$$\text{Sand Cost} = (\$20/\text{ton})\ (18.75\ \text{tons}) - \$375$$

and so the combined sand and pipe cost would be

$$\text{Pipe and Sand Combined Cost} = \$7650 + \$375 = \$8025$$

which is the value reported in Tables 3.1 and 3.2.